UNIVERSITA' DEGLI STUDI DI NAPOLI FEDERICO II

DOTTORATO DI RICERCA IN INGEGNERIA
DEI MATERIALI E DELLE STRUTTURE

XXVIII CICLO

DIPARTIMENTO DI INGEGNERIA CHIMICA, DEI MATERIALI E DELLA
PRODUZIONE INDUSTRIALE

MINIATURIZED BIOSENSORS AND MICRODEVICES BASED ON PEPTIDE FOR FOOD INDUSTRY AND HEALTHCARE

RELATORI
Prof. Filippo Causa
Prof. Paolo Antonio Netti

CANDIDATO
Concetta Di Natale

CORRELATORE
Dott. Edmondo Battista

COORDINATORE
Prof. Giuseppe Mensitieri

…….You’ve got to find what you love. And that is as true for your work as it is for your lovers. Your work is going to fill a large part of your life, and the only way to be truly satisfied is to do what you believe is great work. And the only way to do great work is to love what you do. If you haven't found it yet, keep looking. Don't settle. As with all matters of the heart, you'll know when you find it. And, like any great relationship, it just gets better and better as the years roll on. So keep looking until you find it. Don't settle.

Stay Hungry. Stay Foolish.

Steve Jobs, June 12, 2005.

To Myself, my Strength, my Courage, my Determination, and especially to my PASSION….

Table of Contents

Chapter 1

Introduction

ABSTRACT. The most widely accepted definition of a biosensors is: "a self-contained analytical device that incorporates a biologically active material in intimate contact with an appropriate transduction element for the purpose of detecting (reversibly and selectively) the concentration or activity of chemical species in any type of sample [1].Clark and Lyons developed the first biosensor, an enzyme-based glucose sensor [1]. Since then, hundreds of biosensors have been developed in many research laboratories around the world. The objective of this chapter is to underline the principles of biosensors science and their potential applications in the food, agricultural industries and biomedical fields.

1.1. Biosensors

Molecular recognition events are some of the most significant features of biological and chemical systems. The biomolecular recognition is the ability of a biomolecule to interact selectively with another molecule even in the presence of structurally similar antagonist molecules [2]. This basic principle is not only important from a scientific point of view but also to open an important window in the field of biotechnological applications. The recognition process itself is governed by non-covalent interactions as salt bridges, hydrogen bonds, van der Waals forces, hydrophobic interactions, and entropic effects [3]. Molecular recognition is fundamental for biosensing technique. Before the various types of biosensor technologies and application are discussed, it is first important to understand and define 'biosensor'. A biosensor, according to IUPAC recommendations 1999, is an independently integrated receptor transducer device, which is capable of providing selective quantitative or semi-quantitative analytical information using a biological recognition element [4]. Essentially it is an analytical device made by a biological recognition element to detect specific analyte integrated with a transducer to convert a biological signal into an electrical signal [5]. The aim of a biosensor is to provide rapid, real-time, accurate and reliable information about the studied analyte [6]. In recent years biosensors acquired a significant analytical role in medicine, agriculture, food safety, homeland security, bio-processing, environmental and industrial monitoring [7]. A biosensor consists of three main elements, a

bioreceptor (antibody, proteins, peptide, nucleic acids, that are able to detect the specific target analyte,), a transducer (device that converts the biomedical signal between analyte and bioreceptor in an electrical or chemical signal), and a signal processing system (it is responsible of signal amplification and data processing), [8]. Figure 1 shows a schematic diagram of the typical components in a biosensor.

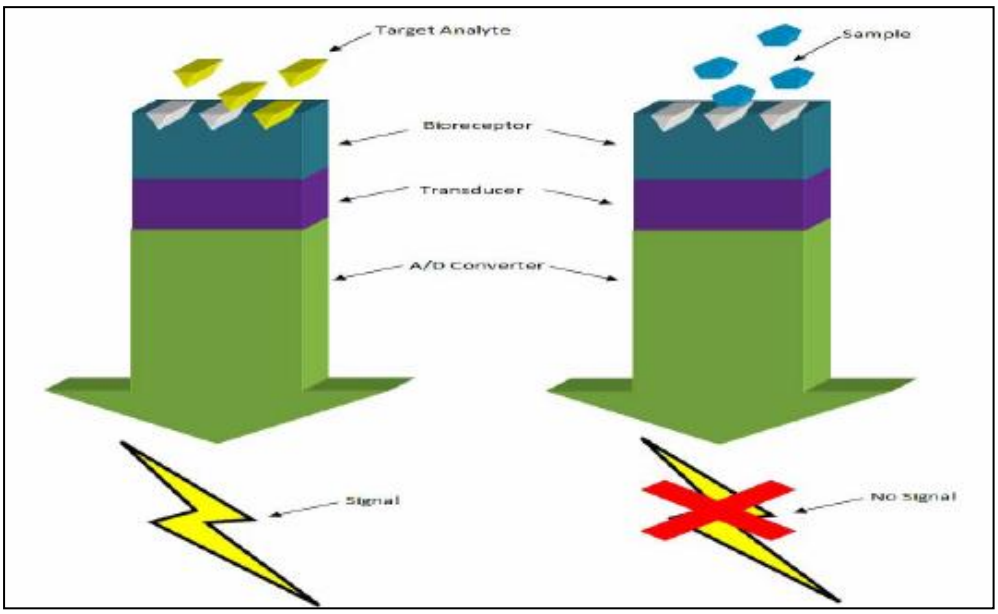

Figure 1.1: Schematic diagram of the typical components in a biosensor.

The first kind of biosensor device was developed in 1967 by Updike and Hicks and it consisted of a molecular recognition element and a transducer. This biosensor was able to detect glucose concentration in the blood basing its functionality on hydrogen peroxide production by glucose oxidase using dissolved oxygen without the aid of mediators and cofactors (Figure 2A). Based on this technology, Yellow Spring Instrument Company, launched the first commercial glucose biosensor in market in 1975 for the direct blood glucose measurement. This kind of device was quickly replaced by a second generation of glucose biosensor that utilized redox mediators to transfer electrons from the enzyme to the working electrode surface (Figure 2B). The use of redox mediators and cofactors eliminated the need of oxygen for electron transfer at the electrode surface overcoming the drawback of limited oxygen pressure observed in the first generation biosensor. In the recent period a third and fourth glucose biosensor generation were developed. The former is based on a direct electron transfer between active centre of enzyme and a carbon nanotube electrode surface (Figure 2C), while the latter is about the use of a non-enzymatic electrode surface such as

active metal micro and nano-particles that mediate oxidation of the adsorbed species (Figure 2D).

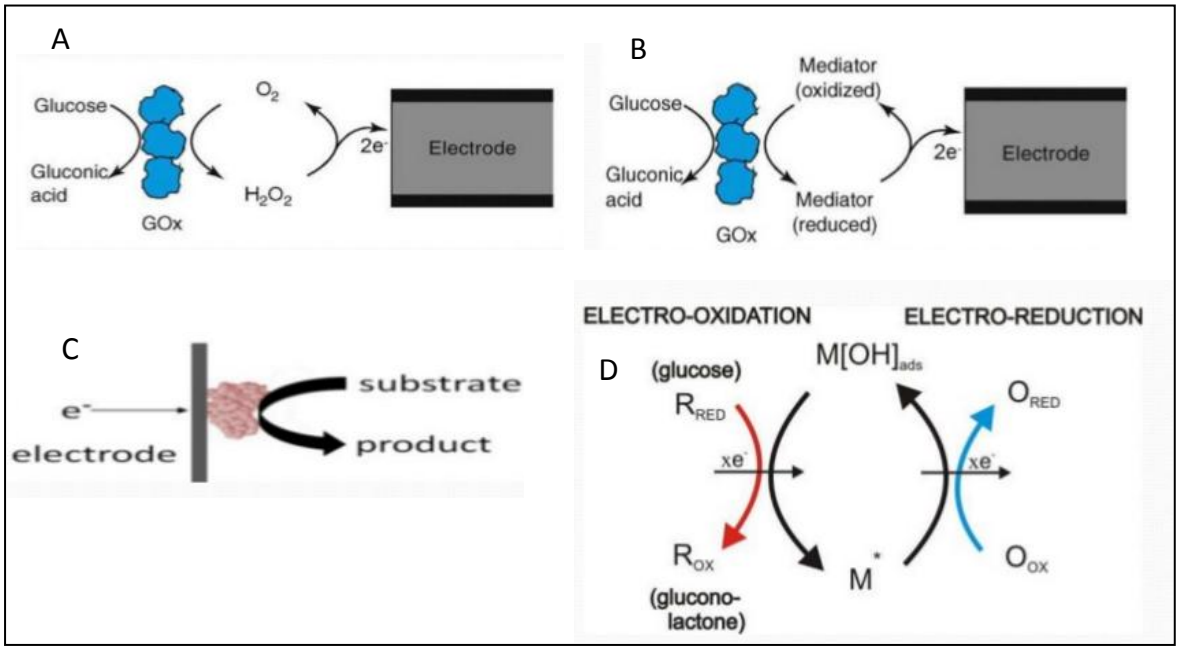

Figure 1.2: Schematic representation of glucose detection biosensors. A) First generation of glucose device made only by analyte and transducer component. Its functionality is based on hydrogen peroxide production by glucose oxidase using dissolved oxygen without the aid of mediators and cofactors. B) The second generation of glucose detection biosensor uses the help of redox mediators to transfer electrons from the enzyme to the working electrode surface, reducing oxygen high pressure observed in the first generation. C) and D) Third and fourth biosensors generation, respectively, based on use of carbon nanotube and metal active micro and nano-particles to a more accurate glucose detection in the blood.

Over the years several techniques have progressively been associated to provide a more accurate detection of target analytes, including different kinds of transducers elements and several biorecognition elements.

1.1.2 Classification of biosensors

Biosensors can be classified on the basis of biological signaling mechanism used or by the type of signal transduction employed. Figure 3 shows the different categories of biosensor.

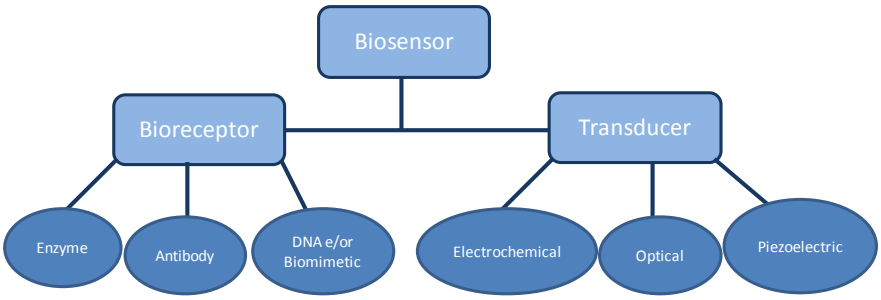

Figure 1.3: Diagram of different categories of biosensors based on bioreceptor and/or transducer element used.

The bioreceptor or biological recognition element is the most important and significant feature of a biosensor. The bioreceptor is the heart of the recognition system of a sensor towards the target analyte. Essentially it is crucial for a bioreceptor to be selective and sensitive towards the specific target in order to prevent the interference by other substance from sample matrix [5]. Generally biosensors can be classified by the type of biological signaling mechanism they utilize. The biological signaling used by biosensors can be divided into three major mechanisms (Figure 3):

Enzyme based sensor: Enzyme based biosensor is the first biosensor introduced by Clark and Lyons in 1962 as an amperometric enzyme electrode for glucose detection in the blood [9]. Since the first biodevice, enzyme based biosensor has a massive growth in usage for various biotechnological applications still present. Enzymes are very efficient biocatalysts, which have the ability to recognize their substrates and to catalyze their transformation in a specific way. These unique properties make the enzymes powerful tools to develop analytical devices [10]. Enzyme-based biosensors associate a biocatalyst-containing sensing layer with a transducer. These devices working primarily on catalytic action and binding capability in order to have a specific analyte detection [8]. The enzyme based biosensors were made of enzyme as bioreceptor which is specific to detect studied analyte from a sample matrix. The lock and key and induced fit hypothesis can apply to explain the mechanism of enzyme action which is highly specific for this type of biosensor. This specific catalytic reaction of the enzyme provides a biosensor with the ability to detect much lower limits than with normal binding techniques. This high specificity of enzyme–substrate interactions and the usually high turnover rates of biocatalysts are the origin of sensitive and specific enzyme-based biosensor devices [10]. Ideally enzyme catalytic action can be influence by several factors such as the concentration of the substrate, temperature, presence of competitive and non-competitive inhibitor and pH [11]. Essentially the Michaelis-Menten equation can be used to further explain the detection limit of enzyme based biosensor [12]. Glucose oxidase

13 (GOD) and horseradish peroxidase (HRP) are the most widely used enzyme based biosensor that has been reported in literature, even if some recent studies have shown that enzyme based biosensor can be used to detect cholesterol, food safety and environmental monitoring, heavy metals and also pesticides [13-17]. Moreover, a recent studies reported the used of an enzyme biosensor with nucleic acid incorporated for DNA detection [18,19].

Immunosensors: An antibodies based biosensor was applied for the first time in the 1950s, opening the doors of immuno-diagnosis [20]. Immunosensors are devices composed by an antigen/antibody as bioreceptor box. An antibody is a 'Y' shaped immunoglobin (Ig) made up of two heavy chains (H) and two light chains (L). However some of human antibodies form dimeric or pentameric structure by utilizing disulphide bonds and an extra protein called the joining or J- chain [21, 22]. Each of the chains has a constant and variable part and this latter one is specific to the antigen that is bound in an highly specific and selective way [23, 20]. The specificity of an antibody towards the binding side of its antigen is a function of its amio acids [24]. Immunosensors play an important role in the improvement of public health in areas such as clinical chemistry, food quality and environmental monitoring thanks their rapid detection, high sensitivity, and specificity properties. The development of immunosensors for bacteria, pathogen and toxins detection opened the doors in the point of care measurement (POC), [25-28]. Some recent studies shown that immunosensor is widely explored toward the detection of cancer/tumor. Because of the traditional diagnostics methods are poor in sensitivity, selectivity and time consuming, immunosensors seem to be promising tools for cancer detection also in its early stages [29].

Nucleic acid sensor: The use of nucleic acids sequences for specific diagnostic applications has developed since the early 1953 and still growing widely [30]. The highly specific affinity binding reaction between two single strand DNA (ssDNA) chains to form double stranded DNA (dsDNA) is utilized in nucleic acids based biosensor . This biosensor works primarily on recognition of the complementary strand by ssDNA to form stable hydrogen bond between two nucleic acids to become dsDNA. For this reason an immobilized ssDNA complementary to the target analyte is used as probe in bioreceptor box. Exposure of target to the probe results in hybridization of complementary ssDNA producing a biochemical reaction that will be amplified and converted in an electrical signal by a transducer. However, literature shows that the present of some linker such as thiol or biotin is needed in the effort to immobilize the ssDNA onto the sensing surface [31, 32]. An important property of DNA is that the nucleic acid ligands can be denatured to reverse binding and the regenerated by controlling buffer ion concentration [12]. DNA based biosensor has potential application in

clinical diagnostic for virus and disease detection [33-35]. In addition, this kind of biosensor possesses a remarkable specificity to provide analytical tools that can measure the presence of a single molecule species in a complex mixture as blood or other biological fluids [36].

Biomimetic sensor: A biomimetic biosensor is an artificial or synthetic sensor that mimics the function of a natural biosensor. These can include aptasensors, where aptamers are the biocomponent used [8]. Aptamers were reported for the first time in the early 1990s and they were described as artificial nucleic acid ligands. They are synthetic strands of nucleic acid that can be designed to recognize amino acids, oligosaccharides, peptides, and proteins. An aptamer has few advantages over antibody based biosensor such as high binding efficiency and avoiding the use of animal that reduces ethical problems. Aptamer properties such as their high specificity, small size, modification and immobilization versatility, regenerability or conformational change induced by the target binding have been successfully exploited to optimize a variety of bio-sensing formats [37]. Aptamer based biosensor has been widely used in various application. Recently great progresses have been made in biomimetics sensor and aptasensor for clinical application [38], including clinical diagnostics to detect pathogen, virus and infectious disease [39-42].

Biosensor are normally categorized according to the transduction method they employ (Figure 3). The transducer plays an important role in the signal detection process. It can be defined as a device that converts a wide range of physical, chemical or biological effects into an electrical signal with high sensitivity and minimum disturbance to the measurement [5]. There are various numbers of transducer methods developed over the decade; but they can be divided in tree big categories: electrochemical, optical and piezoelectric. These groups can be further divided into two general categories; labeled and label free type, which label free type biosensors growing further recently [12].

Electrochemical sensors: Electrochemical biosensors measure the change that results from the interaction between the analyte and the sensing surface of the detecting electrode. The electrical changes can be based on: 1) change in the measured voltage between the electrodes (potentiometric), 2) change in the measured current at a given applied voltage (amperometric), and 3) change in the ability of the sensing material to transport charge (conductometric). Due to their sensitivity, simplicity, low cost and fast response time, these sensors appear more suited for field monitoring applications such as clinical analysis, on-line control processes in industry or environment, and even *in vivo* studies [43,44].

Optical biosensors: Optical sensors transduce a biological event using an optical signal such as absorbance, fluorescence, chemiluminescence, surface plasmon resonance or changes in

light reflectivity [45]. Although are advantageous for screening a large number of samples simultaneously, it is difficult to miniaturize them for insertion into the bloodstream as most optical methods still require sophisticated instruments [44].

Piezoelectric biosensors: Piezoelectric biosensors operate applying an oscillating voltage at a resonance frequency of the piezoelectric crystal and measuring the change in this frequency when the analyte interacts with the crystal surface. Acoustic wave devices, including Surface Acoustic Wave (SAW) and Bulk Acoustic Wave (BAW) are the most common sensors, which bend when a voltage is applied to the crystal. Similarly to optical detection, piezoelectric detection requires large sophisticated instruments to monitor the signal [44].

Piezoelectric biosensors technologies are applied in a wide range of fields for various purposes as environmental, food, clinical and national security uses [46]. Furthermore, pharmaceutical industry requires this kind of biosensors to accelerate the processes of drug discovery and screening. Additionally, public safety has fostered developments in the environmental and food/agricultural industry promoting devices for the detection of pathogens and pollutants in foodstuffs [47].

1.2 Peptide based biosensors

Peptides have been used as components in biological analysis and fabrication of novel biosensors for a number of reasons, including ease of large-scale synthesis, handling, and storage, as well as ready access to multiply modified analogues containing an array of unnatural substituents, highly selectivity for enzymes substrates and low production costs. Bio-conjugation strategies can provide an efficient way to convert interaction information between peptides and analytes into a measurable signal, which can be used for fabrication of novel peptide-based biosensors. Many sensitive fluorophores can respond rapidly to environmental changing their spectral characteristics, hence environmentally-sensitive fluorophores have been widely used as signal markers to conjugate peptides developing the peptide-based molecular sensors. Additionally, nanoparticles, fluorescent polymers, grapheme and near infrared dyes are also used as peptide-conjugated signal markers. Peptides have been utilized as bio-recognition elements to bind various analytes including, proteins, nucleic acid, bacteria, metal ions, enzymes and antibodies in biosensors. The peptides possess the necessary properties as recognition flexibility to adapt sterically to any target, rigidity in secondary structure to converse the binding aptitude and the propensity to form different kinds of non-covalent bonds with potential targets. The recent progresses on microarray

techniques using peptides have facilitated the commercial application of chip-based peptide biosensors in clinical diagnosis.

1.2.1 Peptides as recognition elements

Miniaturized bio-macromolecules offer an alternative strategy to molecular recognition elements with selectivity and affinity properties comparable to their natural compound [48]. In this context, designed short peptides (up to 20 amino acids) are emerging as excellent opportunity for recognition elements development in biosensor field. Short peptides represent a clear option for the design of synthetic receptors for a series of reasons: 1) we can obtained a very high number of different peptides by the combination of the 21 natural amino acids; 2) the availability of both molecular biology and chemical techniques for the fast screening of peptide libraries is less time-consuming; 3) the automated synthesis and purification technologies are much easier than the technologies used for monoclonal antibody preparation; 4) the ease of modifications in a site-specific manner allows for fluorophore coupling and immobilization on solid support; 6) the relatively easy modeling permits more accurate computational studies.

A growing number of peptide-based biosensors systems for different target analytes includes whole cells, proteins, small organic molecule and ions have been reported recently in literature [2].

1.2.2 Selection and synthesis strategies for peptide-based sensors

In the recent years, peptide-based sensors have been developed according to different strategies.

Synthetic design peptides have been designed on the basis of known interactions between single or few amino acids and targets, with attention being paid to the presence of peptide motifs known to allow intermolecular self-organization of the peptides over the sensor surface. Sensitive sensors have been obtained in this way for ions, small molecules and proteins (Figure 4).

Peptides design using computational methods becomes a new and promising way for the rational design of peptide agents targeting specific protein-protein interactions (PPIs). The design is commonly based on bioinformatics methods or molecular modeling techniques, indirectly exploiting structure-activity relationship at the level of peptide sequence or directly deriving lead entities from protein complex architecture [49].

Short peptides from random phage display have been selected in a random way from large, unfocussed, and often preexisting and commercially available libraries with no design

element. Such peptides often perform better that antibodies, but they are difficult to select when the target is a small molecule because often it has no reactive groups for solid support immobilization.

Peptide receptors for ligand sensing are artificial, miniaturized receptors obtained from reduction of the known sequence of a natural receptor down to a synthesizable and yet stable one.

Finally, **peptide ligands for receptor sensing** are short peptides that have been used as active elements for the detection of their own natural receptors. The identification of these natural peptide ligands for cell-surface elements, transmembrane proteins, antibodies, and enzymes provides a good challenge for biosensor development in bacteria and virus detection field. [2].

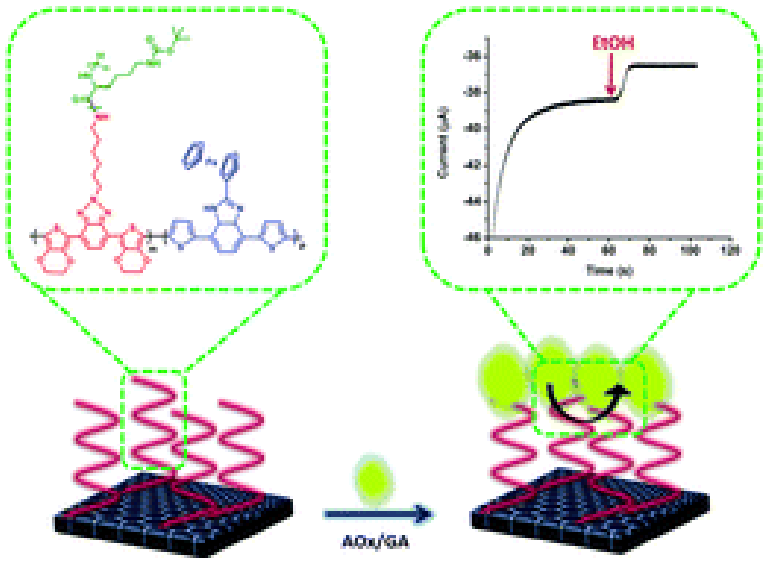

Figure 1.4: Ethanol biosensors based on conducting polymers with peptide and ferrocene on the side chain [50].

1.2.3. Peptide-based fluorescent biosensors

The development of peptide-based sensors over the last two decades has had a considerable success in biotechnology field.

Fluorescent techniques, due to their high sensitivity, selectivity, fast response time, flexibility and experimental simplicity are the key of this approach. FRET (Fluorescence Resonance Energy Transfer) effects or environment-sensitive fluorophore provide reliable design strategies that can be safely implemented to study virtually any biological interaction with minimal efforts [51].

Environment-sensitive fluorophores (Figure 5) are molecules that display emission responsive properties to the chemical surrounding [51]. Physiochemical changes include pH, viscosity, biological analytes and solvent polarity. By conjugating these probes to a molecule (i.e. protein), it is possible to obtain valuable information regarding the state of a protein with high spatial and temporal resolution [52].

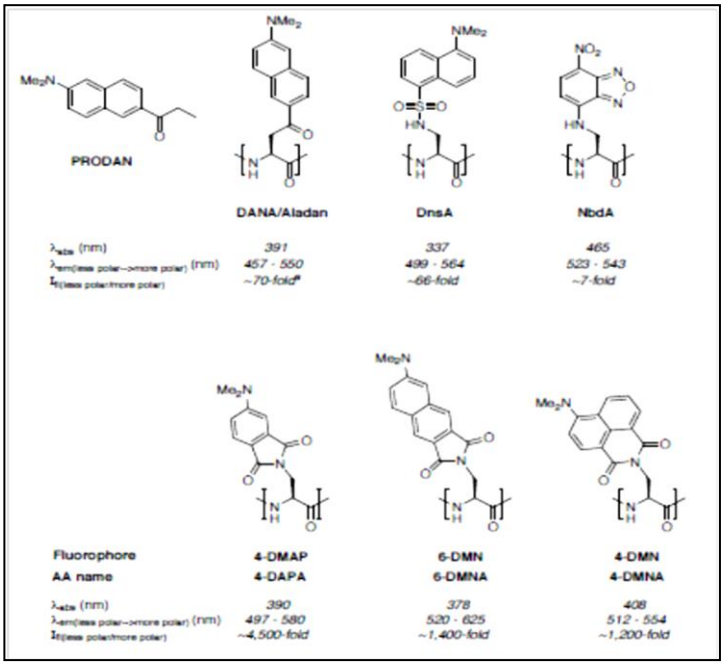

Figure 1.5: Comparison of some environment-sensitive fluorophores and their solvachomatic properties [43]. Abbreviations: 4-DMNA: 4-(N,Ndimethylamino) naphthalimide alanine, 6-DMNA: 6-(N,N-dimethylamino)-2,3-naphtalimide alanine, DANA/Aladan: 6-(2-dimethylamino)-naphthoyl alanine, 4-DAPA: 4-(N,N-dimethylamino)-phalimido alanine, 4-DMAP: 4-(N,N-dimethylamino) phthalimide, DnsA: Dansyl alanine, TAMRA: 5-(and-6)carboxytetramethyl rhodamine, 6-DMN: 6-dimethylamino-1,8-naphthalimide, 4-DMN: 4-dimethylamino-1,8-naphthalimide, NbdA: 7-nitrobenzo-2-oxa-1,3-diazole.

Two main strategies for covalent incorporation of a fluorophore in the peptide can be distinguished. The first one involves post-synthetic coupling at the N-terminal or at the side chains of cysteines or lysines. The second one uses unnatural fluorescent amino acids for peptide synthesis [53]. However the insertion of the fluorophore is restricted topologically to sites in the protein that preserve function and activity while permitting the dye to make necessary contacts that result in measurable fluorescence changes. This consideration

necessitates the use of methods that offer precise control over dye placement within peptide, with minimal perturbation [52].

The Figure 1.6 illustrates the general principle of a fluorescent peptide biosensor, while Table 1 summarizes environmentally sensitive peptide biosensors.

Fluorescent sensor peptides have proven useful in a number of applications, ranging from analyte detection to elucidation PPIs. It is expected that their general applicability with respect to analyte quantification will be expanded by combining combinatorial methods for peptide design with further improvements of fluorophores and fluorescent amino acids in terms of sensitivity to environmental changes [53].

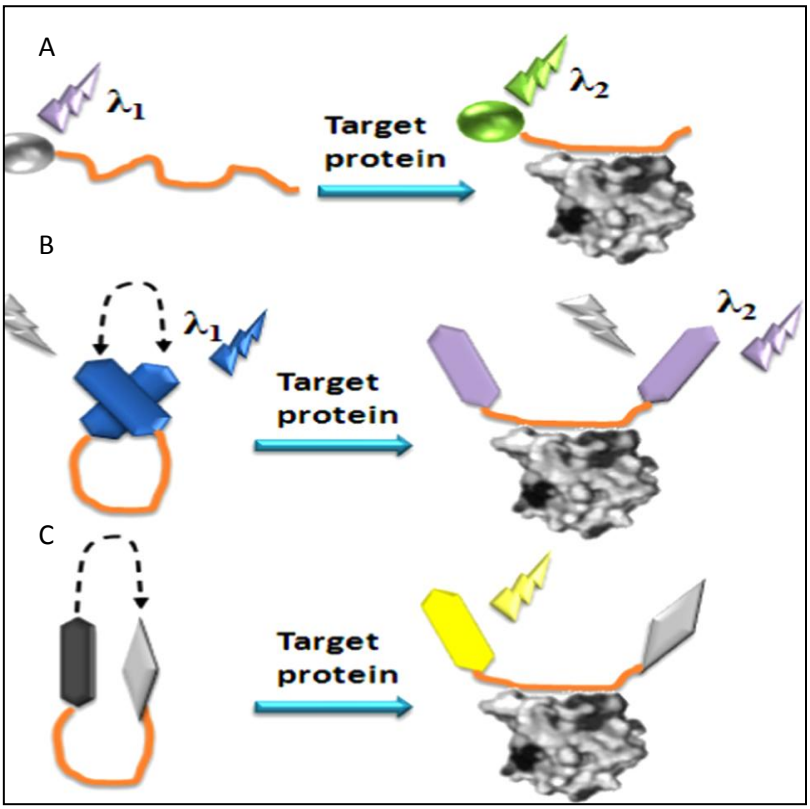

Figure 1.6: Schematic representation of a fluorescent peptide biosensor. A) Peptide probe with environment-sensitive fluorophores assignal markers to respond to the target protein; (B)excimer-pair peptide sensor,the peptide binds to the target protein,changing the spectral property of the fluorophores;(C)FRET/probe–quencher pair peptidesensor,where the distance between the donor–acceptor/probe–quencher was changed by binding of the peptide to the protein.

Table 1: Selected environmentally sensitive peptide biosensors [44].

ANALYTE	RECEPTORS	FLUOROPHORE
DNaK chaperone	Targeting sequence of precursor of aminotransferase	Acrylodan
Cholecystokinin (CCK) receptor	Peptides agonist of the CCK receptor	Alexa 488
α-amilase	Library of designed loop peptides	Fluorescein
Calmodulin	Library of designed α-helical peptides	TAMRA
Double-stranded DNA	Polypeptide derived from the Hin recombinase of *Salmonella typhimurium*	Oxazole yellow
Opioid-receptor	Opioid antagonist	DANA (Aladan)
Class II MHC proteins	HLA-DR-binding peptides	4-DAPA and 6-DMNA

1.3 Conclusions and outlook

The past decade has seen great advancements in the field of biosensor along many fronts. This dynamic tool has been applied in many area of life science research, health care, environmental, food and military application [6]. Biosensor technology seems to be a promising candidate for lower detection limit with rapid analysis time at relatively low cost. Technological advances have brought up use of materials as supports to construct biochip which integrated microfluidic system, probe, sampler, detector, amplifier and logic circuitry. This biochip could be a promising candidate for label free, reagentless, real time monitoring, miniaturization and low cost application. For medical application, this cost advantage will allow the development of extremely low cost, disposable biochips that can be used for in-home medical diagnostics of diseases without the need of sending samples to a laboratory for analysis which time consuming [6].

The main aim of the thesis is the development of different miniaturized biosensors and microdevices based on peptides for food industry and healthcare.

Aim and Outline of the Thesis

Molecular recognition events are some of the most significant features of biological and chemical systems. The biomolecular recognition is the ability of a biomolecule to interact selectively with another molecule even in the presence of structurally similar antagonist molecules [1]. Molecular recognition is fundamental for biosensing technique. A biosensor,

according to IUPAC recommendations 1999, is an independently integrated receptor transducer device, which is capable of providing selective quantitative or semi-quantitative analytical information using a biological recognition element [2]. A biosensor consists of three main elements, a bioreceptor (antibody, proteins, peptide, nucleic acids, that are able to detect the specific target analyte,), a transducer (device that converts the biomedical signal between analyte and bioreceptor in an electrical or chemical signal), and a signal processing system (it is responsible of signal amplification and data processing), [8]. The bioreceptor or biological recognition element is the most important and significant feature of a biosensor. The bioreceptor is the heart of the recognition system of a sensor towards the target analyte. Essentially it is crucial for a bioreceptor to be selective and sensitive towards the specific target in order to prevent the interference by other substance from sample matrix [5]. Peptides have been used as components in biological analysis and fabrication of novel biosensors for a number of reasons, including mature synthesis protocols, highly selectivity for enzymes substrates and low production costs [1]. Bio-conjugation strategies can provide an efficient way to convert interaction information between peptides and analytes into a measurable signal, which can be used for fabrication of novel peptide-based biosensors [1]. Peptides are formed by natural or synthetic amino acids which are linked by peptide bonds with shorter lengths than those of proteins [1]. Peptides have the same building block as proteins, so they may be possible substitutes for proteins in biological analysis [1]. Peptides can be obtained by screening and optimization of artificial peptide libraries and they can provide high affinity to a specific target. In addition, they have a lot of advantages than proteins, including: high chemical and conformational stability, standard synthetic protocol, easy modification and large chemical versatility [1]. For all of these reasons they are chosen as capture agents in the development of our biosystems. Following the outline of the thesis is reported with a brief description of each chapter. The first part of the thesis presents an introduction to the principles of biosensors science and their potential applications in the food, agricultural industries and biomedical fields. Furthermore, peptides based biosensors are presented with a description of their properties, features and advantages. The use of peptides as capture agents and the possibility to exploit their reversibility in biological applications, despite proteins and antibodies, is still very limited and has not been addressed yet. This aspect has been investigated in this first chapter. In **Chapter 2** microfluidic synthesis of novel polymeric microparticles endowed with specific peptide due to its superior specificity for target binding in complex media, is reported. In more details, a peptide sequence is efficiently encapsulated into the polymeric network and protein binding occurred with high affinity (K_D 0.1-0.4 μM).

Fluidic dynamics simulation is performed to optimize the production conditions for monodisperse and stable functionalized microgels. The results demonstrate the easy and fast realization, in a single step, of functionalized monodisperse microgels using droplet-microfluidic technique, and how the inclusion of the peptide within polymeric network improves both the affinity and the specificity of protein capture. In **Chapter 3** the development of a peptide-based biosensor for autofluorescence aflatoxin M1 detection in a sensitive, specific and unsophisticated manner, is reported. To this aim an integrated approach has been developed to select specific peptide motif to capture aflatoxin M1. The integrated approach provides a combination of computation modeling with combinatorial peptide synthesis to screen the sequence with the highest affinity. Peptides sequences selected by the proposed approach have been easily co-polymerized in PEGDA microparticles opening the route towards a direct detection of aflatoxins in small volume both in liquid and solid environments. Such approach can be applied also to other small molecules to develop materials able to sequestrate the target analytes allowing their direct detection directly in the materials. Finally in **Chapter 4** a microdevice for endometriosis diagnosis is developed. In this work, three different peptides (CRP-1, VEGF-114 and ΦG6) are used as capture agents to detect serum levels of vascular endothelial growth factor (VEGF), tumor necrosis factor-alpha (TNF-a), and C-reactive protein (CRP): three serum markers of endometriosis in menstrual blood. The selected peptides have been covalently immobilized on a microfluidic PDMS device, previously derivatized with 10% of PAA (Poly(acrylic acid)) solution. The so built device has been used to capture and recognize endometriosis markers both in buffer and biologic fluids matrices such as human serum with a good specificity and sensitivity.
So the aim of the studies in this work, is to set up miniaturized microdevices that can be used in healthcare and food industry, using peptides as capture agents in order to have sensitive but not invasive and not expansive biosensors.

.

References

[1] De Corcuera J.I.R., and Cavalieri, R.P., Biosensors. Encyclopedia of Agricultural, Food, and Biological Engineering 2007,Dec; 13, DOI: 10.1081/E-EAFE 120007212.

[2] Pavan S., Berti F., Short peptides as biosensor transducers. Anal Bioanal Chem 2012, 402(10):3055-3070.

[3] Tewari A.K., Dubey R., Emerging trends in molecular recognition: Utility of weak aromatic interactions. Bioorg Med Chem 2008 16:126-143.

[4] Thevenot D.R., Toth K., Durst R.A., Wilson G.S., Electrochemical Biosensors Recommended defnitions and classification. Pure Appl Chem 1999, 71: 2333–2348.

[5] Lowe R.S., Overview of Biosensor and Bioarray Technologies. In Marks R.S., Lowe C.R., Cullen D.C., Weetall H.H., Karube I (ed): Handbook of Biosensors and Biochips. Wiley, Weinheim 2007.

[6] Perumal V. and Hashim U., Advances in biosensors: Principle, architecture and applications. Journal of Applied Biomedicine 2014 Jan; 26.

[7] Luong J.H.T., Male K.B., Glennon J.D., Biosensor technology: Technology push versus market pull. Biotechnol. Adv. 26: 492–500, 2008.

[8] Homola J., Yee S.S., Myszka D., Surface plasmon resonance biosensors. In Ligler F, Taitt C 23 (ed): Optical biosensors: today and tomorrow. Elsevier, Amsterdam 2008, pp. 185-242.

[9] Shantilatha R., Varma S., Mitra C.K, Designing a simple biosensor. In Biosensors: Perspectives. In Malhotra BD, Turner APF (ed): Advances In Biosensors: Perspectives In Biosensor. JAI Press, Stamford 2003, pp. 1-36.

[10] Leca-Bouvier B.D., Blum L.J., Enzyme for Biosensing Applications. In Zourob M (ed): Recognition receptors in biosensors. Springer, New York 2010, pp. 177-220.

[11] Cass T. Enzymology. In Marks R.S., Lowe C.R., Cullen D.C., Weetall H.H., Karube I (ed):Handbook of Biosensors and Biochips. Wiley, Weinheim 2007.

[12] Parkinson G and Pejcic B. Using Biosensors to Detect Emerging Infectious Diseases, prepared for The Australian Biosecurity Cooperative Research Centre: pp.1-80, 2005. Retrieved from: http://www.abcrc.org.au/pages/project.aspx?projectid=75.

[13] Amine A., Mohammadi H., Bourais I., Palleschi G., Enzyme inhibition-based biosensors for food safety and environmental monitoring. Biosens Bioelectron. 21: 1405–1423, 2006.

[14] Zapp E., Brondani D., Vieira I.C., Scheeren C.W., Dupont J., Barbosa A.M.J.., Ferreira VS., Biomonitoring of methomyl pesticide by laccase inhibition on sensor containing

platinum nanoparticles in ionic liquid phase supported in montmorillonite. Sens Actuators B Chem. 155: 331–339, 2011.

[15] Nomngongo P.N., Catherine Ngila J., Msagati T.A.M., Gumbi B.P., Iwuoha E.I., Determination of selected persistent organic pollutants in wastewater from landfill leachates, using an amperometric biosensor. Phys Chem Earth Pt A/B/C. 50-52: 252–261, 2012.

[16] Soldatkin O.O., Kucherenko I.S., Pyeshkova V.M., Kukla A.L., Jaffrezic-Renault N., El'skaya A.V., Dzyadevych S.V., Soldatkin A.P., Novel conductometric biosensor based on three enzyme system for selective determination of heavy metal ions. Bioelectrochemistry. 83: 25–30, 2012.

[17] Ju H., and Kandimalla V.B., Biosensors for pesticides. In Zhang X, Ju H, Wang J (ed): Electrochemical Sensors, Biosensors and Their Biomedical Applications. Elsevier, San Diego 2008, pp. 32-50.

[18] He Y, Zhang S., Zhang X., Baloda M., Gurung A.S., Xu H., Zhang X., Liu G., Ultrasensitive nucleic acid biosensor based on enzyme-gold nanoparticle dual label and lateral flow strip biosensor. Biosens Bioelectron. 26: 2018–2024, 2011.

[19] Lin L., Liu Q., Wang L., Liu A., Weng S., Lei Y., Chen W., Lin X., Chen Y., Enzyme-amplified electrochemical biosensor for detection of PML-RARα fusion gene based on hairpin LNA probe. Biosens. Bioelectrons. 28: 277–83, 2011.

[20] Donahue AC and Albitar M,. Antibodies in Biosensing. In Zourob M (ed): Recognition 25 receptors in biosensors. Springer, New York 2010, pp. 221-248.

[21] Wood, P. Understanding Immunology. Pearson Education Limited, Dorchester 2006.

[22] Pohanka M., Monoclonal and polyclonal antibodies production-preparation of potent biorecognition element. J Appl Biomed. 7: 115–121, 2009.

[23] Conroy P.J., Hearty S., Leonard P., O'Kennedy R.J., Antibody production, design and use for biosensor-based applications. Semin Cell Dev Biol. 20: 10–26, 2009.

[24] Fowler J.M., Wong D.K.Y., Halsall H.B., Heineman W.R., Recent developments in electrochemical immunoassays and immunosensors. In Zhang X, Ju H, Wang J (ed): Electrochemical Sensors, Biosensors and Their Biomedical Applications. Elsevier, San Diego 2008, pp. 115-140.

[25] Skottrup P.D., Nicolaisen M., Justesen A.F., Towards on-site pathogen detection using 2 antibody-based sensors. Biosens Bioelectron. 24: 339–348, 2008.

[26] Barton A.C., Collyer S.D., Davis F., Garifallou G.Z., Tsekenis G., Tully E., O'Kennedy R.,Gibson T., Millner P.A., Higson S.P.J. Labeless A.C., Impedimetric antibody-based sensors with pgml(-1) sensitivities for point-of-care biomedical applications. Biosens Bioelectron. 24: 1090–1095, 2009.

[27] Braiek M., Rokbani K.B., Chrouda A., Bakhrouf B.A., Maaref A., Jaffrezic-Renault N. An Electrochemical Immunosensor for Detection of Staphylococcus aureus Bacteria Based on Immobilization of Antibodies on Self-Assembled Monolayers-Functionalized Gold Electrode. Biosensors. 2: 417–426, 2012.

[28] Holford T.R.J., Davis F., Higson S.P.J., Recent trends in antibody based sensors. Biosens Bioelectron. 34: 12–24, 2012.

[29] Ushaa S.M., Nagar N.I., Rao G.M., Design and analysis of nanowire sensor array for prostate ancer detection. Int J Nano Biomater. 3: 239–255, 2011.

[30] Liu A., Wang K., Weng S., Lei Y., Lin L., Chen W., Lin X., Chen., Development of electrochemical DNA biosensors. Trends. Anal. Chem. 37: 101–111, 2012.

[31] Cagnin S., Caraballo M., Guiducci C., Martini P., Ross M., Santaana M., Danley D., West T.,Lanfranchi G.,Overview of electrochemical DNA biosensors: new approaches to detec the expression of life. Sensor. 9: 3122–3148, 2009.

[32] Lazerges M., Perrot H., Rabehagasoa N., Compère C., Thiol- and Biotin-Labeled Probes for Oligonucleotide Quartz Crystal Microbalance Biosensors of Microalga Alexandrium

Minutum. Biosensors. 2: 245–254, 2012.

[33] Chua A., Yean C.Y., Ravichandran M., Lim B., Lalitha P., A rapid DNA biosensor for the molecular diagnosis of infectious disease. Biosens Bioelectron. 26: 3825–3831, 2011.

[34] Liu C.C., Electrochemical Based Biosensors. Biosensors. 2: 269–272, 2012.

[35] Thuy N.T., Tam P.D., Tuan M.A., Le A.T., Tam L.T., Thu V.V., Hieu N.V., Chien N.D.,Detection of pathogenic microorganisms using biosensor based on multi-walled carbon nanotubes dispersed in DNA solution. Curr Appl Phys. 12: 1553–1560, 2012.

[36] Brett A.M.O., DNA based biosensors. In Gorton L (ed): Comprehensive Analytical Chemistry XLIV: Biosensors and Modern Biospecific Analytical Techniques. Elsevier, Amsterdam 2005, pp. 179-208.

[37] Schneider H.J., Lim S., Strongin R.M., Biomimetic Synthetic Receptors as Molecular Recognition Elements. In Zourob M (ed): Recognition receptors in biosensors. Springer, New York 2010, pp. 777-818.

[38] Vallet-Regí M and Arcos DA., Biomimetic Nanoceramics in Clinical Use: From Materials to Applications. RSC publishing, Cambridge 2008.

[39] Strehlitz B., Nikolaus N., Stoltenburg R., Protein Detection with Aptamer Biosensors. Sensors. 8: 4296–4307, 2008.

[40] Torres-Chavolla E., Alocilja E.C., Aptasensors for detection of microbial and viral pathogens., Biosens Bioelectron. 24: 3175–3182, 2009.

[41] Wang Y., Zhang Z., Jain V., Yi J., Mueller S., Sokolov J., Liu Z., Levon K., Rigas B., Rafailovich M.H., Potentiometric sensors based on surface molecular imprinting: Detection of cancer biomarkers and viruses. Sens Actuators B Chem. 146: 381–387, 2010.

[42] Weng C.H., Huang C.J., Lee G.B., Screening of Aptamers on Microfluidic Systems for Clinical Applications. Sensors. 12: 9514–9529, 2012.

[43] Dixon, B. M., Lowry, J. P., & D O'Neill, R. (2002). Characterization in vitro and in vivo of the oxygen dependence of an enzyme/polymer biosensor for monitoring brain glucose. Journal of Neuroscience Methods, 119(2), 135-142.

[44] Luong, J. H., Male, K. B., & Glennon, J. D. (2008). Biosensor technology: technology push versus market pull. Biotechnology advances, 26(5), 492-500.

[45] Fan, X., White, I. M., Shopova, S. I., Zhu, H., Suter, J. D., & Sun, Y. (2008). Sensitive optical biosensors for unlabeled targets: A review. analytica chimica acta, 620(1), 8-26.

[46] Kryscio, D. R., & Peppas, N. A. (2012). Critical review and perspective of macromolecularly imprinted polymers. Acta biomaterialia, 8(2), 461-473.

[47] Terry, L. A., White, S. F., & Tigwell, L. J. (2005). The application of biosensors to fresh produce and the wider food industry. Journal of agricultural and food chemistry, 53(5), 1309-1316.

[48] Cooper, W. J., & Waters, M. L. (2005). Molecular recognition with designed peptides and proteins. Current opinion in chemical biology, 9(6), 627-631.

[49] Zhou P., Wang C., Ren Y., Yang C., Tian F., Computational peptidology: a new and promising approach to therapeutic peptide design. Curr Med Chem. 2013;20(15):1985-96

[50] Kesik M., Akbulut H., Söylemez S., Cevher S.C., Hızalan G., Udum Y.A., Endo T., Yamada S., Çırpan A., Yağc Y. Toppare L., Synthesis and characterization of conducting polymers containing polypeptide and ferrocene side chains as ethanol biosensors. Polym. Chem., 2014, 5, 6295-6306.

[51] Pazos, E., Vazquez, O., Mascarenas, J. L., & Vazquez, M. E. (2009). Peptide-based fluorescent biosensors. Chemical Society Reviews, 38(12), 3348-3359.

[52] Loving, G. S., Sainlos, M., & Imperiali, B. (2010). Monitoring protein interactions and dynamics with solvatochromic fluorophores. Trends in biotechnology, 28(2), 73-83

[53] Choulier, L., & Enander, K. (2010). Environmentally sensitive fluorescent sensors based on synthetic peptides. Sensors, 10(4), 3126-3144.

Chapter 2

Functionalized poly(ethylene glycol) diacrylate microgels by microfluidics: in situ peptide encapsulation for in serum selective protein detection

ABSTRACT. Polymeric microparticles represent a robustly platform for the detection of clinically relevant analytes in biological samples; they can be functionalized encapsulating a multiple types of biologics entities, enhancing their applications as a new class of colloid materials. Microfluidic offers a versatile platform for the synthesis of monodisperse and engineered microparticles. In this work, we report microfluidic synthesis of novel polymeric microparticles endowed with specific peptide due to its superior specificity for target binding in complex media. A peptide sequence was efficiently encapsulated into the polymeric network and protein binding occurred with high affinity (K_D 0.1-0.4 μM). Fluidic dynamics simulation was performed to optimize the production conditions for monodisperse and stable functionalized microgels. The results demonstrate the easy and fast realization, in a single step, of functionalized monodisperse microgels using droplet-microfluidic technique, and how the inclusion of the peptide within polymeric network improves both the affinity and the specificity of protein capture.

The work described in this Chapter has been submitted for publication: Giorgia Celetti, Concetta Di Natale, Filippo Causa, Edmondo Battista, Paolo A. Netti: "*Functionalized poly(ethylene glycol) diacrylate microgels by microfluidics: in situ peptide encapsulation for in serum selective protein detection".*

2.1 INTRODUCTION

In the recent years, hydrogels-based technologies has been widely developed for a range of biotechnology applications including diagnostic [1-3], drug delivery [4,5], and tissue engineering [6,7]. Due to their biocompatible and highly tunable nature they represent ideal candidates for biosensing applications. Their microstructure and interfacial proprieties can also be rendered responsive to various stimuli through chemical and physical cues resulting in "smart" materials which can respond to their local environment [9]. In particular, hydrogels can be engineer with different biological entities such as nucleic acids or peptides [5] for capture and detection of proteins, DNA, mRNA and microRNA [10]. Hydrogels are typically prepared and processed as bulk materials such as monolithic structures or supported films. However, emerging applications require miniaturization and tailoring of hydrogel architecture at increasingly small length scales for delivery and transport purposes in microscopic environments. This has spurred the development of various processes for the synthesis of colloidal and microparticle hydrogels, or "microgels" [9]. Hydrogel microparticles have been suggested as diagnostic tools for the rapid, multiplexed screening of biomolecules due to their advantages in detection and quantification [11-13]. Compared to traditional planar arrays, particle-based arrays offer easier probe-set modification, more efficient mixing steps, and higher degrees of reproducibility [14]. However appropriate methods for achieving the functionalization of large microparticles have not yet been developed [15].

Among the various approaches for synthesizing hydrogel microparticles, microfluidics represent one of the most promising methods for the production and the functionalization of monodisperse microgels, including droplet microfluidics [16-18] and flow lithography [18]. In particular, droplet microfluidics facilitates fabrication of spherical microparticles (i.e., microspheres) or microparticles with complex chemical compositions [18], and potentially enables higher throughput synthesis [19]. Prior reports have demonstrated the ability of microfluidic-based platforms to synthesize, functionalize and encode microparticles with multiple bioactive agents [18,20,21], in a single step, overcoming the conventional emulsion polymerization methods [9]. Here we present a novel droplet microfluidics method that allows an easy and fast functionalization of polymeric microparticles for selective biomolecules detection in complex biologic matrix.

Due to its biocompatibility and low-biofuling properties poly(ethylene glycol) (PEG) has been widely used for hydrogels particles-based assays [10]. Various approaches have explored PEG's utility as biosensor platform including direct physical entrapment [22] or covalently linking the biomolecules to the polymer network [23].

Most of the validated detection strategies use monoclonal antibodies as target recognition moieties, however the use of these large macromolecules has several limitations, including poor stability and high production costs [24,25]. Contrariwise, small molecules like peptides can be prepared synthetically and mimic the antibody binding site by using only a small cluster of residues, even though with lower affinity and specificity toward biomolecule target [26]. Hydrogel networks endowed with bioactive peptides have been already reported for applications such as tissue engineering, where short peptide sequences were demonstrated to elicit specific cell functions or change the materials network upon specific cell responses [27]. However, the capability of hydrogel microparticles, functionalize with a small molecules in a single step, to increase the affinity and the specificity of a protein capture has not yet been explored.

In this work, we use droplet microfluidics for one step synthesis of monodisperse and stable micrometer poly(ethylene glycol) diacrylate (PEGDA) hydrogels, in which label Strep-tagII peptide sequence was incorporated in order to create a functional microparticles for selective protein detection in complex fluid (Figure 1). Droplet-microfluidics was used to produce water in oil emulsion in which reactive and label peptide was included directly in flow, eliminating the need for costly and time-consuming labeling steps. Computational fluidic dynamics simulation (CFD) was used to optimize the design of the device investigating the parameters that influence droplet formation. After UV polymerization the capability of PEGDA-peptide microgels to detect Streptavidin protein in buffer and in complex biological medium was demonstrated by confocal and fluorescence spectroscopy methods. This tool-system promises to be useful for producing a novel, efficient and sensitive polymeric microparticles to detect bio-molecular targets with higher affinity in complex medium.

Figure 2.1: Schematic representation of Strep-tagII microgels synthesis able to detect Streptavidin protein in human serum. Such approach includes: phase modeling; microfluidic fabrication and validation; and assay validation for selective protein detection.

2.2 MATERIALS AND METHODS

2.2.1 Materials

Poly(ethylene glycol) diacrylate (PEGDA, 700 MW), the non polar solvent light mineral oil and the nonionic detergent sorbitan monooleate (Span 80) were purchased from Sigma Aldrich. Crosslinking reagent Darocur 1173 was purchased from Ciba. Reagents for peptide synthesis (Fmoc-protected amino acids, resins, activation, and deprotection reagents) were purchased from Iris Biotech GmbH (Waldershofer Str. 49-51 95615 Marktredwitz, Deutschland) and InBios (Naples, Italy). Solvents for peptide synthesis and HPLC analyses and Streptavidin ATTO-425 were purchased from Sigma-Aldrich; reversed phase columns for peptide analysis and the LC–MS system were supplied respectively from Agilent Technologies and Waters (Milan, Italy). Pooled human serum from healthy donors was supplied by Lonza (Life Technology Ltd, Paisley, UK). All chemicals were used as received.

2.2.2 Microfluidic device

Microfluidic device consists of two inlets for the continuous and disperse phase, a narrow orifice in which the main channel and the two opposite channels converge, and a serpentine in which droplets were polymerized. The dimensions of the device are 50 × 35 µm (width × depth) for the channels solutions, 35 × 35 µm at the junction (width × depth); the serpentine is 10 cm long. The microfluidic device was fabricated by combining the conventional photolithographic and soft-lithographic techniques. Briefly, negative photoresist (Mr-DWL 40 phtoresist, Microresist technology) was spun onto a silicon wafer at 2000 rpm for 30 s to make a 35 µm thick layer of photoresist. Then, the photoresist was baked and subsequently

exposed using DWL 66 Fs LASER technology system (Heidelberg instruments). After the exposed sample had been post-baked and developed, the microfluidic flow focusing device master was prepared. The surface of the device mold was treated with tridecafluoro-1,1,2,2-tetrahydrooctyl-1-trichlorosilane to facilitate the peeling off of the polydimethyl-siloxane (PDMS, Sylgard 184, Dow Corning) replica. PDMS (10:1 polymer to curing agent) was poured on the patterned silicon wafer containing negative-channels. The PDMS-based microfluidic device was peeled off from the wafer and bonded on a glass slide with oxygen plasma treatment.

2.2.3 CFD simulation

To optimize the design of the device, computational fluid dynamics simulations were performed using COMSOL Multiphysics 4.2b software. During the simulation, all geometries were created two-dimensional based on the dimensions of the designed microfluidic device. A two-dimensional model was chosen to reduce complexity and computation time. The momentum and mass balances were modeled by Navier-Stokes equations and the level set method (LSM) was used to model the two phases. The principle on which LSM is based is the assignment of a so-called level set function $\Phi(x, t)$ to the space occupied by an interface, where x denotes the co-ordinates of a point within that space at a time t. The function is initialized at time t_0, and then a numerical scheme is used to approximate the value of $\Phi(x, t)$ over small time increments, thus enabling the propagation of the interface to be tracked in time. The interface is represented by the zero contour of the level set function Φ. $\Phi > 0$ on one side of the interface and $\Phi < 0$ on the other. The level set function is chosen such that the position of the water–oil interface is described by the 0.5 contour of the level set function Φ and for $\Phi > 0.5$ the break off occurs and the droplet is formed.(Dendukuri and Doyle 2009) Channel geometries were meshed using the free meshing tool and the channel walls were specified as wetted walls with a constant contact angle, measured experimentally using the instrument Contact Angle CAM 200. The interfacial tension between the continuous phase and the prepolymer solution was changed from 4.27 to 1.68 mN/m to investigate the influence of the surface tension (γ) on the droplet sizes. In particular, three prepolymer solutions of PEGDA (20, 40, 60 *wt* %) and three oil solutions (with 5, 10, 15 % of surfactant) were chosen and for each PEGDA/oil solutions γ was measured by pendant drop CAM 200. The viscosity of the two fluids was measured with 50 mm flat-plate geometry by rheometer.

2.2.4 Microgel synthesis

Microgels were synthesized using light mineral oil containing nonionic surfactant Span 80 (5 wt%) as a continuous phase and poly(ethylene glycol)diacrylate (PEGDA) (20 wt%) with photoinitiator (0.1 wt%) and Strep-tagII-FITC (0.5 mg/mL) as disperse phase. Droplet emulsions were formed injecting prepolymer solution, disperse phase, through the central channel and oil solution, continuous phase, through two opposite side channels. The uniform PEGDA-peptide droplets were crosslinked in flow to form monodisperse microgels. To photopolymerize droplets DAPI microscopy filter (9.8 mW, λ=360 nm) was used, focusing the UV light on the serpentine and regulating the diaphragm aperture of the microscope, for 15 s. After photopolymerization, microgels were collected in an eppendorf and washed three times with a solution of ethanol (35 v/v%) and acetone (10 v/v%) to remove the oil. After washing, microgels containing Strep-tagII-FITC were analyzed by confocal microscopy. Polyethylene tubes were connected to the inlets and outlets and the solutions were injected using high-precision syringe pumps (neMesys-low pressure) to ensure a reproducible, stable flow. This system was mounted on an inverted microscope (IX 71 Olympus) and the droplets formation was visualized using a 4× objective and recorded with a CCD camera Imperx IGV-B0620M.

2.2.5 Peptide synthesis

Strep-tagII-peptide ((WSHPQFEKD(OAll))) synthesis was performed on a fully automated multichannel peptide synthesizer Biotage® Syro Wave™. Preparative RP-HPLC was carried out on a Waters 2535 Quaternary Gradient Module, equipped with a 2489 UV/Visible detector and with an X-Bridge^{TM} BEH300 preparative 10× 100 mm C18, 5μm column. LC–MS analyses were carried out on an Agilent 6530 Accurate-Mass Q-TOF LC/MS spectrometer. Zorbax RRHD Eclipse Plus C18 2.1 x 50 mm, 1.8 μm columns were used for the analyses. The Strep-tagII-peptide was synthesized in the acetylated/amidate version, employing the solid phase method on a 50 μmol scale following standard Fmoc strategies. Rink-amide resin (substitution 0.45 mmol/g) was used as solid support. Activation of amino acids was achieved using HBTU/HOBt/DIPEA (1:1:2). All couplings were performed for 15 min and deprotections for 10 min. To monitor peptide entrapment, Lysine side chain amine fluorescein labeling was achieved by on-resin treatment with fluorescein isothiocyanate (FITC) after removing methyltrityl (Mtt) protecting group using 1% TFA in DCM for 30 min. Peptide was then removed from the resin, by treatment with a TFA/TIS/H_2O (95:2.5:2.5, v/v/v) mixture for 90 min at room temperature; then, crude peptide was precipitated in cold ether, dissolved in a water/acetonitrile (1:1, v/v) mixture, and

lyophilized. Product was purified by RP-HPLC applying a linear gradient of 0.1% TFA CH_3CN in 0.1% TFA water from 5% to 70% over 30 min using an X-Bridge^{TM} BEH300 preparative 10× 100 mm C18, 5μm column at a flow rate of 10 mL/min. Peptide purity (95%) and identity (1488 amu) was confirmed by LC–MS (data not shown). Purified peptide was lyophilized and stored at −20 °C until use.

2.2.6 Peptide encapsulation and characterization

Peptide was encapsulated adding Strep-tagII-FITC (0.5 mg/mL) to the disperse phase prior to microgel synthesis. Fluorescent microgels without peptide, used as negative control, were obtained dissolved 0.1 mg of Rhodamine B in 10 mL of water solution. Fluorescence analysis was performed by Leica SP5 confocal microscope. Bright field and fluorescence images using a HCX IRAPO L 25×/0.95 water objective were acquired; 488nm line of the Argon laser as excitation sources for FITC-peptide was used and detection occurred at the 500-530 nm band. Images were acquired with a resolution of 1024 × 1024 pixels, zoom 1, 2.33A.U. pinhole. All our experiments were performed at room temperature.

2.2.7 CD analysis

CD spectra were recorded using a JascoJ-1500 spectropolarimeter in a 1.0 cm quartz cell at room temperature. The spectra were recorded from 300 to 190 nm, with a band width of 1 nm, a time constant of 16 s, and a scan rate of 10 nm/min. Spectra were recorded subtracting them from blank samples.

2.2.8 Streptavidin Atto-425 binding and characterization

Binding experiments were performed incubating Strep-tagII-microgels and microgels without peptide (Control-microgels) with Streptavidin-Atto-425 (peptide/protein ratio 5/1) in PBS (pH 7.4) and human serum from healthy donors (final volume 200 mL) at room temperature for 2 h. After incubation Strep-tagII-microgels and Control-microgels were centrifuged for 5 min at 10000 rpm and the supernatant was measured by fluorescence spectroscopy (λ_{exc} 436 – λ_{em}484) using a Perkin Elmer 2300 Enspire Plate Reader.

To demonstrate the ability of our system to detect specific protein, 100 μL of Strep-tagII-microgels were suspended in 1 mL of PBS and different concentrations of Streptavidin protein, ranging from 0.16 μM to 1.6 μM (Figure S4), were added and these solution were incubated for 2 h. After the incubation, microgels were washed three times and their fluorescence was analyzed. The same protocol was used for microgels without peptide, as a

negative control, and for *Strep-TagII*-microgels in serum analysis as well. Fluorescence analysis was performed by Zeiss LSM700 confocal microscope. For this experiment 20× dry objective was used. Two-channel fluorescence images, simultaneously, using multitrack mode were acquired. 480 nm and a 405 nm DAPI solid state lasers as excitation sources were used for peptide-FITC and Streptavidin-Atto-425-protein 435, respectively. Their detection in fluorescence was 500-530 nm and 410-450 nm bands, respectively.

2.2.9 Statistical analysis

The results of confocal experiments were analyzed by software GraphPad Prism version 5.04 and experimental data were expressed as mean ± standard deviation. One-tailed analysis of variance with an Unpaired t-Test was performed to compare all experimental groups and to determine statistical significance of $p < 0.05$. The evaluation of K_D was calculated by a non-linear fitting approach using GraphPad Prism version 5.04 software.

2.3 RESULTS AND DISCUSSIONS

2.3.1 Microfluidic design

Microfluidic design, showed in Figure 2.2, is optimized to obtain monodisperse and stable functionalized microgels in order to create a tool-system for diagnostic and sensing. Droplet formation process is affected by several physical parameters such as flow rates, viscosity of the fluid, dimensions of the geometry, capillary number (Ca) and surface tension [28]; therefore, the design of optimal microfluidic device for the production of monodisperse and stable emulsion relies on controlling such parameters.

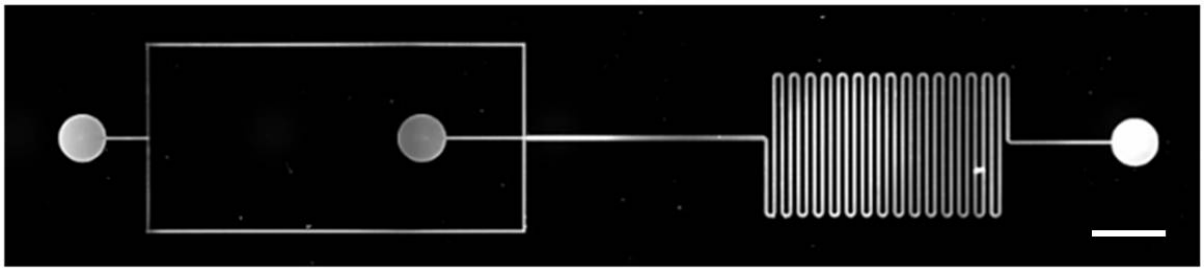

Figure 2.2: Microfluidic flow-focusing device. Scale bar are 100 µm.

In the first set of simulations the influence of geometry and Ca on droplet production was investigated. Firstly the dimensions of the junction were changed; in particular, different widths (25, 30, 35 and 40 µm) and lengths (50, 100 and 500 µm) were modeled. These studies revealed that monodispersity and stability of droplets can be ensured choosing

junction geometry appropriately, maintaining the flow rate constant. Based on the simulation results, junction size of 50 × 35 × 50 µm (width × depth × length) was chosen.

Droplet formation is driven by the competition between the viscous stress and the surface tension of two immiscible fluids, and occurs at a critical Capillary number (Ca), Ca=µU/γ [29]. For this reason, the influence of Ca on emulsion stability was investigated, maintaining the dimensions of the device constant. Ca can be modified by varying the flow rate of the continuous phase (Q_{oil}); a diagram of flow patterns was used to investigate on stable droplet formation (Figure 2.3). Simulation results shows three different flow patterns after the junction: elongation flow pattern, stable emulsions and unstable emulsions (Figure 2.3 A, 2.3 B, 2.3 C).

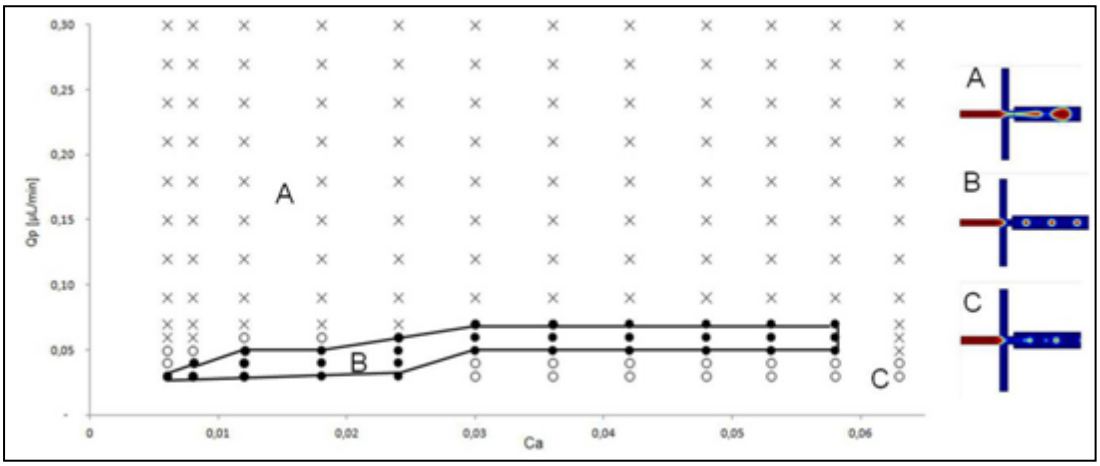

Figure 2.3: Flow diagram as function of PEGDA prepolymer flow rate (Qp) and capillary number (Ca). Three distinct regions were observed: a) elongation flow of thread, b) stable droplets, c) unstable droplet formation.

It is difficult generate stable emulsion at high flow rates of prepolymer solution ($Q_p > 8\times10^{-2}$ µl/min) (Figure 2.3); in fact, W/O emulsion could not separate uniformly from the junction due to the unstable hydrodynamic pressure of PEGDA prepolymer phase. When the flow of the oil phase relatively increases, the flow of prepolymer solution reverses into channels. When the value of Ca is in a limited range 0.005 ~ 0.055 and the value of PEGDA flow rate is between 3×10^{-2} µl/min and 8×10^{-2} µl/min, the prepolymer phase breaks into a stable emulsions (regime of stable emulsions Figure 2.3B). Choi *et al.* also investigated on the flow patterns to obtain stable polymeric droplets [30]. They found that stable and monodisperse emulsions were generated in a limited range of Ca (0.5×10^{-2}~ 0.5×10^{-1}) and a flow rate of disperse phase (0.2~1.1 µL/min). it is higher than the flow rate chosen in our simulation due to the different channels dimensions.

Precise control of particle size and monodispersity are critical for many applications of microgels; microfluidic platform allows this control over a wide range of sizes [31]. For this reason, in the second set of simulations the influence of Q_{oil} on the droplet size was investigated, while Q_p was kept constant. Once the dimensions of the device had been fixed, microgels with a wide range of sizes, ranging from 10 to 90 µm, were produced. Droplets diameter was calculated during the simulation analysis. In particular, droplet size was determined by the flow rates of the two phases and the flow rate ratio, as proposed by Collins *et al*. Therefore, maintaining the ratio of the disperse and the continuous phase flow rates appropriate [30], droplets size decreased as Q_{oil} increased. In order to stabilize droplets against uncontrolled coalescence, the use of a surfactant is necessary. These molecules populate the water/oil interface and prevent droplet coalescence. In emulsification processes, the effect of the interfacial tension on droplet size and stability is significant [32, 33]. For this reason, we investigated on the influence of the surface tension (γ); in particular, γ was changed from 4.27 to 1.68 to mN/m (Figure 2.4) and it was observed that when γ increased, droplets diameter increased (Figure 2.5).

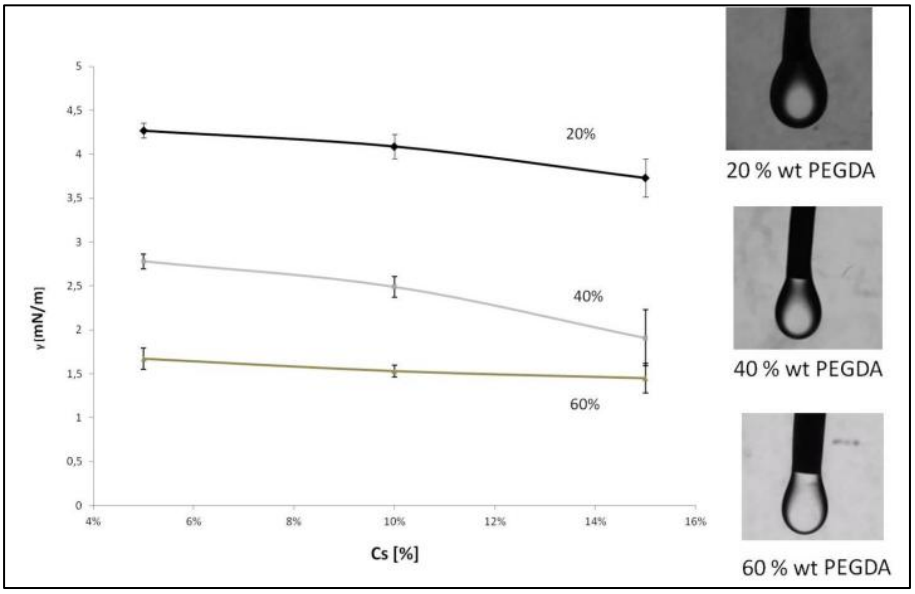

Figure 2.4: The measures of surface tension between PEGDA prepolymer solution (20, 40, 60 wt %) and oil solution (with 5, 10, 15 % of surfactant) by pendant drop CAM 200 were showed. With increase of the concentration of the surfactant (Cs) the surface tension decrease. The surface tension depends also on the PEGDA concentration, in particular increasing PEGDA concentration the surface tension decrease.

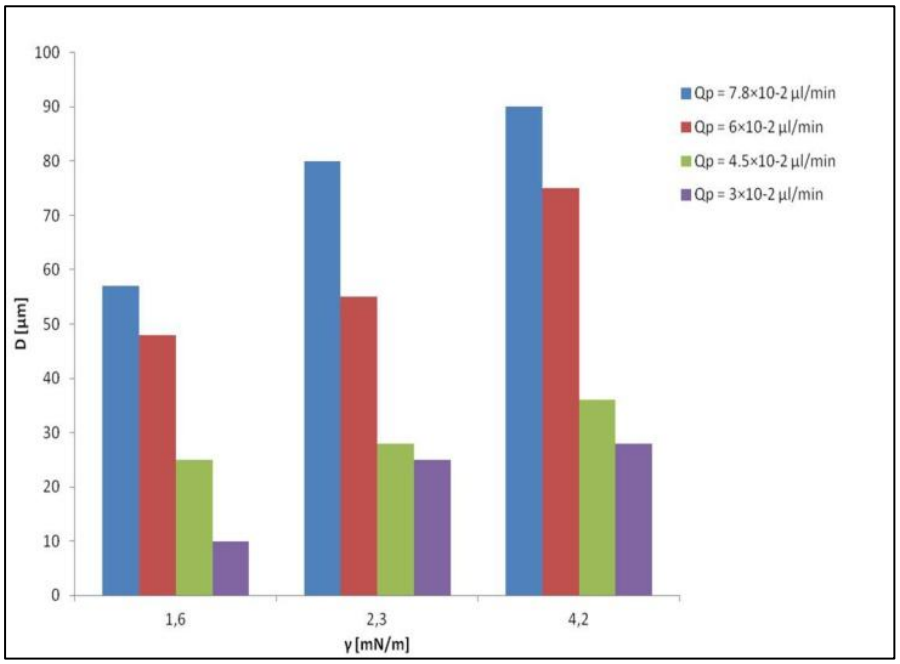

Figure 2.5: The mean diameter of generated microgels as a function of surface tension. Simulation results of 3 groups of cases with various values of interfacial tension: (a) 1.6 mN/m, (b)2.3 mN/m, (c) 4.2 mN/m, at different Q_{peg}.

Another parameter that influences the viscosity and, consequently, the interfacial tension between the two phases is the polymer concentration in water solution. A solution with prepolymer concentration lower than 20 wt % can be used to form droplets, but UV curing requires long time and these droplets could be display deformation and loss of mechanical stability under flow conditions [10]. Instead, a solution with PEGDA concentration higher than 60 wt % can be cured by UV light in less time; however, it is difficult to control the stability of the droplets because of its high viscosity [34]. For this reason, a prepolymer solution at 20 wt.% of PEGDA was used and the length of the serpentine at 10 cm was optimized to ensure droplet polymerization.

2.3.2 PEGDA-peptide microgels synthesis and characterization

Here microfluidic synthesis of biodegradable PEGDA-peptide microgels for diagnostic applications is reported. The encapsulated peptide is Strep-tagII, an eight amino acid peptide (H_2N–WSHPQFEK–COOH) selected from a random peptide library as an artificial ligand for streptavidin protein [35]. It is usually used for efficient protein purification in a simple single

step and -because of its independence from metal ions- it is also important in the study of metallo-proteins [36]. Microgels synthesis is shown in Figure 2.6 A and described in Experimental Section. Briefly, the pre-polymer solution containing peptide Strep-tagII-FITC was injected through the central channel of the microfluidic device, as disperse phase, and oil solution with surfactant through its two opposite side channels, as continuous phase. Under optimized flow rate conditions, estimated by CFD simulation, disperse phase was sheared into monodisperse droplets by continuous phase. The amount of embedded peptide was calculated to be 50 µg in 100 µL of microgels (data not show). Based on flow conditions, the yield of microgel production was around 300 microgel/minutes.

With regards to the homogeneity of microgels size and the peptide encapsulation, microfluidic set up allows robust and rapid synthesis of functionalized and uniform polymeric microparticles in a single step, overcoming the limits of the conventional suspension polymerization methods. Strep-tagII-microgels obtained are monodisperse in size with a coefficient of polydispersity (PDI) < 0.003 and peptide encapsulation was confirmed by confocal image (Figure 2.6). Despite the addition of such biologics may lead to a slight increase in the deviation of diameter, the resulting microgels remained largely uniform, thereby demonstrating the ability of our approach to encapsulate biomolecules in polymeric microparticles.

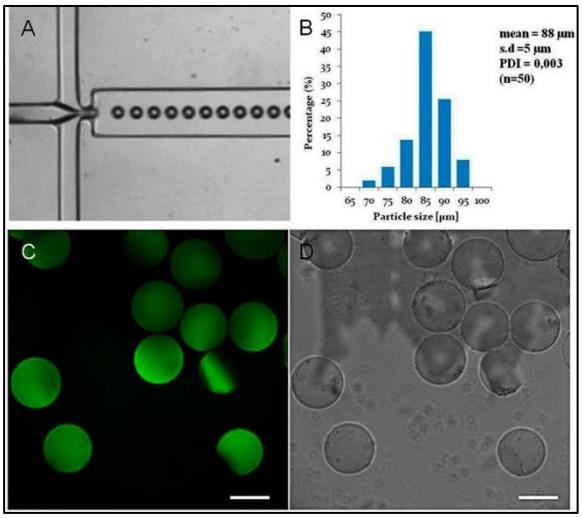

Figure 2.6: PEGDA-peptide microgel (20%PEGDA, 0.1%Darcour,0.5mg/ml peptide).
A) StreptagII microgels synthesis by microfluidic device. B) Size distribution of PEGDA-peptide peptide microgels. C) Fluorescent image of StreptagII FITC encapsulation. D) Phase contrast image of microgels. Scale bare are 100µm.

PEGDA has been chosen for its advantages over other polymers and its specific proprieties, such as good biocompatibility, non-toxicity, low immunogenicity *in vivo*, and resistance to protein adsorption. Moreover, polyethylene glycol (PEG) hydrogels are widely used in biomedical fields such as drug delivery and tissue engineering [37, 38].

Finally, to verify the secondary structure of the peptide in solution and inside the microgels circular dichroism (CD) was performed. CD spectra of peptide registered in aqueous buffer solution (Figure 2.7A) revealed a random coil content due to the absence of Cotton bands at 205, 222 nm that are typical of helix conformations. As showed in Figure 2.7A the addition of different TFE concentrations results in an increase of helical content, in particular at 60% of TFE peptide spectrum shows a presence of little Cotton bands at 205 and 222 nm. The same experiments were carried out for peptide incorporated into the microgels. CD data confirmed that Strep-tagII peptide retains its structure (random-coil as it expect for small peptides) after its encapsulation, as previously reported for other peptides [39, 40]. Figure 2.7 B shows CD spectrum of Step-tagII peptide and Strep-TagII microgels. In order to analyze the structural behavior of the peptide encapsulated into the microgels, CD spectrum at 60% of TFE was recorded. In contrast of peptide spectrum at 60% of TFE, peptide encapsulated didn't change its conformation even with high TFE content, showing only a slight band at 220nm. Figures 2.7 C and D show CD data of Strep-tagII-microgels recorded at 0 and 60% of TFE and peptide spectrum in solution and incorporated inside microgels at the same TFE concentration.

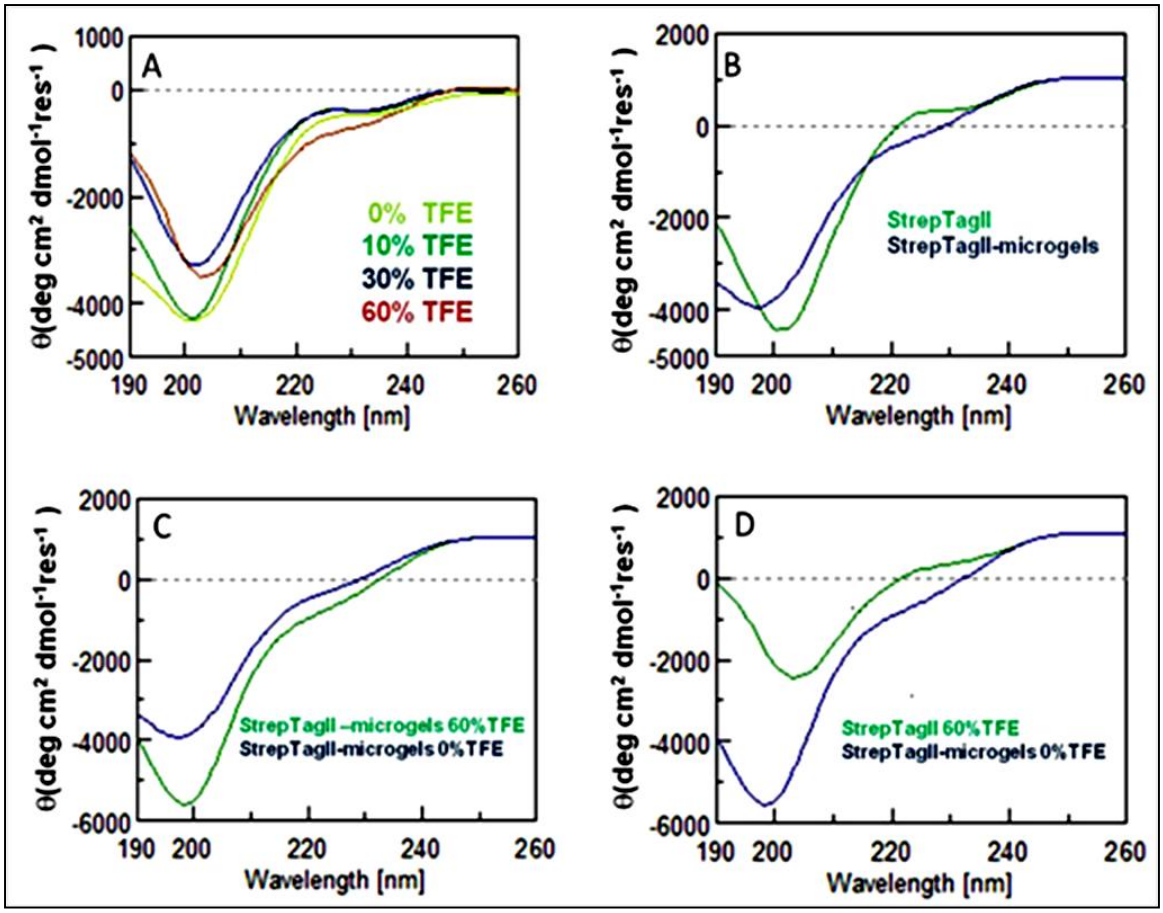

Figure 2.7: CD analysis of Strep-tagII peptide and Strep-tagII peptide-microgels, in phosphate buffer 10 mM pH 7. Overlay of Strep-tagII peptide CD spectra recorded (A) with increasing amounts of TFE (from 0 to 60%), Overlay of StreptagII-peptide and StreptagII-microgels CD spectra in buffer solution (B), Overlay of StrepTagII microgels CD spectra recorded (C) with 0% and 60% of TFE and Overlay of StrepTagII peptide and microgels recorded (D) with 60% of TFE.

Because of the uniformity of the microgels diameter and the homogeneity of the peptide into the microgels, this approach may serve as a consistent method for selective protein detection. Importantly, our strategy is relatively simple and robust, and encapsulated molecules retain their structure during microgels processing. Moreover, we demonstrate that CFS allows a robust control over microgels synthesis, avoiding fabrications of many different microfluidic devices.

2.3.3 Protein-binding analysis in PBS and human serum

One motivation for using peptide-binding proteins in polymeric networks is employ them as platform to have a selective protein detection in complex mixtures [41]. Protein-binding peptide is described in Experimental Section with more details. It occurred adding to Strep-tagII-microgels different concentrations of Streptavidin protein, ranging from 0.16 µM to 1.6 µM. Figure 2.9B shows *Streptavidin-Atto-425* fluorescence on Strep-tagII- microgels after 2h of incubation at room temperature in PBS. The selective binding of our system was demonstrated using the same protocol for Control-microgels labeled with Rhodamine B (Figure 2.8 E). *Atto-425* fluorescence signal occurred only on Strep-tagII-microgels and its intensity increased with increasing protein concentration (Figure 2.8 L), giving a reasonable specific binding signal. It is evident that *Streptavidin-Atto-425* recognition is specific and dose-response on Strep-tagII-microgels, unlike Control-microgels (Figure 2.9 A), with an estimated K_D of 0.40±0.11 µM, which demonstrate a good affinity toward Streptavidin protein. As reported the maximum constant affinity between such peptide and protein is about 70 µM [42, 43], therefore microgel is able to improve the sensitivity and specificity of protein detection. Furthermore we assumed an uniform distribution of bound protein on microgels and a saturation point at 1.6 µM (Figure 2.9). Limit of detection of 0.2 µM is obtained with about 3.6×10^3 particles in 100 µL of volume reaction. Indirect-assay, performed by spectrofluorometer, confirmed the ability of Strep-tagII-microgels to recognize Streptavidin, unlike Control-microgels (Figure 2.10).

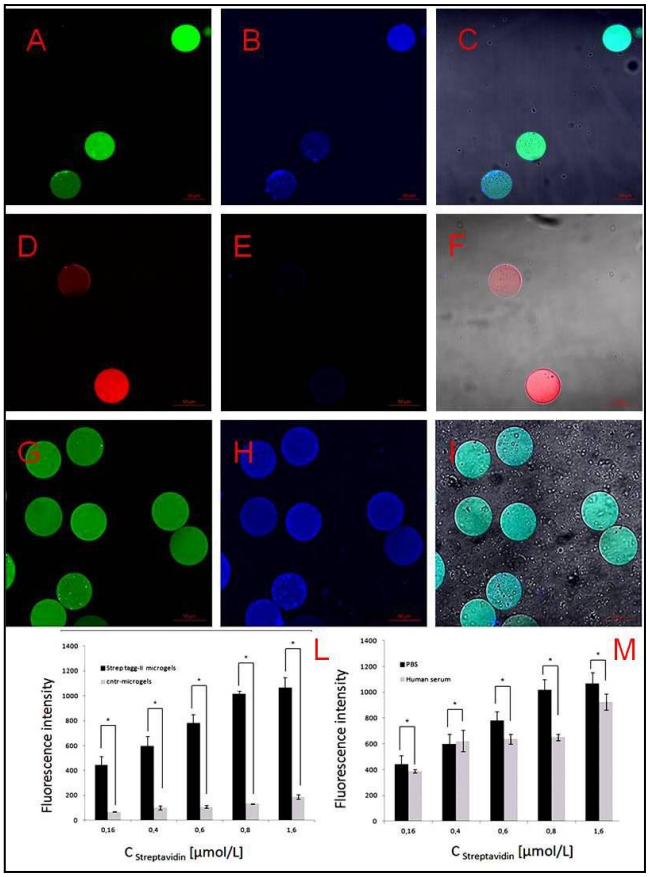

Figure 2.8: Fluorescence detection of specific and unspecific binding both in PBS and in human serum. Single component detection: (A) strep-tagII-microgels (green) and (B) Streptavidin binding microgels (blue); (C) Overlay image. The single component images demonstrate that there is no occurrence of overlapping signals. (D) PEGDA microgels labeled with Rhodamine B (red) as a control of unspecific signal; (E) fluorescence image of streptavidin on control microgels; (F) overlay channel; (G) Strep-tagII-microgels (green) and (H) Streptavidin binding microgels (blue) in human serum; (I) Overlay image for specific protein-binding peptide in human serum; (L) Bioassay system efficiency of microgels-bounding; (M) Performance of bioassay system for protein detection in PBS and in human serum. The binding event is detected by measuring the fluorescence intensity of Atto-425 conjugated Streptavidin directly on 50 microgel particles. Statistical difference between Strep tag II-microgels and control microgels *$p<0.05$ (mean±SD n=2) in PBS and *$p>0.05$ (mean±SD n=2) in human serum.

Since most of the interesting proteins are located in biological complex matrices such as human serum, we evaluated the accuracy of our system directly in biological environment. Fluorescence image (Figure 2.9H) confirms the protein-binding peptide and the accuracy of the microgel-based assay also in complex matrix. Moreover Figure 2.10B shows that the

fluorescence intensity of the Streptavidin-Atto-425 is dose-responsive and specific in serum as well, with a K_D of 0.12±0.047 µM [44-46]. Such performance is ascribable to the capability of the polymeric network to offer antifouling properties, thus improving the specificity of the capture.

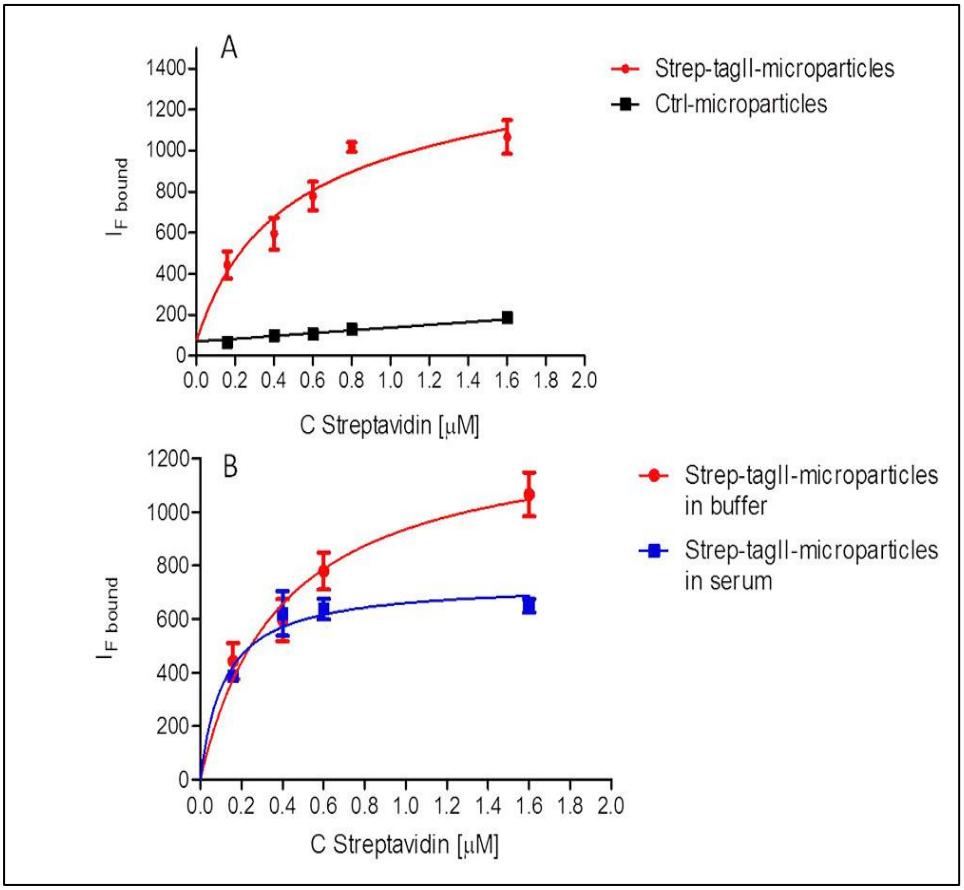

Figure 2.9: Strep-tagII-microgels-protein binding confocal results. (A) the Streptavidin-ATTO-425 recognition (red curve) is specific, unlike Control-microgels (black curve) (mean±SD n=2). (B) Comparison of confocal binding by non linear fitting in buffer (red curve) and in serum (blue curve).

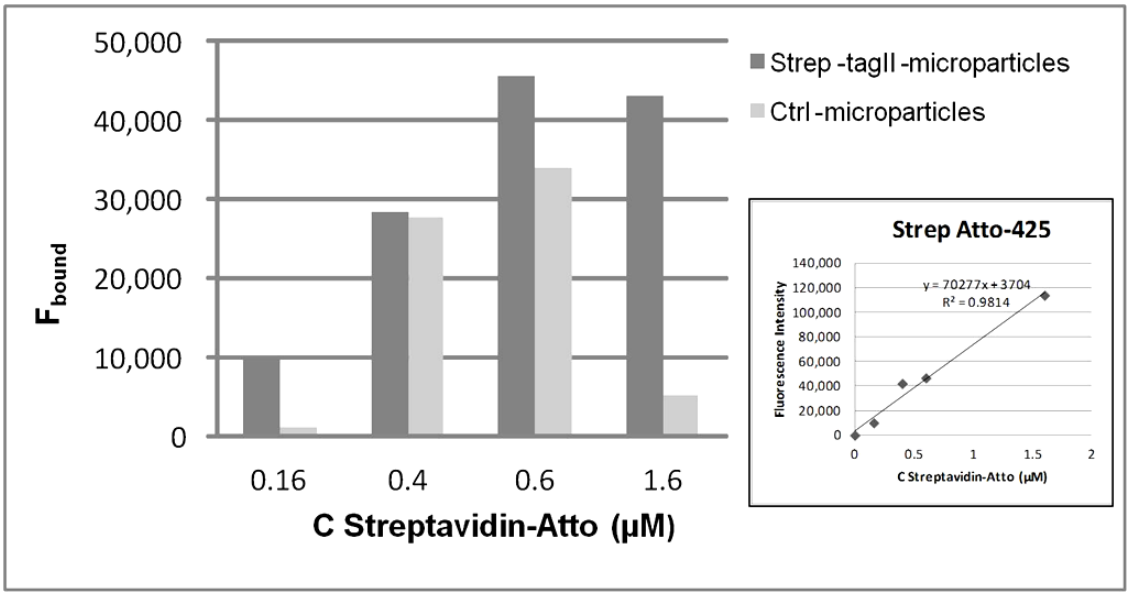

Figure 2.10: Fluorescence spectroscopy binding assay between Strep-tagII-microgels and Streptavidin-Atto 425 protein. Different amount of unbound protein, ranging from 0.16 to 1.6uM, were collected and analyzed by spectrofluorometer (λ_{exc} 436 – λ_{em}484). The fraction of bound protein reported was calculated by subtracting the emission of the unbound protein to total one. Inset the tritation curve of Streptavidin-Atto 425 used for the total protein fluorescence calculation. The differences in the amount of bound protein between Strep-tagII-microgels (dark grey) and Control-microgels (light grey) were underlined by a lack of a specific binding in the control one.

With our approach we synthesized "smart" microgels for selective protein detection both in PBS and in complex fluid, using droplet-microfluidics. This method is relative simple, rapid and support the use of the microfluidic device as a manufacturing platform for diagnostic use.

We believe that the reported system can be broadly applicable for rapid synthesis of microgels for different application like biosensing or food and environmental contaminants detection, using different biopolymers and small molecules.

2.4 CONCLUSIONS

In conclusion, here we report droplet-microfluidics method for the easy and rapid synthesis of biodegradable PEGDA-peptide microgels for selective biomolecules capture in complex medium, unlike conventional techniques. Based on numerical simulations, we fabricate microfluidic device to produce stable and monodisperse microgels. Uniform distribution of the specific peptide within the microgel was achieved and the efficiency of peptide-to–protein

binding both in PBS and human serum was confirmed. The use of microfluidic platform easily leads the control on size, shape, and chemical proprieties of microgels as well as on the content and distribution of the encapsulated peptide. Such peptide-functionalized microparticles allows the enhancement of binding affinity and the specificity in complex media. About this point it is very important to modulate the peptide density into microgels, in order to avoid proteins crowding or to leave many gaps using very low peptide concentration. So the amount of integrated peptide plays a strong and a limiting role in the affinity studies. Our system is easy and flexible towards the detection of different molecules, does not require additional reagents and allows for the specific detection in complex media because of its antifouling properties. The control of physical and chemical properties of polymeric microparticles obtained by droplet microfluidic, the hydrophilic characteristics and the flexibility of the molecular encapsulation of proposed microgel represent a modular platform that can be generalized for any direct bio-detection in complex media, and, thus, applied to a wide spectrum of biomedical applications.

References

[1] Langer R, Tirrell DA. Designing materials for biology and medicine. Nature 2004;428(6982):487–92. http://dx.doi.org/10.1038/ nature02388.

[2] Rubina AY, Kolchinsky A, Makarov AA, Zasedatelev AS. Why 3-D? gel-based microarrays in proteomics. Proteomics 2008;8(4):817–31. http://dx.doi.org/10.1002/pmic.200700629 .

[3] Helgeson ME, Chapin SC, Doyle PS. Hydrogel microparticles from lithographic processes: novel materials for fundamental and applied colloid science. Curr Opin Colloid Interface Sci 2011;16(2):106–17. http://dx.doi.org/10.1016/j.cocis.2011.01.005.

[4] Peppas NA, Keys KB, Torres-Lugo M, Lowman AM. Poly(ethylene glycol)-containing hydrogels in drug delivery. J Controlled Release 1999;62(1–2):81–7. http://dx.doi.org/10.1016/S0168-3659(99)00027-9.

[5] Peppas NA, Hilt JZ, Khademhosseini A, Langer R. Hydrogels in biology and medicine:

from molecular principles to bionanotechnology. Adv Mater 2006;18(11):1345–60. http://dx.doi.org/10.1002/adma.200501612.

[6] Lee KY, Mooney DJ. Hydrogels for tissue engineering. Chem Rev 2001;101(7):1869–79. http://dx.doi.org/10.1021/cr000108x.

[7] Nguyen KT, West JL. Photopolymerizable hydrogels for tissue engineering applications. Biomaterials 2002;23(22):4307–14. http://dx.doi.org/10.1016/S0142-9612(02)00175-8.

[8] Slaughter BV, Khurshid SS, Fisher OZ, Khademhosseini A, Peppas NA. Hydrogels in regenerative medicine. Adv Mater 2009;21(32–33):3307–29. http://dx.doi.org/10.1002/adma.200802106.

[9] Matthew E. Helgeson, Stephen C. Chapin, Patrick S. Doyle. Hydrogel microparticles from lithographic processes: Novel materials for fundamental and applied colloid science. Current Opinion in Colloid & Interface Science 2011: 16(2): 106-117. http://dx.doi:10.1016/j.cocis.2011.01.005.

[10] Gaelle C. Le Goff, Rathi L. Srinivas, W. Adam Hill, Patrick S. Doyle. Hydrogel microparticles for biosensing. European Polymer Journal 2015; 72: 386-412. http://dx.doi.org/10.1016/j.eurpolymj.2015.02.022.

[11] Pregibon, D. C.; Toner, M.; Doyle, P. S. Science 2007, 315, 1393–1396.

[12] Wilson, R.; Cossins, A. R.; Spiller, D. G. Angew. Chem., Int. Ed. 2006, 45, 6104–6117.

[13] Birtwell, S.; Morgan, H. Integr. Biol. 2009, 1, 345–362.

[14] Ki Wan Bong, Stephen C. Chapin, and Patrick S. Doyle. Magnetic Barcoded Hydrogel Microparticles for Multiplexed Detection 2010; 26(11): 8008-8014. http://dx.doi.10.1021/la904903g.

[15] Droplet Microfluidics for Producing Functional Microparticles. 2013. http://dx.doi.org/10.1021/la403220p.

[16] Baret, J. C. Surfactants in droplet-based microfluidics. Lab Chip 2012, 12 (3), 422−33.

[17] Dendukuri, D.; Doyle, P. S. The Synthesis and Assembly of Polymeric Microparticles Using Microfluidics. Adv. Mater. 2009, 21 (41), 4071−4086.

[18] Duncanson, W. J.; Lin, T.; Abate, A. R.; Seiffert, S.; Shah, R. K.; Weitz, D. A. Microfluidic synthesis of advanced microparticles for encapsulation and controlled release. Lab Chip 2012, 12 (12), 2135− 45.

[19] Nisisako, T.; Torii, T. Microfluidic large-scale integration on a chip for mass production of monodisperse droplets and particles. Lab Chip 2008, 8 (2), 287−93.

[20] Xu, Q.; Hashimoto, M.; Dang, T. T.; Hoare, T.; Kohane, D. S.; Whitesides, G. M.; Langer, R.; Anderson, D. G. Preparation of monodisperse biodegradable polymer microparticles using a microfluidic flow-focusing device for controlled drug delivery. Small 2009, 5 (13), 1575−81.

[21] Kesselman, L. R. B.; Shinwary, S.; Selvaganapathy, P. R.; Hoare, T. Synthesis of Monodisperse, Covalently Cross-Linked, Degradable "Smart" Microgels Using Microfluidics. Small 2012, 8 (7), 1092−1098.

[22] Torres-Lugo, M.; Peppas, N. Preparation and Characterization of P(MAA-g-EG) Nanospheres for Protein Delivery Applications. J. Nanopart. Res. 2002, 4 (1−2), 73−81.

[23] Zisch, A. H.; Lutolf, M. P.; Ehrbar, M.; Raeber, G. P.; Rizzi, S. C.; Davies, N.; Schmokel, H.; Bezuidenhout, D.; Djonov, V.; Zilla, P.; Hubbell, J. A. Cell-demanded release of VEGF from synthetic, biointeractive cell ingrowth matrices for vascularized tissue growth. FASEB J. 2003, 17 (15), 2260−2.

[24] Chirinos-Rojas, C. L.; Steward, M. W.; Partidos, C. D., A peptidomimetic antagonist of TNF-α-mediated cytotoxicity identified from a phage-displayed random peptide library. The Journal of Immunology 1998, 161 (10), 5621-5626.

[25] Cusano, A. M.; Causa, F.; Della Moglie, R.; Falco, N.; Scognamiglio, P. L.; Aliberti, A.; Vecchione, R.; Battista, E.; Marasco, D.; Savarese, M., Integration of binding peptide selection and multifunctional particles as tool-box for capture of soluble proteins in serum. Journal of The Royal Society Interface 2014, 11 (99), 20140718.

[26] Banner, D. W.; D'Arcy, A.; Janes, W.; Gentz, R.; Schoenfeld, H.-J.; Broger, C.; Loetscher, H.; Lesslauer, W., Crystal structure of the soluble human 55 kd TNF receptorhuman TNFβ complex: implications for TNF receptor activation. Cell 1993, 73 (3), 431-445.

[27] Jing, J.; Fournier, A.; Szarpak-Jankowska, A.; Block, M. R.; Auzély-Velty, R., Type, Density, and Presentation of Grafted Adhesion Peptides on Polysaccharide-Based Hydrogels Control Preosteoblast Behavior and Differentiation. Biomacromolecules 2015, 16 (3), 715-722.

[28] Dendukuri, D.; Doyle, P. S., The synthesis and assembly of polymeric microparticles using microfluidics. Advanced Materials 2009, 21 (41), 4071-4086.

[29] Shepherd, R. F.; Conrad, J. C.; Rhodes, S. K.; Link, D. R.; Marquez, M.; Weitz, D. A.; Lewis, J. A., Microfluidic assembly of homogeneous and janus colloid-filled hydrogel granules. Langmuir 2006, 22 (21), 8618-8622.

[30] Choi, C.-H.; Jung, J.-H.; Hwang, T.-S.; Lee, C.-S., In situ microfluidic synthesis of monodisperse PEG microspheres. Macromolecular Research 2009, 17 (3), 163-167.

[31] Headen, D. M.; Aubry, G.; Lu, H.; García, A. J., Microfluidic-Based Generation of Size-Controlled, Biofunctionalized Synthetic Polymer Microgels for Cell Encapsulation. Advanced Materials 2014, 26 (19), 3003-3008.

[32] Joscelyne, S. M.; Trägårdh, G., Membrane emulsification—a literature review. Journal of Membrane Science 2000, 169 (1), 107-117.

[33] Xu, J.; Luo, G.; Chen, G.; Tan, B., Mass transfer performance and two-phase flow characteristic in membrane dispersion mini-extractor. Journal of membrane science 2005, 249

(1), 75-81.
[34] Dang, T.-D.; Kim, Y. H.; Kim, H. G.; Kim, G. M., Preparation of monodisperse PEG hydrogel microparticles using a microfluidic flow-focusing device. Journal of Industrial and Engineering Chemistry 2012, 18 (4), 1308-1313.

[35] Schmidt, T. G.; Skerra, A., The random peptide library-assisted engineering of a Cterminal affinity peptide, useful for the detection and purification of a functional Ig Fv fragment. Protein Engineering 1993, 6 (1), 109-122.

[36] Korndörfer, I. P.; Skerra, A., Improved affinity of engineered streptavidin for the Strep-tag II peptide is due to a fixed open conformation of the lid-like loop at the binding site. Protein science 2002, 11 (4), 883-893.

[37] Teh, S.-Y.; Lin, R.; Hung, L.-H.; Lee, A. P., Droplet microfluidics. Lab on a Chip 2008, 8 (2), 198-220.

[38] Chung, B. G.; Lee, K.-H.; Khademhosseini, A.; Lee, S.-H., Microfluidic fabrication of microengineered hydrogels and their application in tissue engineering. Lab on a Chip 2012, 12 (1), 45-59.

[39] Amiram, M.; Luginbuhl, K. M.; Li, X.; Feinglos, M. N.; Chilkoti, A., Injectable protease-operated depots of glucagon-like peptide-1 provide extended and tunable glucose control. Proceedings of the National Academy of Sciences 2013, 110 (8), 2792-2797.

[40] Black, K. A.; Priftis, D.; Perry, S. L.; Yip, J.; Byun, W. Y.; Tirrell, M., Protein encapsulation via polypeptide complex coacervation. ACS Macro Letters 2014, 3 (10), 1088-1091.

[41] Zhang, Z.; Zhu, W.; Kodadek, T., Selection and application of peptide-binding peptides. Nature biotechnology 2000, 18 (1), 71-74.

[42] Freitag, S.; Le Trong, I.; Klumb, L. A.; Chu, V.; Chilkoti, A.; Stayton, P. S.; Stenkamp, R. E., X-ray crystallographic studies of streptavidin mutants binding to biotin. Biomolecular engineering 1999, 16 (1), 13-19.

[43] Skerra, A.; Schmidt, T. G., Applications of a peptide ligand for streptavidin: the Streptag. Biomolecular engineering 1999, 16 (1), 79-86.

[44] Deng, J.; Sun, M.; Zhu, J.; Gao, C., Molecular interactions of different size AuNP–COOH nanoparticles with human fibrinogen. Nanoscale 2013, 5 (17), 8130-8137.

[45] EL-Sharif, H. F.; Hawkins, D. M.; Stevenson, D.; Reddy, S. M., Determination of protein binding affinities within hydrogel-based molecularly imprinted polymers (HydroMIPs). Physical Chemistry Chemical Physics 2014, 16 (29), 15483-15489.

[46] Nakamoto, M.; Hoshino, Y.; Miura, Y., Effect of physical properties of nanogel particles on the kinetic constants of multipoint protein recognition process. Biomacromolecules 2014, 15 (2), 541-547.

Chapter 3

Miniaturized peptide-based biosensor for Aflatoxin M1 in milk samples: from Peptide Screening to Biosensor Development.

ABSTRACT. Mycotoxins are fluorescent low-molecular-weight natural products produced as secondary metabolites by fungi in milk and dried fruits. These metabolites are chemically stable molecules that cause disease and death in human beings [1]. In particular, they are teratogenic, mutagenic, nephrotoxic, immunosuppressive and carcinogenic. They are highly resistive in nature and hence remain in the food chain. Therefore, a rapid, sensitive and specific assay technique is required for the routine analysis of foods, and beverages. Current analytical determination includes immuno-and bio-luminescent assays, HPLC (fluorescence detection), TLC, gas and liquid chromatography coupled to mass spectroscopy [2]. However all of them present high costs and skilled quality control operators. Our idea is to develop a peptide-based biosensor for aflatoxin M1 detection in a sensitive, specific and unsophisticated manner. To this aim an integrated approach has been developed to select specific peptide motif to capture aflatoxin M1. The integrated approach provides a combination of computation modeling with combinatorial peptide synthesis to screen the sequence with the highest affinity. In particular, computation modeling using a C-docker alghoritm was performed to determine the Binding energy of all possible peptide combinations against toxin, using as building blocks eight different amino-acids chosen by considering their different chemical properties. The combinatorial peptide libraries were obtained with the same building blocks and best alfatoxin binders were selected by SPR (Surface Plasmon Resonance). Peptides sequences selected by the proposed approach have been easily integrated in PEGDA microparticles opening the route towards a direct detection of aflatoxins in small volume both in liquid and solid environments. Such approach can be applied also to other small molecules to develop materials able to sequestrate the target analytes allowing their direct detection directly in the materials.

3.1 INTRODUCTION

Mycotoxins are low-molecular-weight natural products (i.e., small molecules) produced as secondary metabolites by filamentous fungi. These metabolites constitute a toxigenically and chemically heterogeneous assemblage that are grouped together only because the members can cause disease and death in human beings and other vertebrates. Not surprisingly, many mycotoxins display overlapping toxicities to invertebrates, plants, and microorganisms [1].

The term mycotoxin was coined in 1962 in the aftermath of an unusual veterinary crisis near London, England, during which approximately 100,000 turkey poults died. This mysterious turkey X disease was linked to a peanut (groundnut) meal contaminated with secondary metabolites from *Aspergillus flavus* (aflatoxins) [1].

Mycotoxins are not only hard to define, they are also challenging to classify. Due to their diverse chemical structures and biosynthetic origins, their myriad biological effects, and their production by a wide number of different fungal species, classification schemes tend to reflect the training of the person doing the categorizing. Clinicians often arrange them by the organ they affect [3]. Thus, mycotoxins can be classified as hepatotoxins, nephrotoxins, neurotoxins and immunotoxins [4]. Cell biologists put them into generic groups such as teratogens, mutagens, carcinogens, and allergens. Organic chemists have attempted to classify them by their chemical structures (e.g., lactones, coumarins); biochemists according to their biosynthetic origins (polyketides, amino acid-derived,etc.); physicians by the illnesses they cause (e.g., St. Anthony's fire, stachybotryotoxicosis), and mycologists by the fungi that produce them (e.g., Aspergillus toxins, Penicillium toxins) [1].

Currently, more than 300 mycotoxins are known, but most of studies are focused on aflatoxins, ochratoxin, trichothecenes, zearalenone and fumonisin [5]. The synthesis of mycotoxins occurs during different stages of food production, and in particular, they are found in the growing and storage. They can cause several pathologies in animals and people. Aflatoxins, for example, cause liver damage, decreased production of milk and eggs and immune deficiency in animals which have consumed low amounts of contaminated food without any obvious clinical manifestations. Typical clinical signs are: gastrointestinal dysfunction, reduced reproduction, loss of appetite and anemia [6,7]. Aflatoxins are a group of toxins furanocoumarins polyketides produced by certain species of Aspergillus and their most toxic and carcinogenic member is the aflatoxin B1. By reported cases seems that the mold Aspergillus is diffused in warmer climates, and the optimum temperature for its growth is 30°C but it can also grow in a temperature range between 10°C and 45°C.

Numerous types of aflatoxins have been identified but the most important are: the aflatoxin B1, B2, G1, G2 and their metabolic derivatives M1 and M2 present in particular in the milk of animals that have ingested contaminated food [8].

The metabolism of AFB1 is determined primarily by cytochrome P450 (CYP450). Typically isoforms CYP1A2 and CYP3A4 are the most involved in the activation of AFB1 with the formation of the 2,3 epoxide responsible for binding with nucleic acids and the subsequent activity on protein synthesis and hepato-carcinogenic function (Figure 3.1). The AFM1 derives its name from "milk" and it is the unique AFB1 metabolite that passess in significant quantities in milk; However, it is also present in other body fluids (blood and urine), as well as in organs such as liver and kidney.

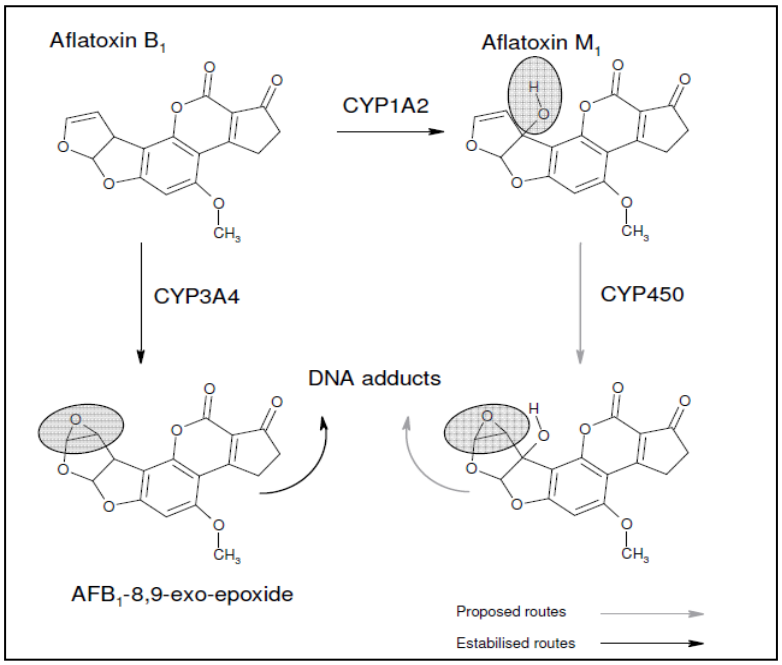

Figure 3.1: Mechanism of AFM1-DNA binding [8].

It is formed by aflatoxin B1 through a process of hydroxylation in the liver and kidney and is subsequently eliminated in the milk, while a small portion is deposited in the muscle. The AFM1 in milk begins to appear after about 12 hours from start of administration of contaminated food. The toxic effect is due to the toxin-nucleic acids and toxin-nucleoproteins binding, and the result is a weakening of the immune system, carcinogenicity and teratogenicity (birth defects). AFM1 food limits are regulated by *Normativa 10 del 9-6-99; recepimento Reg.CEE 1528/98* as follows:

- **Milk products 0.05 ppb (50 ppt).**
- **Infant food 0.01 ppb.**

Most of the mycotoxin are molecules chemically stable that remain unchanged during storage and production. The best strategy to control the mycotoxin presence in the food chain is the prevention. Low molecular weight mycotoxins possess a variety of chemical structures which is the main constraint to develop one standard technique for analysi. There has been a major international research effort, aimed at the identification and quantification of mycotoxins and evaluation of their biological effects in humans and animals [3].

Conventional techniques used for the detection of mycotoxins

The analytical determination is important for the evaluation of toxins: immuno-chemiluminescent and bioluminescent assays are generally used for the analysis of mycotoxins. Currently, however, the most used techniques for the determination of mycotoxins are chromatographic ones: HPLC (fluorescence detection), TLC, gas and liquid chromatography coupled to mass spectroscopy [2], (Figure 2.1). Also the comparison of genomic DNA sequences can be used for the identification of the fungal species responsible for the synthesis of mycotoxins and this cDNA can also be useful to determine if the genes for the biosynthesis of these molecules are expressed in a specific way or not.

The determination at molecular level is carried out by: PCR and RT-PCR. Another method used for the detection of toxins is the ELISA assay. In this assay, the wells of the plate containing an antibody against these toxins. The detection reagent is a covalent complex between the mycotoxin and an enzyme, usually horseradish peroxidase or alkaline phosphatase. ELISA typically uses a fluorimetric or colorimetric method for the detection. However, substrates may also be used with products that can be measured electrochemically; in this case the immunoreagent are immobilized on the surface of an electrode. The advantage of electrochemical assays is the low cost of production of the electrodes. Applications based on these types of assays have included the detection of AFM1 in milk [9], AFB1 in barley and rice [10,11] and OTA in wheat [12]. Though these methods are well known for their accurate and precise detection of mycotoxin in food or feed samples, they require skilled operators, extensive sample pretreatment, equipment and may lack accuracy at low analyte concentration [13,14]. Therefore, a rapid, sensitive and specific assay technique is required for the routine analysis of foods, and beverages.

The biosensors are instruments that use biological molecules, such as antibodies or enzymes, which come into contact with a substance, such as a toxin, react and undergo changes which are then "translated" into a measurable electrical signal or impulse. These devices have an high sensibility, high selectivity, low cost, offering the chance to be reborn and have many potential applications. Biosensors can be easily used in the food industry to determine the

presence of mycotoxins in food [15]. Among the most widely used for this purpose there are: the piezoelectric biosensors (simple, rapid and highly selective) and microarray (simultaneous detection of molecules with high, medium and low molecular weight). Over the last few years the use of "Lateral flow tests" also increased. The lateral flow tests are simple devices designed to detect the presence (or absence) of a target analyte in the sample (matrix) without the need for specialized, expensive equipment; one of the most recent used for the detection of aflatoxin M1 was designed by the **CHARM**. It is the only lateral flow test that detects the presence of aflatoxin M1 in parts per trillion (ppt) in raw milk. It is designed to respect the U.S.A. FDA limit of 500 ppt (0.5 ppb).

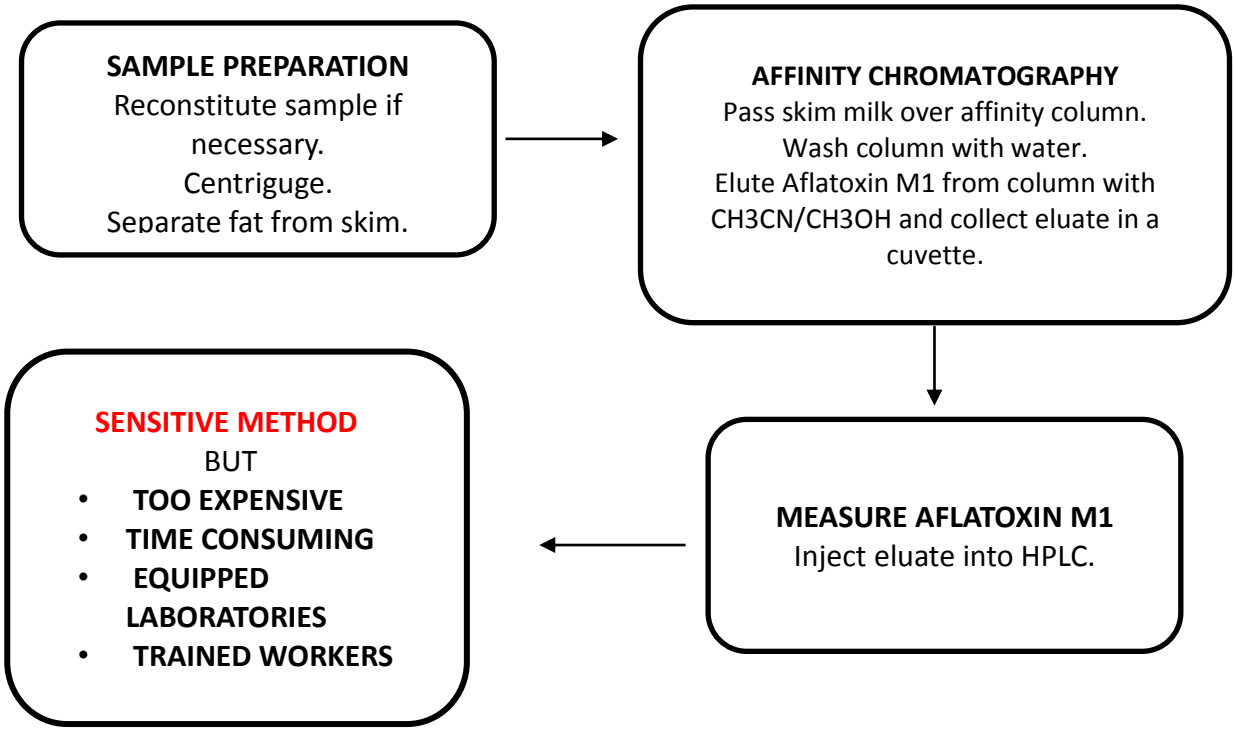

Figure 3.2: HPLC detection of AFM1 in raw milk (advantages and disadvantages).

In this work we described a miniaturized peptide-based biosensor for rapid, sensitive and specific detection of Aflatoxin M1 in complex milk samples. To this aim we developed an integrated approach to select specific peptide motif to capture aflatoxin M1. The integrated approach provides a combination of computation modeling with combinatorial peptide synthesis to screen the sequence with the highest affinity. In particular, computation modeling using a C-docker alghoritm was performed to determine the Binding energy of all possible peptide combinations against toxin, using as building blocks eight different amino-acids chosen by considering their different chemical properties. The combinatorial peptide libraries were obtained with the same building blocks and best alfatoxin binders were

selected by SPR (Surface Plasmon Resonance). Peptide sequences selected by proposed approach were easily integrated in PEGDA microparticles through a droplet microfluidic strategy in order to open the route towards a direct detection of aflatoxins in small volume both in liquid and solid environment. Droplet-microfluidics was used to produce water in oil emulsion in which reactive peptide was included directly in flow, eliminating the need for costly and time-consuming labeling steps. Computational fluidic dynamics simulation (CFD) was used to optimize the design of the device investigating the parameters that influence droplet formation. After UV polymerization the capability of PEGDA-peptide microgels to detect Aflatoxin M1 in buffer and in complex milk medium was demonstrated by confocal spectroscopy. This tool-system could be useful for producing a novel, efficient and sensitive peptide integrated microparticles to detect bio-molecular targets with higher affinity in complex medium. Our approach could be also applicable to other small molecules or contaminants whose sensitive detection is indispensable for food, biochemical or medical applications.

3.2 MATERIALS AND METHODS

3.2.1 Materials

Poly(ethylene glycol) diacrylate (PEGDA, 700 MW), the non polar solvent light mineral oil and the nonionic detergent sorbitan monooleate (Span 80) were purchased from Sigma Aldrich. Crosslinking reagent Darocur 1173 was purchased from Ciba. Reagents for peptide synthesis (Fmoc-protected amino acids, resins, activation, and deprotection reagents) were purchased from Iris Biotech GmbH (Waldershofer Str. 49-51 95615 Marktredwitz, Deutschland) and InBios (Naples, Italy). 1-ethyl-3-(3-dimethylaminopropyl)car-bodiimide hydrochloride(EDC) ,N-hydroxysuccinimide(NHS aflatoxinM1 (AFM1) and the conjugate of AFM1 with bovine serum albumin(BSA–AFM1) were fromSigma-Aldrich. Solvents for peptide synthesis and HPLC analyses were purchased from Sigma-Aldrich; reversed phase columns for peptide analysis and the LC–MS system were supplied respectively from Agilent Technologies and Waters (Milan, Italy). All SPR reagents and chips were purchased from AlfaTest (Rome, Italy). All chemicals were used as received.

3.2.2 Peptide Synthesis

Peptide libraries and single peptides were prepared by the solid phase method on a 50 μmol scale following the Fmoc strategy and using standard Fmoc-derivatized amino acids. Briefly, synthesis were performed on a fully automated multichannel peptide synthesizer Biotage® Syro Wave™. Rink amide resin (substitution 0.71 mmol/g) was used as solid support. Activation of amino acids was achieved using HBTU-HOBt-DIEA (1:1:2), whereas Fmoc deprotection was carried out using a 40% (v/v) piperidine solution in DMF. All couplings were performed for 15 minutes and deprotections for 10 minutes. For peptides library; 8 different amino acids were chosen to build the library based on their chemical and physical properties. The selected amino acids for the library construction were Arg, Asn, Pro, Trp, Leu, Ala, Asp and Thr. The resin (4,55g) was split into 64 different tubes and each reactor holds the combination of the eight amino acids, selected for the library construction, as first and second coupling. At the end of coupling procedures previously reported, we obtained 64 different di-peptides that constituted the first peptide library. The di-peptide with the best binding properties (selected by SPR technique) was chosen for the second library as two fixed amino acids present at the C-terminal of the new tetrapeptide library . Thus we split the dipeptide resin into 64 different tubes and we bound the third amino acid to the amine group of the second amino acid. At the end the fourth amino acid was linked to the third one by the same synthesis procedures. We obtained a second library composed by 64 tetrapeptides that have the same two amino acids at the C-terminus but the first two amino acids at the N-terminal are randomized with eight different building blocks . The best binding tetra-peptides, selected by SPR, were functionalized with rhodamine to monitor their entrapment in microparticles. Lysine side chain amine rhodamine labeling was achieved by on-resin treatment with rhodamine isothiocyanate (TRITC) after removing methyltrityl (Mtt) protecting group using 1% TFA in DCM for 30 min.

3.2.3 Computer Modeling

Modeling and docking studies were conducted with software package Discovery Studio version 4.5, (BIOVIA 5005 WateridgeVista Drive, San Diego, CA 92121,USA).

3.2.3.1 The aflatoxin M1 structure .

The first part of the work was to determine the structural conformation of the aflatoxin M1 molecule. A search was executed in the Protein Data Bank (PDB) for structures which contain the aflatoxin M1 molecule. Several molecules were found with the AFB1 -8, 9-exo-epoxide bound to a DNA chain; however none contained the aflatoxin M1 molecule alone. Since no structure of the aflatoxin M1 molecule was available, we tried to design it, through the Discovery Studio software with "Sketch and Edit molecules tools". Aflatoxin M1 does not contain any chiral centres. The molecule was then charged by CharMm method and molecular mechanics was applied to minimized structure using the We perfomed 200 steps of energy minimization using the "Smart Minimizer algorithm" which performs Steepest Descent, followed by Conjugate Gradient minimization. In figure 3.3 the Aflatoxin M1 sketched structure was reported.

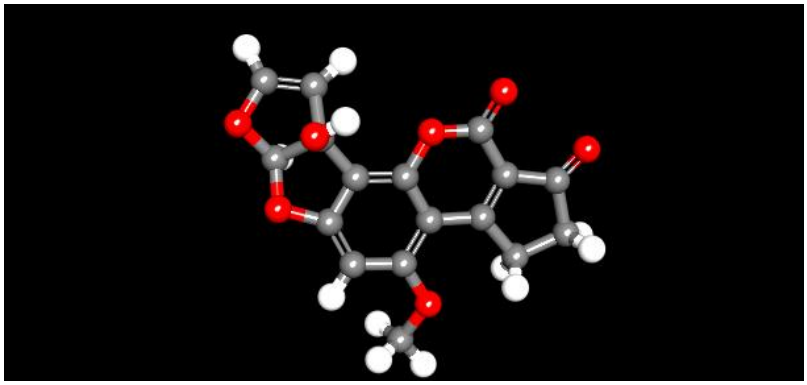

Figure 3.3: Aflatoxin M1 sketched structure by "Sketch and Edit molecules tools".

3.2.3.2 Library design.

The dataset for the monomers was set using a customized protocol to build peptides of a given length developed through the Pipeline Pilot software (version 9.5) following the scheme showed in figure 3.4. Only 8 amino acids, selected on the basis of their chemical properties, were used as building blocks of the library (A,T,D,N,R,P,W,I). The generated di-library was validated using a computational approach composing by molecular dynamics, docking algorithms and binding energy estimation. The docking procedure was used to obtain a scoring of the best di-peptide binding sequences, against the target toxin, that were used as start point to generate another tetra-peptide library using the same amino-acids, previously mentioned, as building blocks. All 64- tetra-peptides generated were validated again by the same computational approach..

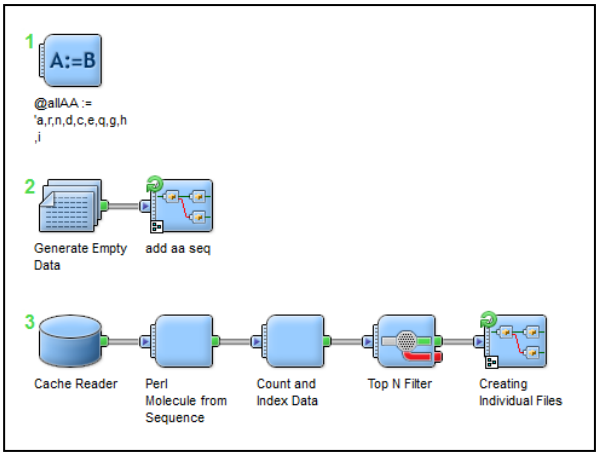

Figure 3.4: Flow chart of the protocol implemented in the Pipeline Pilot software used in this work to generate di- and tetra- peptide library.

3.2.3.3 Molecular dynamics simulation and C-docker procedure

All the 64 peptides of the di-and tetrameric library were typed with CHARMn (Biovia) force field. We perfomed 200 steps of energy minimization using the "Smart Minimizer algorithm" which performs Steepest Descent, followed by Conjugate Gradient minimization. Minimized peptide structures were solvated inside an orthorombic water box ionized with a 0.145 M salt concentration. We performed molecular dynamics simulation of the solvated peptides using the following protocol: an initial minimization stage using 1000 steps of Steepest Descent algorithm, a second minimization stage 2000 steps of Conjugate Gradient method, an 4 ps heating stage to increase the temperature from 50 K to 300 K, a 10 ps equilibration stage at 300 K and a production stage 1 ns molecular dynamics at 300 K in the NPT ensemble. Final peptide conformations from molecular dynamics were used as input receptor structures for a docking procedure. We used the CDocker protocol (BIOVIA) to generate a complex of each peptide with Aflatoxin molecule in order to calculate the binding energies between the two species and obtain the most interactive peptides against the Aflatoxin. For the best Aflatoxin M1 binding peptide discovered at the end of all screening steps, we calculated the binding energy of the complex with the "Calculate Binding Energies protocol" that estimates the binding energy between a receptor and a ligand. The binding energy was calculated using the following equation: EnergyBinding = EnergyComplex - EnergyLigand – EnergyReceptor [22].

3.2.4 Surface plasmonic resonance

The interactions between all 64 di-peptides and tetra-peptides were measured using the SPR technique with SensiQ Pioneer from AlfaTest (Rome, Italy). In order to measure the affinity of the peptides (analyte) against the aflatoxin (ligand), AflatoxinM1-conjugated BSA was immobilized at a concentration of 50 µg/mL in a 10 mM acetate buffer pH 3.7 (flow 10 µL/min, injection time 20 min) on a COOH1 SensiQ sensor chip, using EDC/NHS chemistry (0.4 M EDC - 0.1 M NHS, flow 25µl/min, injection time 4 min), achieving a 7000 RU signal. Groups reactive residues were deactivated by treatment with ethanolamine hydrochloride 1 M, pH 8.5. In order to study the aspecific binding of peptides against BSA, the reference channel was prepared by activation with EDC/NHS and immobilized with the BSA protein alone at a concentration of 50ug/mL and reaching the same RU signal of the toxin-BSA (7000). The binding assays were performed at 25 µL/min, with a contact time of 4 min, all peptides were diluted in the buffer stroke, HBS (10 mM Hepes, 150 mM NaCl, 3 mM EDTA, pH 7.4).The injection of analytes (100 µL) was performed at the indicated concentrations. The association phase (k_{on}) was followed for 180 s, whereas the dissociation phase (k_{off}) was followed for 300 s. The complete dissociation of formed active complex was achieved by addition of 10 mM NaOH, for 60 s before each new cycle start. To subtract the signal of the reference channel and evaluate the kinetic and thermodynamic parameters of the complex, the software QDAT analysis package (SensiQ Pioneer, AlfaTest) was used. For tetra-peptide library binding experiments were conducted by Fast step injection. Fast Step is an in situ-dilution method that enables stepped analyte gradient injections to be performed, where the concentration of sample steps up, or down, according to a predefined profile without reliance on dispersive mixing in a flow channel. The analyte concentration is modulated en route to the flow cell on-the-fly. This eliminates the overhead associated with multiple loading, injecting and clean up cycles making substantial reductions in time and complexity possible. The dissociation of analyte can be accurately estimated from a single dissociation phase curve recorded after the step injection is complete. The sample throughput can be increased by >10-fold compared to conventional methods. In this case an analyte concentration of 1mM was used with a flow rate of 200µL/min , a contact time of 20 sec and a dissociate time of 120 sec. As to bulk standard cycles, a 20% of sucrose was used. Kinetic parameters for all tetra- peptides were estimated assuming a 1:1 binding model and using QDAT software (SensiQ Technologies).

3.2.5 Microfluidic device

Microfluidic device consists of two inlets for the continuous and disperse phase, a narrow orifice in which the main channel and the two opposite channels converge, and a serpentine in which droplets were polymerized. The dimensions of the device are 50 × 35 µm (width × depth) for the channels solutions, 35 × 35 µm at the junction (width × depth); the serpentine is 10 cm long. The microfluidic device was fabricated by combining the conventional photolithographic and soft-lithographic techniques. Briefly, negative photoresist (Mr-DWL 40 phtoresist, Microresist technology) was spun onto a silicon wafer at 2000 rpm for 30 s to make a 35 µm thick layer of photoresist. Then, the photoresist was baked and subsequently exposed using DWL 66 Fs LASER technology system (Heidelberg instruments). After the exposed sample had been post-baked and developed, the microfluidic flow focusing device master was prepared. The surface of the device mold was treated with tridecafluoro-1,1,2,2-tetrahydrooctyl-1-trichlorosilane to facilitate the peeling off of the polydimethyl-siloxane (PDMS, Sylgard 184, Dow Corning) replica. PDMS (10:1 polymer to curing agent) was poured on the patterned silicon wafer containing negative-channels. The PDMS-based microfluidic device was peeled off from the wafer and bonded on a glass slide with oxygen plasma treatment.

3.2.6 Synthesis of Hybrid Peptide-Microgels .

Microgels were synthesized using light mineral oil containing nonionic surfactant Span 80 (5 wt%) as a continuous phase and poly(ethylene glycol)diacrylate (PEGDA) (20 wt%) with photoinitiator (0.1 wt%) and the three best Aflatoxin binding peptides (WNDNRD-(O-allyl)), WNDDRD-(O-allyl)), WNDPRD-(O-allyl)) at 80µM as disperse phase. Droplet emulsions were formed injecting prepolymer solution, the disperse phase, through the central channel whereas an oil solution, the continuous phase, through two opposite side channels. The uniform PEGDA-peptide droplets were crosslinked in flow to form monodisperse microgels. To photopolymerize droplets DAPI microscopy filter (9.8 mW, λ=360 nm) was used, focusing the UV light on the serpentine and regulating the diaphragm aperture of the microscope, for 15 s. After photopolymerization, microgels were collected in an eppendorf and washed three times with a solution of ethanol (35 v/v%) and acetone (10 v/v%) to remove the oil. After washing, microgels containing selected rhodamine-derivatized peptides were analyzed by confocal microscopy. Polyethylene tubes were connected to the inlets and outlets and the solutions were injected using high-precision syringe pumps (neMesys-low pressure) to ensure a reproducible, stable flow. This system was mounted on an inverted

microscope (IX 71 Olympus) and the droplets formation was visualized using a 4× objective and recorded with a CCD camera Imperx IGV-B0620M.

Peptides were dissolved into the disperse phase and thanks to the allyl group at the C-terminus of the sequences they could co-polymerize with the PEG for the microgels synthesis. Fluorescent rhodaminated peptides were used to control the efficient microgels synthesis. Fluorescence analysis was performed by Leica SP5 confocal microscope. Bright field and fluorescence images using a HCX IRAPO L 40×/0.95 water objective were acquired; 540 nm line of the Argon laser as excitation sources for Rhodamine-peptide was used and detection occurred at the 600-700 nm band. Images were acquired with a resolution of 1024 × 1024 pixels, zoom 1, 2.33A.U. and maximum of pinhole (Figure 3.5). All our experiments were performed at room temperature.

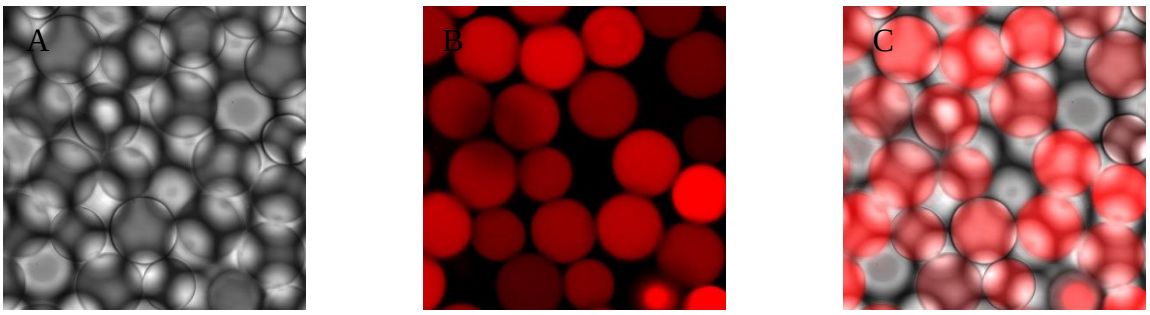

Figure 3.5: Confocal microscope images of Rhodamine-peptide microgels. A and B) Bright field and fluorescence images using a HCX IRAPO L 40×/0.95 water objective were acquired; 540 nm line of the Argon laser as excitation sources for Rhodamine-peptide was used and detection occurred at the 600-700nm band. C) Overlay of Bright field and fluorescent channels.

3.2.7 Microgels Recovery by washing steps and SEM (Scanning electron miscroscopy) characterization

Oil-dispersed microgels were recovered by an optimized washing protocol. Briefly, 1 mL of a mixed acetone/isopropanol/water solution (30:10:60) was added to the biphasic-system followed by centrifugation at 10000 rpm for 5 minutes, two times [16]. In this way the supernatant containing oil was eliminated and microgels were re-suspended in PBS buffer pH 7.4 and stored at 4°C.

In order to evaluate the correct oil elimination, SEM characterization with EDS analysis (Energy Dispersive X-ray Spectroscopy) was performed. SEM analysis was performed with a

Ultra Plus FESEM scanning electron microscope (Zeiss, Germany). 10 µL of peptide microgels and PEG-microgels (without peptides, control negative microgels) solution of 0.1mg/mL were mounted on microscope stubs, dried overnight and sputter coated with gold (approximately 7 nm thickness). The same conditions were used for microgels before and after washing protocol.

3.2.8 Fluorescamine assay

Thanks to the α amino group of the Aflatoxin binding peptides, we evaluated the efficient and homogeneous peptide co-polymerization into microgels by a fluorescamine-based assay [17]. Fluorescamine was dissolved in HPLC grade acetone (3 mg/mL) to obtain a 1 mM solution.. After 250 µM solution of fluorescamine was added to prepared samples and mixed for 15 minutes. Sample was loaded in ibidi channels and fluorescence analysis was performed by multiphoton confocal laser scanning microscopy (Leica SP5) using a two photon laser at 700nm. Objective: HCX IRAPO L 40.0x0.95 WATER section thickness 3 µm, scan speed 400 Hz, excitation MP laser 700nm, λ_{em} range 500–540nm, image size 1024 × 1024 μm^2, zoom 1, 2.33A.U. and 600µm pinhole. All experiments were conducted at room temperature. The fluorescamine assay was perfomed both for peptide microgels and control negative microgels. All captured images were analysed with a public domain image-processing program, IMAGEJ (v. 1,43i, NIH, Bethesda, MD, USA). The images were briefly thresholded by the Otsu algorithm and then processed with the ImageJ Analyze Particles function to computationally determine the number of single fluorescent particles in the range of 20 µm.

3.2.9 Aflatoxin binding and characterization in buffer and milk samples

Binding experiments were performed incubating Aflatoxin binding peptide-microgels and microgels without peptide (Control-microgels) with Aflatoxin M1-BSA conjugated in PBS (pH 7.4) at room temperature for 2 h. To demonstrate the ability of our system to detect aflatoxin, 5µL of Aflatoxin binding peptide-microgels were suspended in 100µL of PBS and different concentrations of AFM1-BSA ranging from 0.0025nM to 2nM were added and incubated for 2 h. After the incubation, microgels were directly loaded in ibidi channels without any washing in order to not affect binding equilibrium between microgels and AFM1-BSA molecules; and the auto-fluorescence of AFM1-BSA in microgels was analyzed. The same protocol was used for microgels without peptide, as a negative control. Fluorescence analysis was performed by multiphoton confocal laser scanning microscopy (Leica SP5) using a two photon laser at 700nm. Objective: HCX IRAPO L 40.0x0.95 WATER section thickness 3 µm, scan speed 400 Hz, excitation MP laser 700nm, λ_{em} range

400-500nm, image size 1024 × 1024 μm^2, zoom 1, 2.33A.U. and 600µm pinhole. All experiments were conducted at room temperature. The same experiments were performed both for peptide-microgels and control microgels dispersed into milk solutions. Skim milk was purchased from a local grocery store and spiked with the same AFM1-BSA solutions used in the protocol for buffer samples. Before binding experiments, the milk was diluted with water (1:10) in order to decrease milk-proteins concentrations and avoid aspecific signals. For milk samples experiments, even AFM1 toxin without BSA conjugation was used. All captured images were analysed with a public domain image-processing program, IMAGEJ (v. 1,43i, NIH, Bethesda, MD, USA). The images were briefly thresholded by the Otsu algorithm and then processed with the ImageJ Analyze Particles function to computationally determine the number of single fluorescent particles in the range of 20 µm.

3.3 RESULTS AND DISCUSSIONS

The aim of this work was to obtain a synthetic system that could mimic recognition properties of the antibodies and possibly substitute them into the affinity media. We exploited combinatorial chemistry to synthesize libraries from which we could select a compound with recognition properties towards Aflatoxin M1. We performed two different combinatorial approaches: Computational and Experimental. Peptides sequences selected by proposed approach was then easily co-polymerized into PEGDA microparticles opening the route towards a direct detection of aflatoxins in small volume both in liquid and solid environments.

3.3.1 Experimental library design and synthesis

The aim of this work was to obtain a synthetic system that could mimic recognition properties of the antibodies and possibly substitute them into the affinity media. We decided to exploit combinatorial chemistry to synthesize libraries from which we could select a compound with recognition properties towards Aflatoxin M1 with high affinity. We combined two different approaches: Computational and Experimental. Peptides sequences selected by proposed approach were then easily integrated in PEGDA microparticles opening the route towards a direct detection of aflatoxins in small volume both in liquid and solid environments.

Because of their chemical properties (i.e. solubility, different functional groups), their high availability and their low cost, we decided to use amino-acids to construct our library [18]. The amino-acids chosen to prepare library were Alanine (A), Arginine (R), Aspartic Acid

(D), Asparagine (N), Threonine (T), Proline (P), Isoleucine (I), Tryptophan (W), which have different functional groups in their side chains and different chemical properties; in particular we tried to choose one amino-acid for each chemical category and so we simplified the composition of the library by neglecting other amino-acids. In this way we could easily obtain a known linear peptide sequence using an 8x8 amino-acids matrix as reported in figure 3.6. As a solid phase Rink amide resin (substitution 0.71 mmol/g) was used; this support was suitable for the synthesis work because of their large size (50–100 mesh) and their easiness to handle and separate. In this way 64 different linear di-peptides were obtained. After SPR screening (See Chapter 3.3.3 for details), di-peptide "ND" with the best binding properties towards the aflatoxin M1 was used as starting point for the synthesis of a new linear tetrapeptide library. The same amino-acids previously employed were added as building blocks. The Aflatoxin M1 binding tetra-peptides were subsequently screened by SPR technique (See Chapter 3.3.3.2 for details) in order to find a high affinity binder.

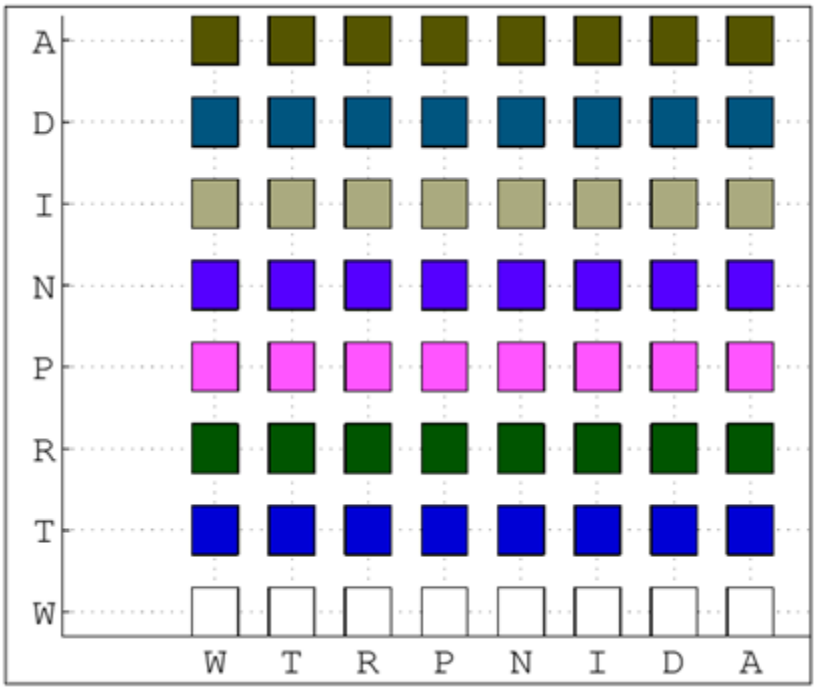

Figure 3.6: Design of parallel peptide simplified library (one amino-acid for each chemical property): 8x8 aminoacids library matrix : 8^2 = 64 possible di-peptides for each step. The same scheme was used for the construction of the tetra-peptide library using as starting point (first and second amino-acid) the best Aflatoxin M1 binding peptides screened by SPR.

3.3.2 In silico screening – Cdocker results

In silico is an expression used to mean "performed on computer or via computer simulation." It is a computational technique used in drug discovery to search libraries of small molecules in order to identify those structures which are most likely to bind to a drug target, typically a protein receptor or enzyme [19]. Given a set of structurally diverse ligands that bind to a receptor, a model of the receptor can be built by exploiting the collective information contained in such set of ligands. These are known as pharmacophore models. A candidate ligand can then be compared to the pharmacophore model to determine whether it is compatible with it and therefore likely to bind [20]. CDOCKER is a CHARMm-based docking algorithm. Using a CHARMm-based MD simulation scheme,CDOCKER docks ligands in a receptor binding site. In this method, random ligand conformations generated from a high-temperature MD are first translated into the binding site. The binding poses are searched using random rigid-body rotations, followed by simulated annealing with a grid potential. A final minimization with full forcefield potential is used to refine the ligand poses [21]. Molecular Docking experiments between Aflatoxin M1 and 64 different peptides were performed using Cdocker, an algorithm available within Discovery Studio software. In particular, all 64 structures obtained from the library (See Experimental Section for details of library construction) have been properly designed, parameterized and minimized. After this both the toxin and peptide sequences were balanced by molecular dynamic. For the assignment of the charges we have chosen CharMm method and the force-field used was the “Momany-Rone” available within the program. So the minimized sequences and toxin were analyzed by Cdocker algorithm in order to have a binding energy of the interaction. This screening was repeated twice in order to have tetrapeptides able to bind Aflatoxin M1. As to the second screening, in according to Cdocker data of the first one and the SPR data, the di-peptide sequence “ND” was chosen as starting point for the construction of the tetra-peptide library. In Figure 3.7 the binding energies of the first and second screening were reported, while best sequences of first and second screening were reported in figure 3.8. The docking results of all sequences for first and second screening were reported in Appendix of chapter 3.

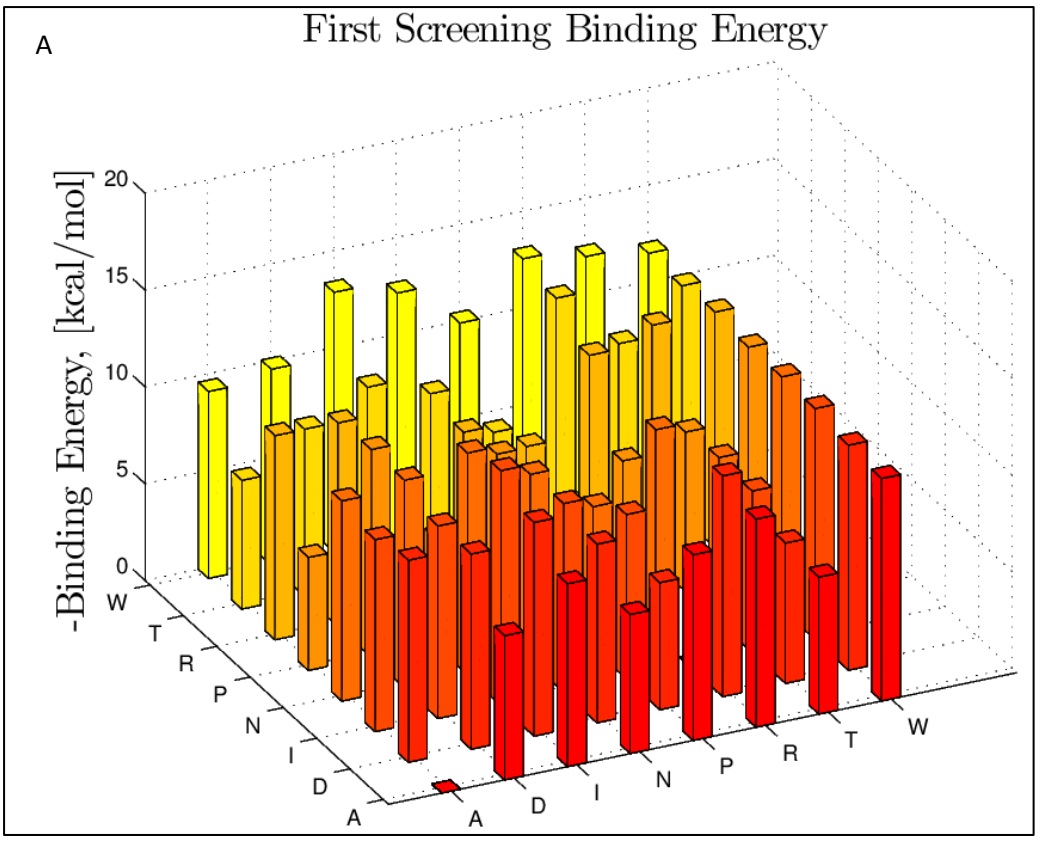

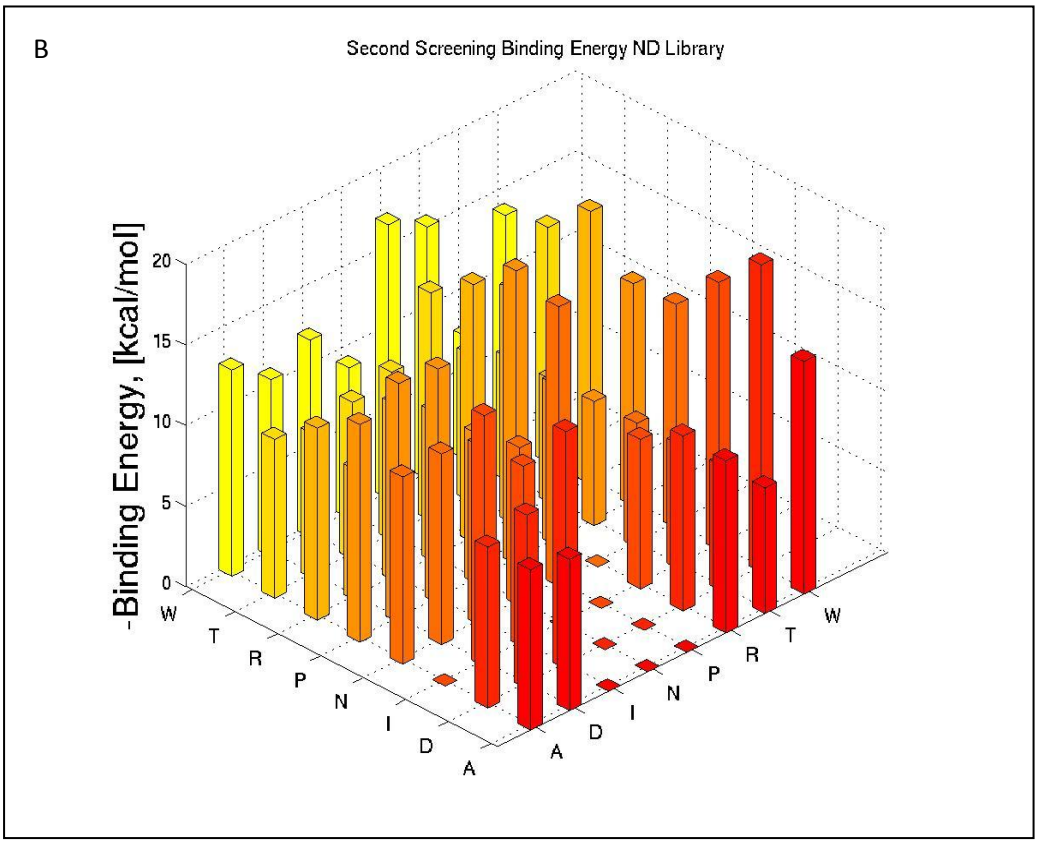

Figure 3.7: Cdocker results of first and second screening: A) Binding energy values of di-

peptide library towards Aflatoxin M1. B) Binding energy values of tetra-peptide library towards Aflatoxin M1.

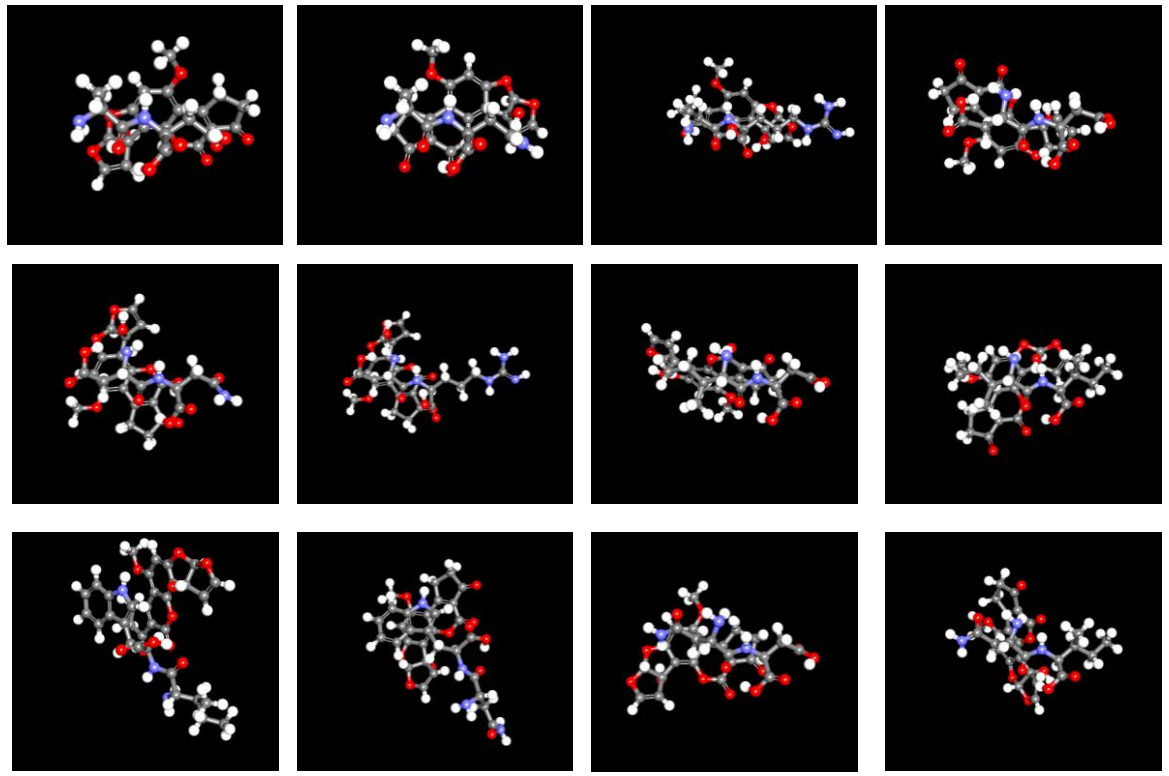

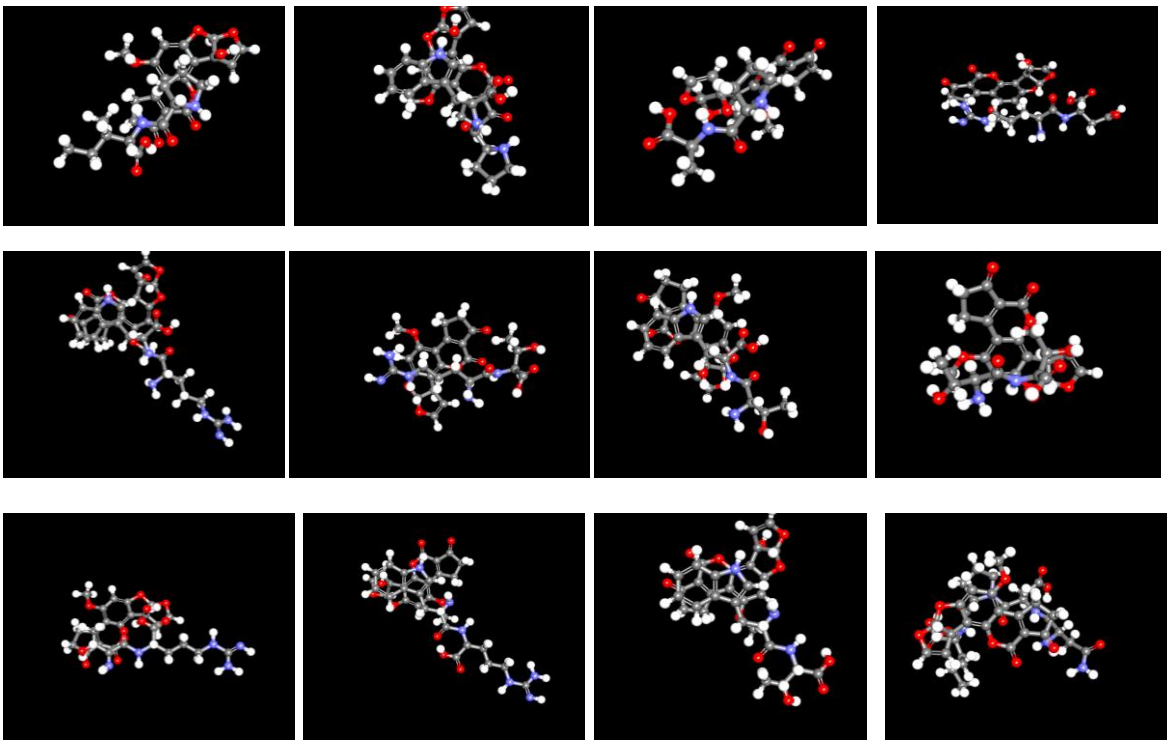

FIGURE 3.8: Best Aflatoxin M1 binding di-peptide sequences selected from first screening performed by Cdocker results. From top left to the bottom the di-peptide sequences are: AD,AN,AR,DD,DN,DR,II,IN,IW,NI,NN,NW,PI,PW,PA,RW,RT,RD,TW,TR,TT,WW,WR, WN.

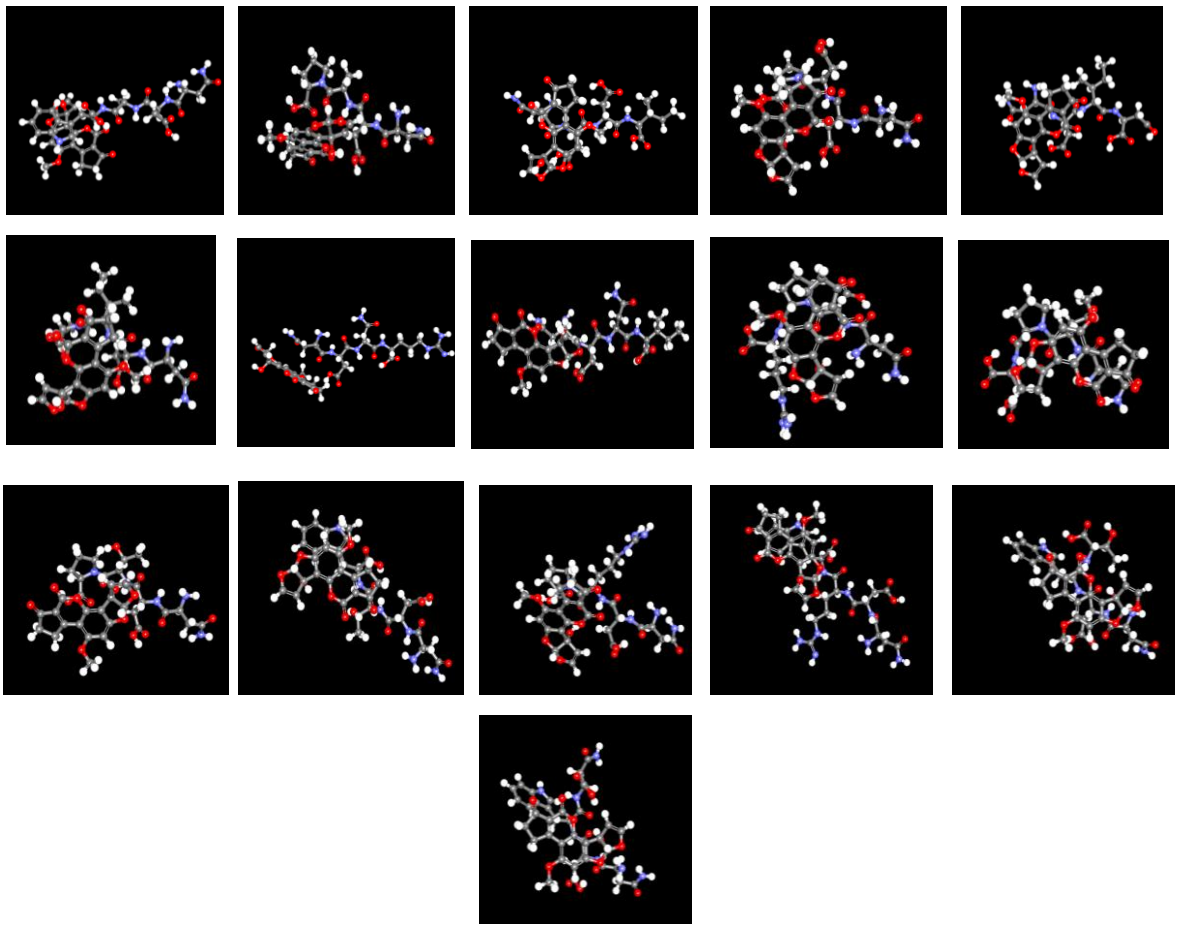

FIGURE 3.9: Best Aflatoxin M1 binding tetra-peptide sequences selected from second screening performed by Cdocker results.

From top left to the bottom the tetra-peptide sequences are: NDAP,NDAW,NDDI,NDDP,NDID,NDIP,NDNR,NDNI,NDPR,NDPD,NDTP,NDTW,NDRP,NDRW,NDWN,NDWT.

3.3.2.1 Calculation of binding energy of the complex between the best tetra-peptide sequences and Aflatoxin M1.

In according to SPR screening (See paragraph 3.3.3 for details) and Cdocker results for the tetra-peptide library, three best Aflatoxin M1 binding peptides (WNDNR,WNDDR,WNDPR) were selected to calculate also the real Binding Energy value of the formed complex between peptides and toxin [22]. In addition, we also added a tryptophan residue (W) at the N-terminal end of these three sequences in order to increase the affinity of them towards Aflatoxin M1. We decided to add this amino- acid as a sort of tag because of its aromatic properties that seem to be preferred by toxin both in Docking and SPR experiments. The tag addition increased the affinity between WNDPR peptide and toxin but it was negligible for WNDNR and WNDDR peptides. For this last two sequences, in-fact, it was not able to calculate the Binding Energy value of the total complex formed within the toxin. Despite of this we decided to use even this two peptides for material integration in according to good SPR obtained results. In figure 3.10, the complex formed by toxin and WNDPR peptide was reported and the Binding Energy value was calculated to be -48.4442 kcal/mol.

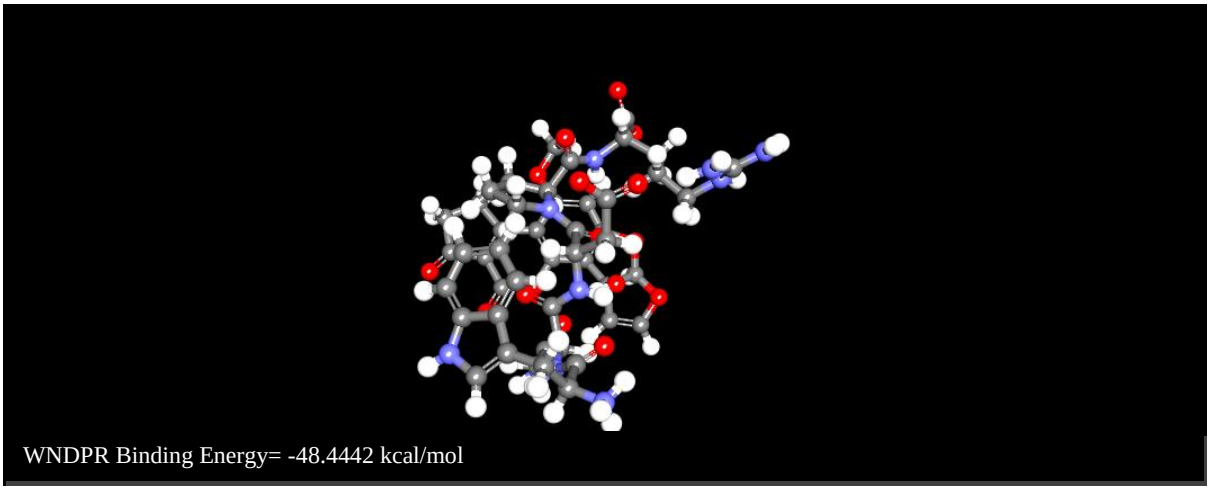

Figure 3.10: Binding Energy calculation of Aflatoxin M1/WNDPR complex.

3.3.3 Surface plasmonic resonance (SPR) results

All 64 synthesized peptides were analyzed by SPR experiments in order to evaluate their ability to bind aflatoxin. In SPR experiment Aflatoxin-M1-conjugated BSA was used as ligand and immobilized on the chip COOH1, achieving 7000 RU immobilization level according to reported conditions (see Experimental section for details).

For the first screening, the direct binding between toxin-BSA and all 64 peptides were performed by injecting a fixed concentration of 3mM of all 64 peptides using a standard

protocol. As it is possible to see in figure 3.11, the highest RU signal was given by di-peptides containing W (tryptophan) residues but they gave a high non specific signal on BSA reference channel as well (data not shown, we reported the RU values from channel one subtraction to channel 3). For this reason the Asparagine-Aspartic acid di-peptide (one letter code: ND) was chosen as starting point for the tetra-peptide library construction. This sequence, in-fact, gave a reasonable RU signal on toxin channel and no signal on BSA reference channel, highlighting the presence of a real specific binding between this di-peptide and Aflatoxin M1. For the "ND" peptide, a dose response experiment towards aflatoxin-BSA was also performed by injecting peptide solutions at increasing concentrations from 1.5µM to 1mM. Employing a 1:1 interaction model, a high micromolar dissociation value for ND peptide/ Aflatoxin M1-BSA complex was shown. A good fitting was obtained using a 1:1 interaction model. In figure 3.12 the dose-response overlay of ND sensorgrams and K_D calculation was reported. All fitted sensorgrams for entire library were reported in Appendix of chapter 3.

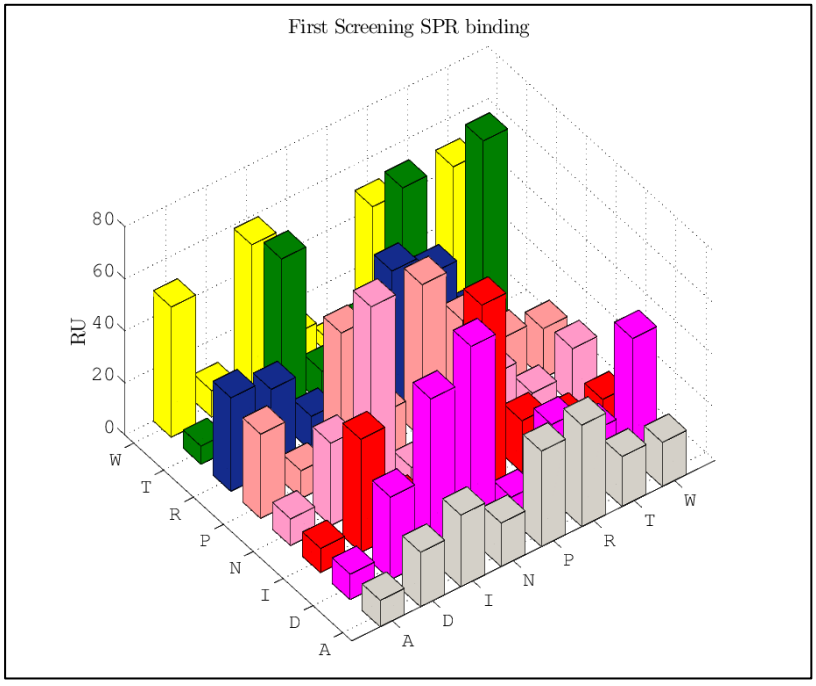

Figure 3.11: RU values of all 64 di-peptides of first screening towards Aflatoxin-M1 channel. For each peptides a fixed concentration of 3mM was injected. The final RU signal was obtained by subtracting the BSA reference channel.

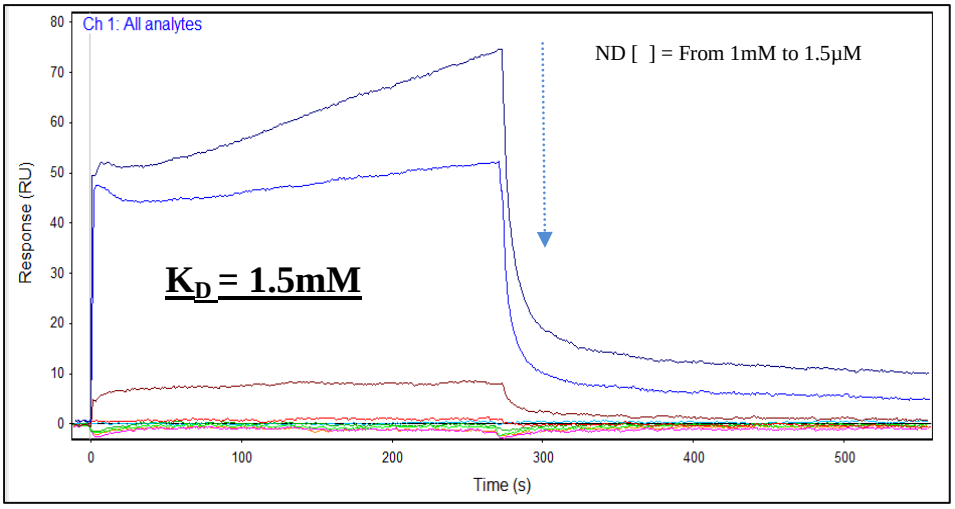

Figure 3.12: Binding of ND peptide and Aflatoxin M1 molecule. Conventional SPR experiment, analyte concentration from 1.5 µM to 1mM.

In order to improve the affinity of selected ND peptide towards toxin, a tetra-peptide library was synthesized using ND sequence as starting point. So a SPR screening of this second library was performed. To avoid aspecific signals on reference channels (Channel 2 and BSA-channel 3), due to the entrapment of small peptides on polymer surface of sensor chip using conventional method, we decided to perform a Fast injection for the second screening. Fast Step is an in situ-dilution method that enables stepped analyte gradient injections to be performed where the concentration of sample steps up, or down, according to a predefined profile without reliance on dispersive mixing in a flow channel. The analyte concentration is modulated en route to the flow cell on-the-fly [23]. This eliminates the overhead associated with multiple loading, injecting and clean up cycles making substantial reductions in time and complexity possible (Figure 3.13). The dissociation of analyte can be accurately estimated from a single dissociation phase curve recorded after the step injection is complete. The sample throughput can be increased by >10-fold compared to conventional methods.

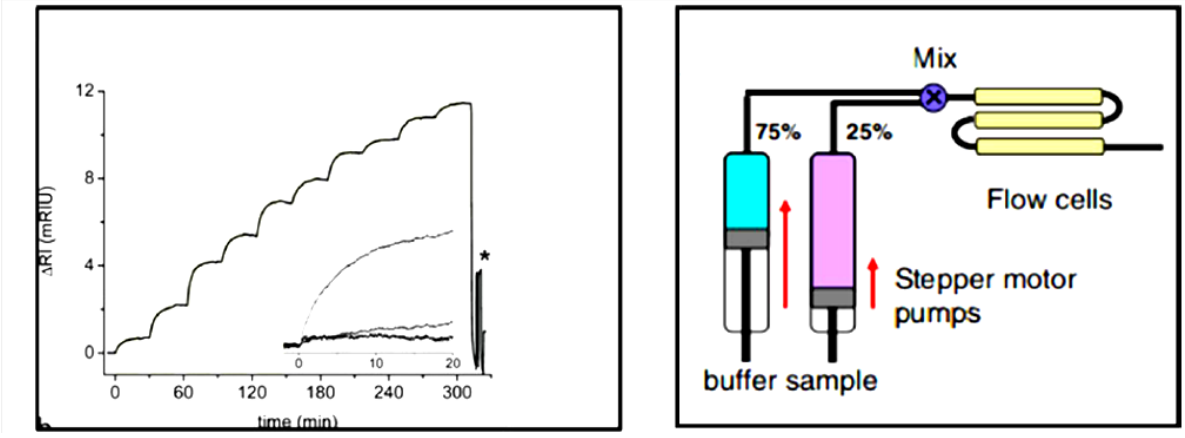

Figure 3.13: Fast step methodology.

So returning on our experiment, a fixed concentration of 500 M of all 64 tetra-peptides was injected and diluted directly into instrument flow-cell. Employing a 1:1 interaction model, a micromolar dissociation value (both with kinetic and equilibrium parameters) for six peptides (NDNR, NDRN, NDDR, NDRD, NDRP, NDPR) of the entire library was calculated as reported in figure 3.14a and b and in table 2, while for the other tetra-peptides there was no a clear association to the toxin showing typical aspecific sensorgrams with a low millimolar dissociation value, (See Appendix of chapter 3 for all fitted sensorgrams)

a

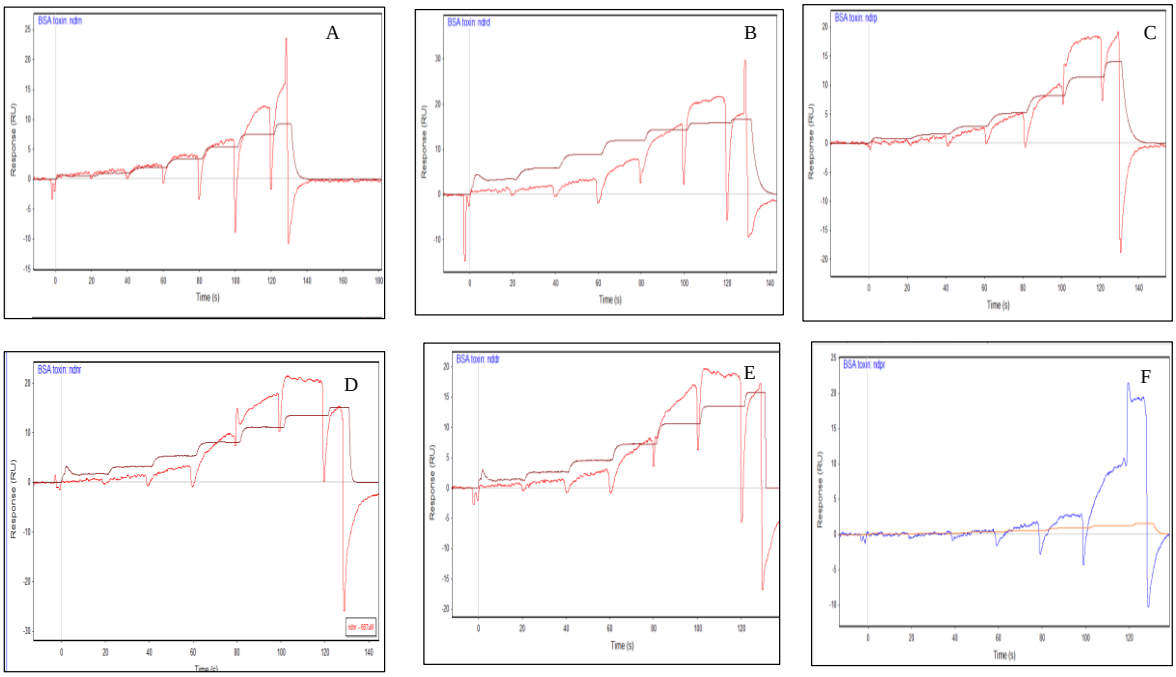

b

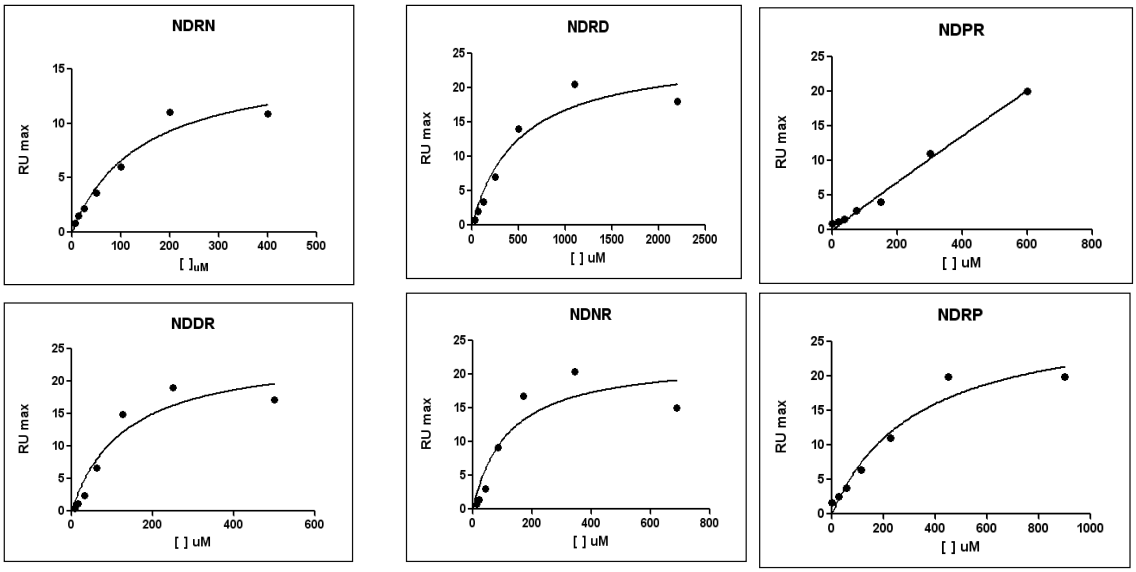

Figure 3.14: Fast step results of the best six tetra-peptides from the second screening. Fast step fitted sensorgrams using kinetic parameters (a) and equilibrium parameters (b). (a)From the top left the sequences reported are: NDRN, NDRD, NDRP, NDDR, NDNR, NDPR. The K_D values are reported in table below.

Table 2: KD evaluation with kinetic and equilibrium parameters.

Best sequence	**Kinetic**	**Equilibrium**
	K_D (μM)	K_D (μM)
NDRN	**161±20**	**139C**
NDRD	**49±100**	**500±100**
NDRP	**330±20**	**328±117**
NDNR	**98±30**	**116±41**
NDDR	**100±21**	**129±20**
NDPR	Not detectable	800±10

In according to Docking experiments three of these sequences (NDNR,NDDR,NDPR) were selected for material integration and for biosensors development. In particular even if the

sequence NDPR had a high K_D constant value, we decided to choose it on the basis of docking results because it was the best Aflatoxin M1binding peptide selected from docking screening.

To these three sequences, we decided as previously mentioned to add a W residue at the N-terminal portion with the aim to improve more the affinity of the NDNR, NDDR and NDPR peptides towards Aflatoxin M1.

As Docking results, the tag addition was very satisfying for NDPR sequence but was negligible for NDNR and NDDR peptides. Even in this experiment a Fast step injection was performed using a fixed concentration of 500µM for all three peptides. A low micro-molar dissociation value, employing a 1:1 interaction model was calculated as reported in figure 3.15. All RU signal were subtracted to BSA reference channel.

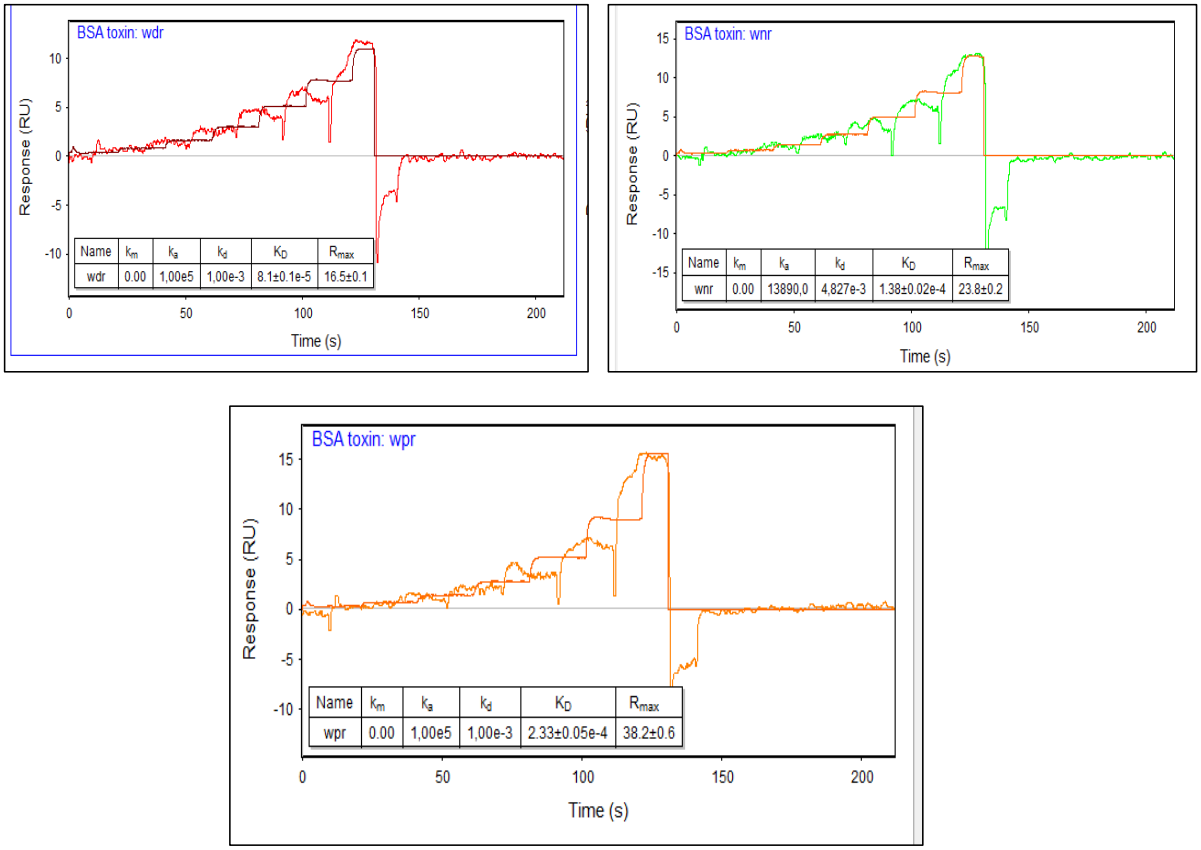

Figure 3.15: Fast step injection of the best three selected tetra-peptides with tag (W residue) addition. From the top left the sequence are: WNDDR, WNDNR,WNDPR. For all peptides a concentration of 500µM was used and a low micro-molar dissociation value, employing a 1:1 interaction model was calculated. For WNDDR the KD was about 81±0.5µM, for WNDNR was 138±0.02 µM and for WNDPR was about 233±0.05µM.

So at the end of all library screening we decided to use the sequences: WNDNR, WNDDR,WNDPR to development and synthesized the final biosensor.

3.3.4 PEGDA-peptide microgels synthesis and characterization

Here microfluidic synthesis of biodegradable PEGDA-peptide microgels for Aflatoxin M1 detection was reported. To functionalize the microgels we used three different tetra-peptides sequences selected from Docking experiments and SPR technology. In order to co-polymerize these sequences with PEG into microgels, an allyl group at the C-terminal end of each peptide was added. Microgels synthesis and peptide attachment was described in Experimental Section. Briefly, the pre-polymer solution containing selected peptides (WNDNRD(allyl), or WNDDRD(allyl), or WNDPRD(allyl)) was injected through the central channel of the microfluidic device, as disperse phase, and an oil solution with surfactant was flushed through its two opposite side channels, as continuous phase. Under optimized flow rate conditions, estimated by CFD simulation, disperse phase was sheared into monodisperse droplets by continuous phase. Based on flow conditions, the yield of microgel production was around 300 microgel/minutes and the number of microgels was about $2x10^6$ particles/mL. This number was calculated using a cell counting chamber (data not shown). Alfatoxin M1 binding peptide-microgels obtained are monodisperse in size and peptide encapsulation was confirmed by confocal image (Figure 3.5 in Experimental section). PEGDA has been chosen for its advantages over other polymers and its specific proprieties, such as good biocompatibility, non-toxicity, low immunogenicity *in vivo*, and resistance to protein adsorption. Moreover, polyethylene glycol (PEG) hydrogels are widely used in biomedical fields such as drug delivery and tissue engineering [24, 25].

3.3.5 Microgels Recovery by washing steps and SEM (Scanning electron miscroscopy) characterization

In order to evaluate the correct oil elimination, SEM characterization with EDS analysis (Energy Dispersive X-ray Spectroscopy) was performed. For recovery protocol a solution of acetone/isopropanol/water (30/10/60) was used. This mixture caused a significant change in particle shape and surface morphology, as shown in Figure 3.16 A and B, where microgels washed and not washed were represented. In particular washed microgels had a good sphericity and a rough surface. The roughness was once more due to use of dehydrating solvents. Water extraction appears to change the PEGDA microgels network. Unlike, not good sphericity and smooth surface was detected on not washed microgels structure. The smooth and dense microgels surface were due to residual surfactants and oil (data confirmed

also by UV spectra, not shown here), as it is possible to see in EDS experiments (figure 3.17) [16]. All these considerations were validated both for peptide-microgels and control-negative microgels.

A

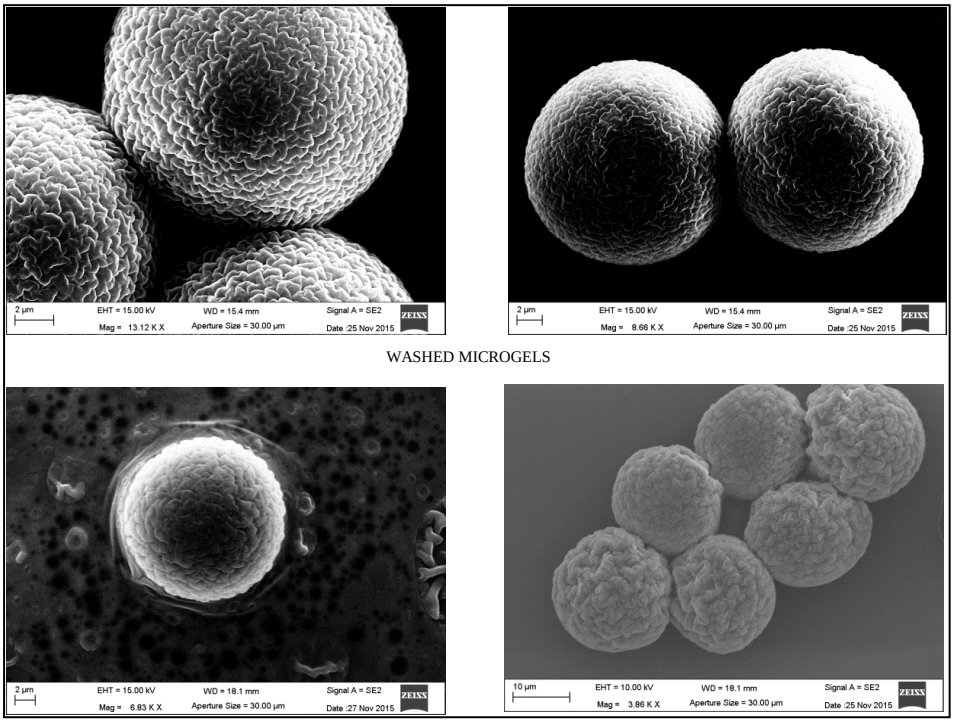

B

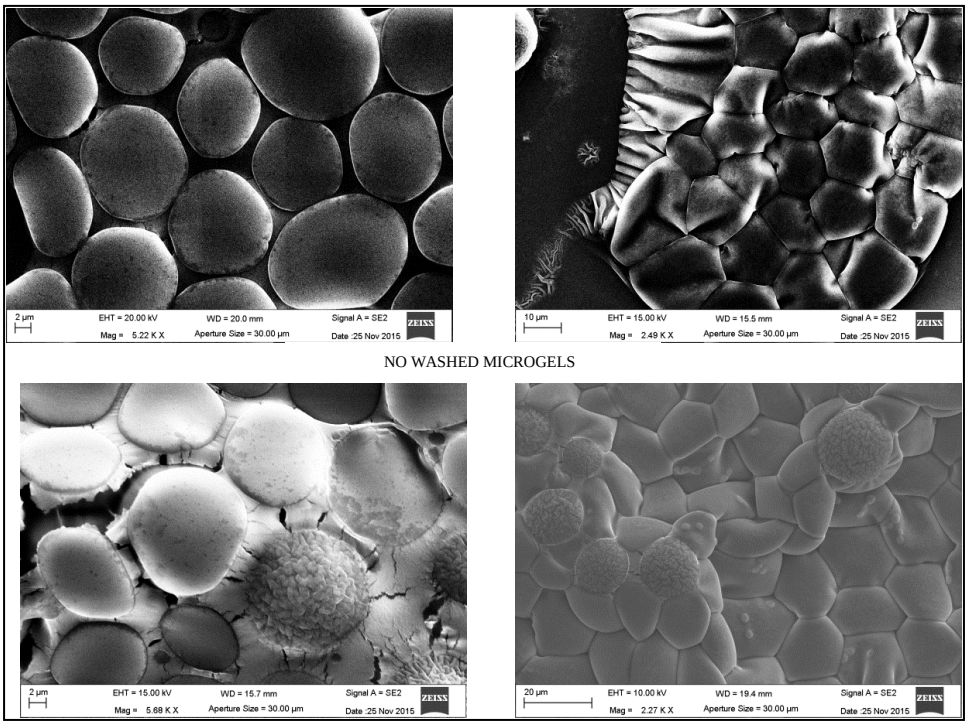

Figure 3.16: SEM images of peptide and control negative microgels. A) Washed microgels: From the top left the WNDPR, WNDNR, WNDDR and PEG microgels were represented. They showed a good sphericity and a rough surface. The roughness was once more due to use of dehydrating solvents. B) No washed microgels: From the top left the WNDPR, WNDNR, WNDDR and PEG microgels were represented; They had not good sphericity and smooth surface. The smooth and dense microgels surface were due to residual surfactants and oil.

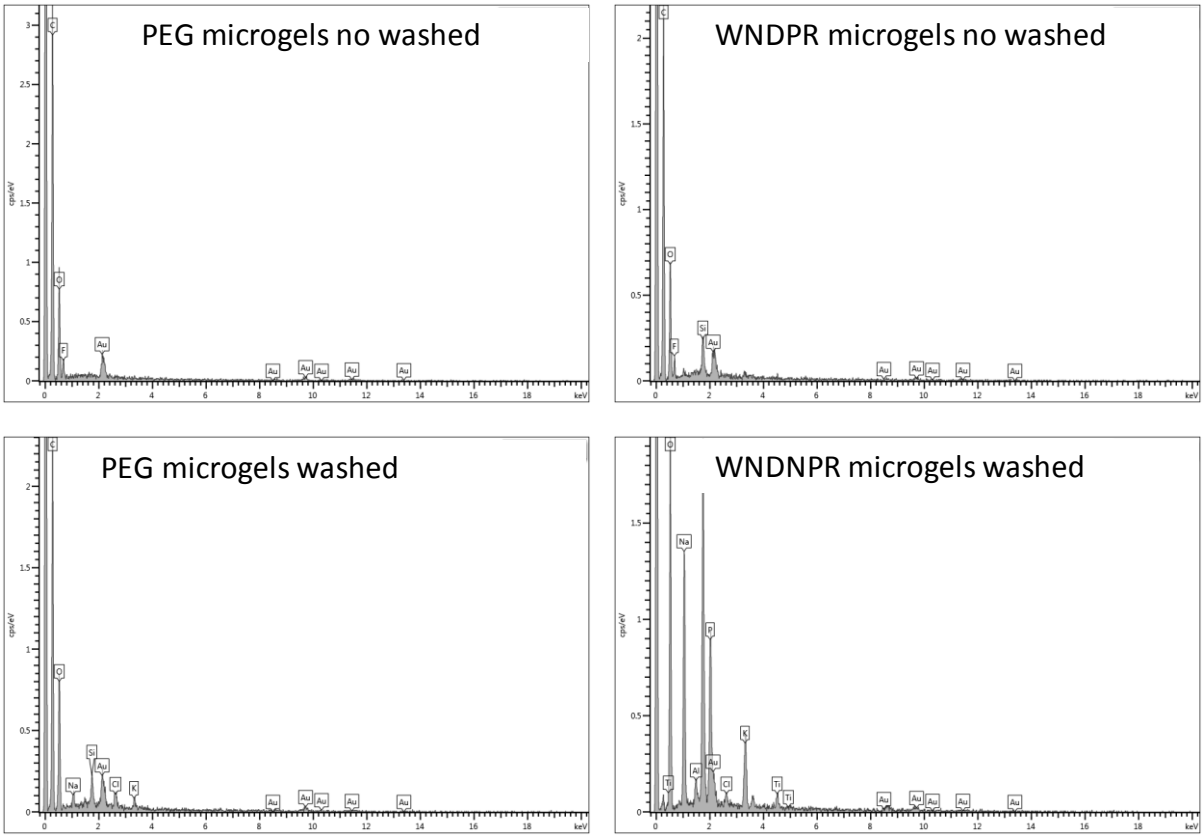

Figure 3.17: Example of EDS images for control negative microgels and WNDPR ones. On the top the no washed microgels were represented. In this image it is possible to see the presecence of oil and surfactants retained on microgels surface. On the bottom of the figure, the washed microgels were reported. In this case it is possible to see only the presence of cationic and anionic elements presented in buffer solution.

3.3.6 Fluorescamine assay

Thanks to the α amino group of the Aflatoxin binding peptides, we evaluated the efficient and homogeneous peptide co-polymerization into microgels by a fluorescamine-based assay. Fluorescamine is a common probe used to quantify protein or peptides in complex solutions. The non-fluorescent compound, fluorescamine, reacts rapidly with primary amines in

proteins, such as the terminal amino group of peptides and the e-amino group of lysine, to form highly fluorescent moieties [26-28]. In our work, four different samples for each peptide microgels were treated with 250μM of fluorescamine solution for 15 minutes. The images were performed by multiphoton confocal laser scanning microscopy using a two photon laser at 700nm and the fluorescence analyzed by ImageJ tools (Figure 3.19), (See Experimental section for details). As we can see in the figure 3.18, the amount of peptides all over microgels structure was homogeneous. The same experiment was performed for control negative microgels.

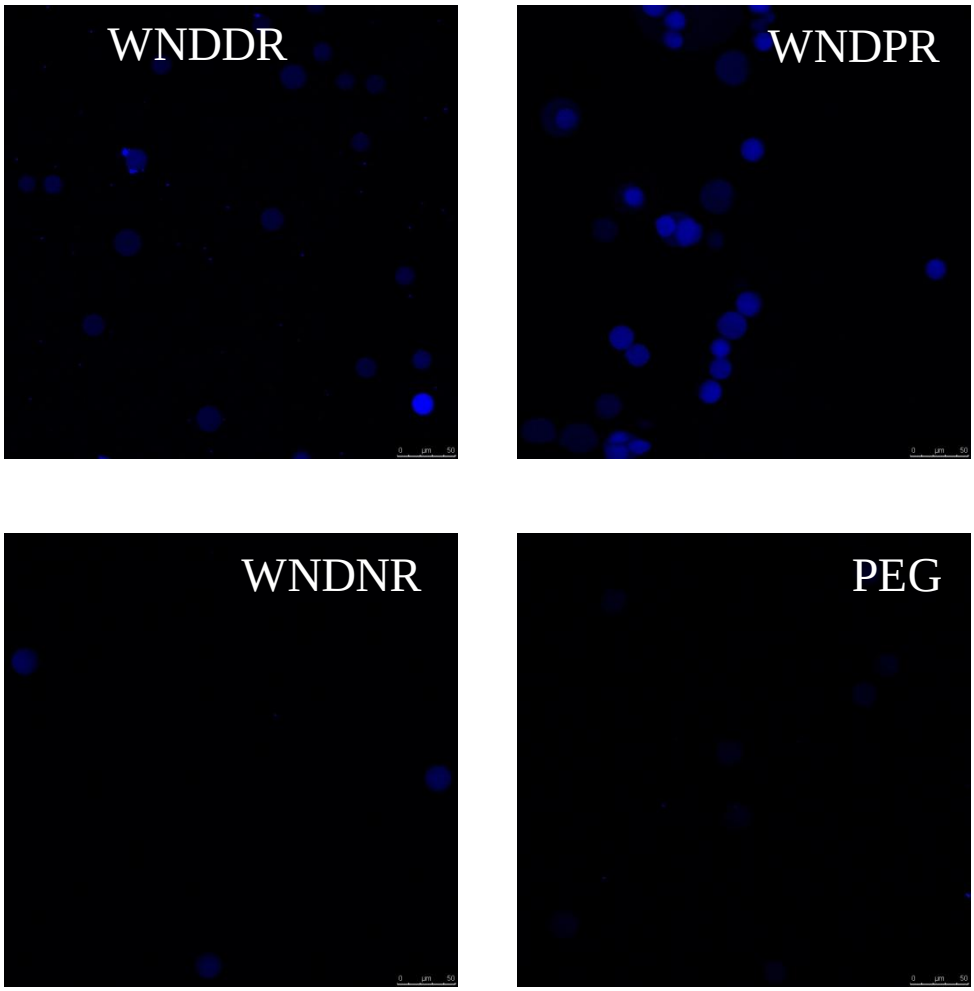

Figure 3.18: Fluorescamine assay. Multiphoton confocal laser scanning miroscopy images, excitation laser 700nm. The amount of peptide into microgels was homogeneous. For control negative microgels, the signal was very low similar to the laser background.

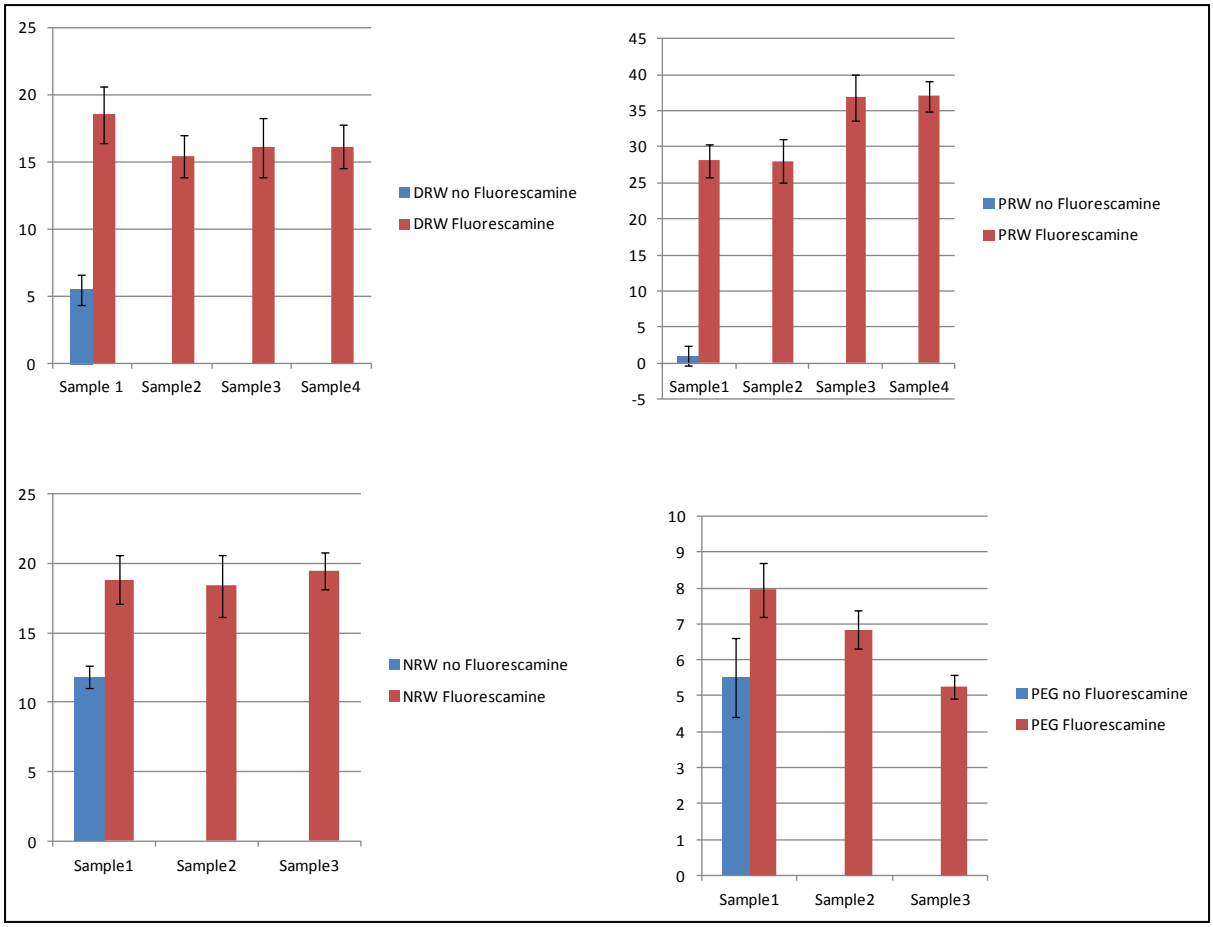

Figure 3.19: Fluorescence quantification by Image J tool. The amount of peptides into microgels was reproducible and homogeneous. The fluorescence signal of control negative microgels was very low, similar to no functionalized microgels.

3.3.7 Aflatoxin M1-BSA conjugated binding and characterization in buffer samples

The use of peptide-binding small molecules in polymeric networks is useful to have a selective platform for small molecules detection in complex mixtures. The binding between Aflatoxin M1-conjugated BSA and WNDNR,WNDDR,WNDPR peptides were determined suspending peptide-microgels in several buffer solutions containing different concentrations of toxin (see Experimental section for details). The selective binding of our system was demonstrated using the same protocol for control negative-microgels synthesized without peptide. All images were perfomed by multiphoton confocal scanning microscopy using 700 nm as excitation laser. The quantification of Aflatoxin M1-BSA into microgels was performed by ImageJ tools, analyzing the fluorescence of the toxin into the single microgel. All three peptides were able to bind toxin, even if the best sequence is the peptide WNDPR in according with Docking results as well. In particular, in-fact, the WNDNR and WNDDR were not able to reach a saturation point in the range of concentrations used in this work,

while the WNDPR peptide reached a saturation just at concentration of 0.1nM, that was the legal accepted limit by *Normativa 10 del 9-6-99; recepimento Reg.CEE 1528/98.* So the integration of this new discovered peptide in a PEGDA microgel was very useful for the development of a biosensor for Aflatoxin contamination detection in foodstuff at very low concentrations. In figure 3.20 A, B, and C the fluorescence images of binding between aflatoxin and peptide-microgels were reported, also the control-negative microgel images were represented (Figure 3.20 D). In figure 3.21, the quantification of fluorescence intensity of WNDPR microgels after binding was reported. It was dose-responsive and specific with a K_D about picomolar range. The fitting of other sequences was not reported because of their not saturation point reaching. For this reason and because of the accepted limit of Aflatoxin M1 in food are very low, we decided to select only WNDPR peptide for experiments in milk solutions.

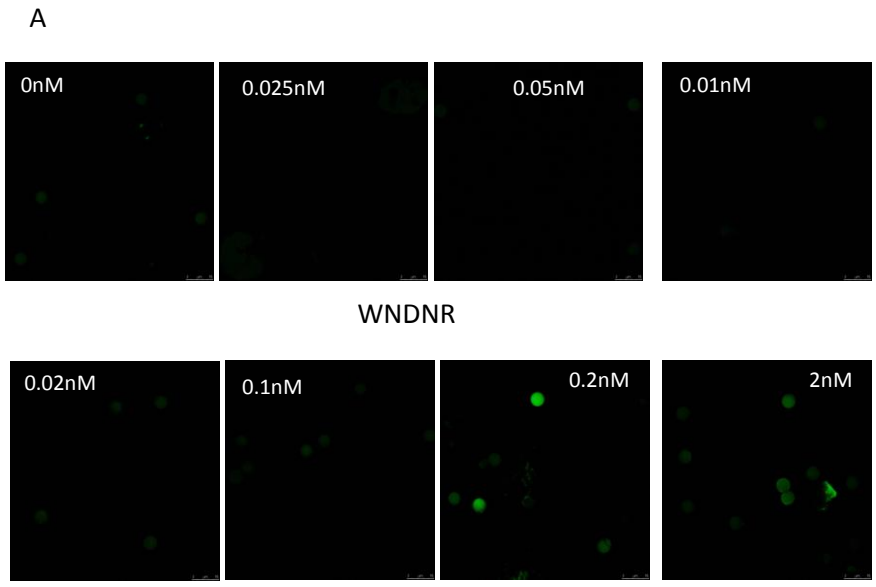

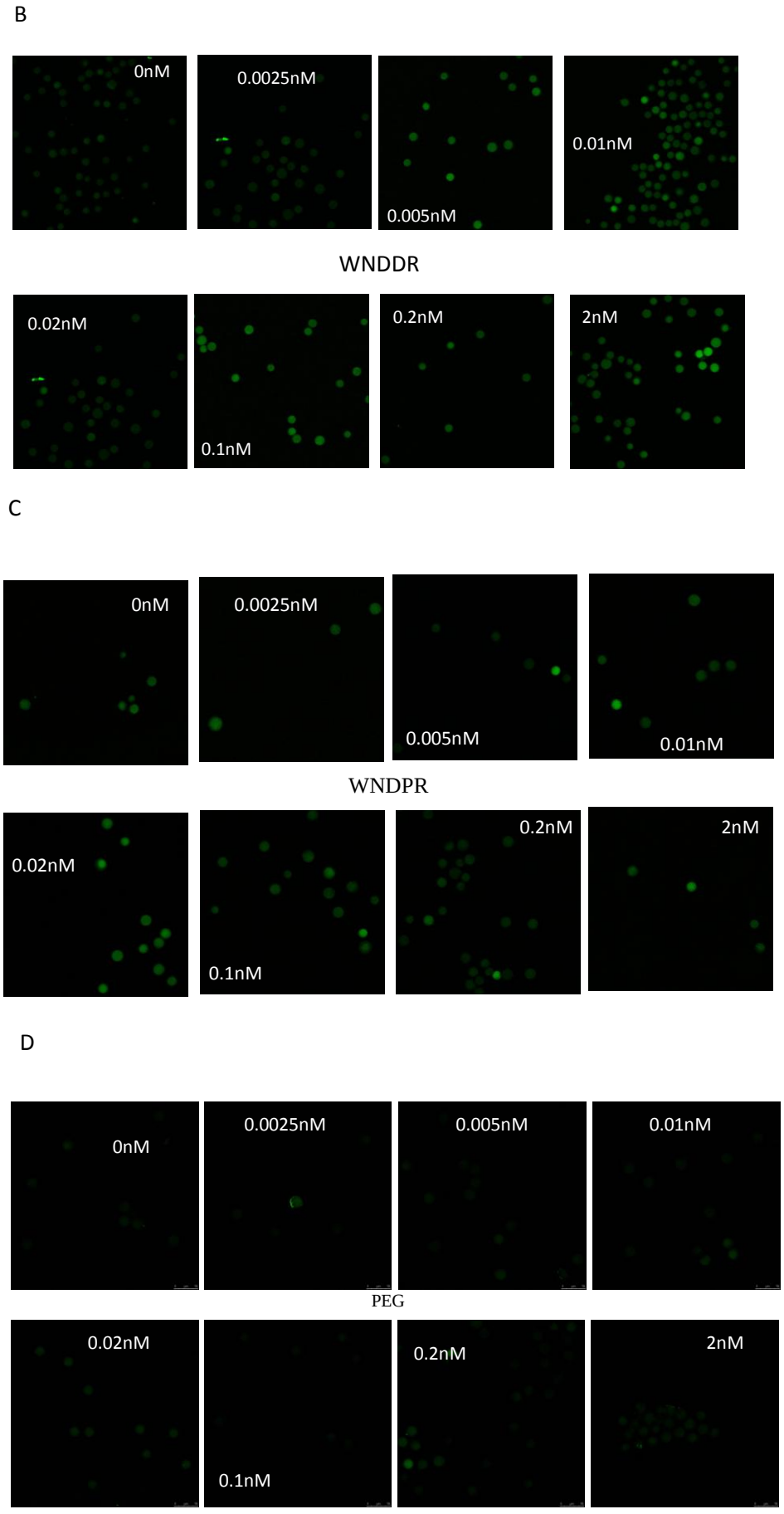

Figure 3.20: Multiphoton confocal images of binding between Aflatoxin M1-BSA conjugated

and WNDNR (A), WNDDR (B), WNDPR (C) and control negative microgels (D). Excitation laser 700nm, emission 400-500nm.

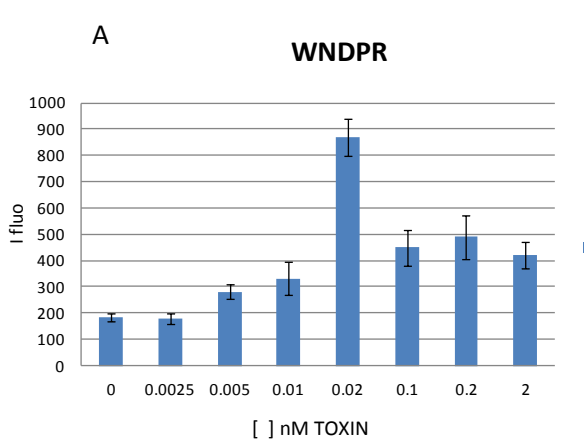

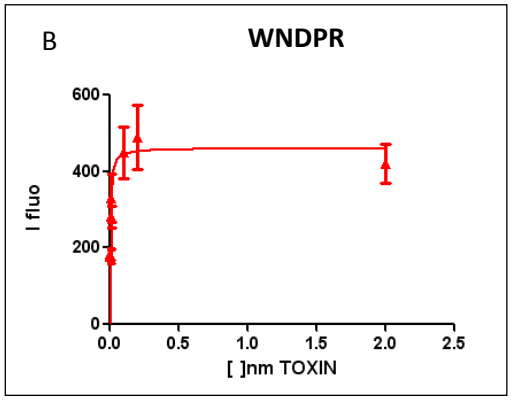

K_D= 3.59±2.0 pM

C

One site -- Specific binding	
Best-fit values	
Bmax	460.8
Kd	0.003591
Std. Error	
Bmax	51.67
Kd	0.002018
95% Confidence Intervals	
Bmax	327.9 to 593.6
Kd	-0.001598 to 0.008779
Goodness of Fit	
Degrees of Freedom	5
R^2	0.6162
Absolute Sum of Squares	36528
Sy.x	85.47
Number of points	
Analyzed	7

Figure 3.21: Quantification of fluorescent intensity of WNDPR microgels. A) Quantification of fluorescent of single microgels using ImageJ tools. B) Fitting of binding event between WNDPR peptide and Aflatoxin M1-conjugated BSA using a One-site specific binding as model with a non linear regression approach (C).

3.3.8 Aflatoxin M1-BSA conjugated binding and characterization in milk samples

Aflatoxin M1 (AFM1) in milk and milk products is considered to pose certain hygienic risks for human health. Human beings that ingest aflatoxin B1 contaminated diets eliminate into milk amounts of the principal 4-hydroxylated metabolite known as “milk-toxin” or aflatoxin M1,(figure 3.1) [29]. International Agency for Research on Cancer (IARC, 1993) classified AFB1 and AFM1 as class 1 and 2B (or probable) human carcinogens, respectively, (milk review). It seems that milk has the greatest demonstrated potential for introducing aflatoxin residues from edible animal tissues into human diet. Moreover, as milk is the main nutrient for growing young, whose vulnerability is notable and potentially more sensitive than that of adults, the occurrence of AFM1 in human breast milk, commercially available milk, and milk

products is one of the most serious problems of food hygiene [29]. Because of the complexity of milk matrix, it is very difficult to process and destroy Aflatoxin M1 contamination without losing milk properties. For this reason we develop a peptide-based biosensor that is able to recognize aflatoxin in a very sensitive way.

On the basis of experiments of previous paragraphs, we decided to use only WNDPR as selected peptide to synthesize and develop our final biosensor. This peptide sequence, in-fact, showed the best binding properties towards Aflatoxin M1 when it was integrated in PEGDA microgels. These results were consistent with Docking experiments as well. Skim milk was purchased from a local grocery store and spiked with the same AFM1-BSA solutions used in the protocol for buffer samples (See Experimental section for details). Before binding experiments, the milk was diluted with water (1:10) in order to decrease milk-proteins concentrations and avoid aspecific signals. The selective binding of our system was demonstrated using the same protocol for control negative-microgels synthesized without peptide. All images were performed by multiphoton confocal scanning microscopy using 700 nm as excitation laser and 400-500 nm as emission laser. The quantification of Aflatoxin M1 autofluorescence into microgels was performed by ImageJ tools, analyzing the fluorescence of the single microgel. Even in this case, the peptide WNDPR showed a very good and specific recognition properties towards toxin also at very low aflatoxin concentrations respecting the legal accepted limit by *Normativa 10 del 9-6-99; recepimento Reg.CEE 1528/98.* This confirm the ability of our peptide to detect aflatoxin also in milk sample in a very sensitive way. In figure 3.22 A the fluorescence images of binding between aflatoxin and WNDPR microgels were reported, also the control-negative microgel images were represented (Figure 3.22 B). In figure 3.23 A the quantification of fluorescence intensity of WNDPR microgels after binding was reported. It was dose-responsive and specific signal with a K_D about low nanomolar range (B-C). For control negative microgels the fluorescence signal was very low respect to WNDPR microgels and the fitting was not evaluable, (figure 3.24 A,B,C,D).

A

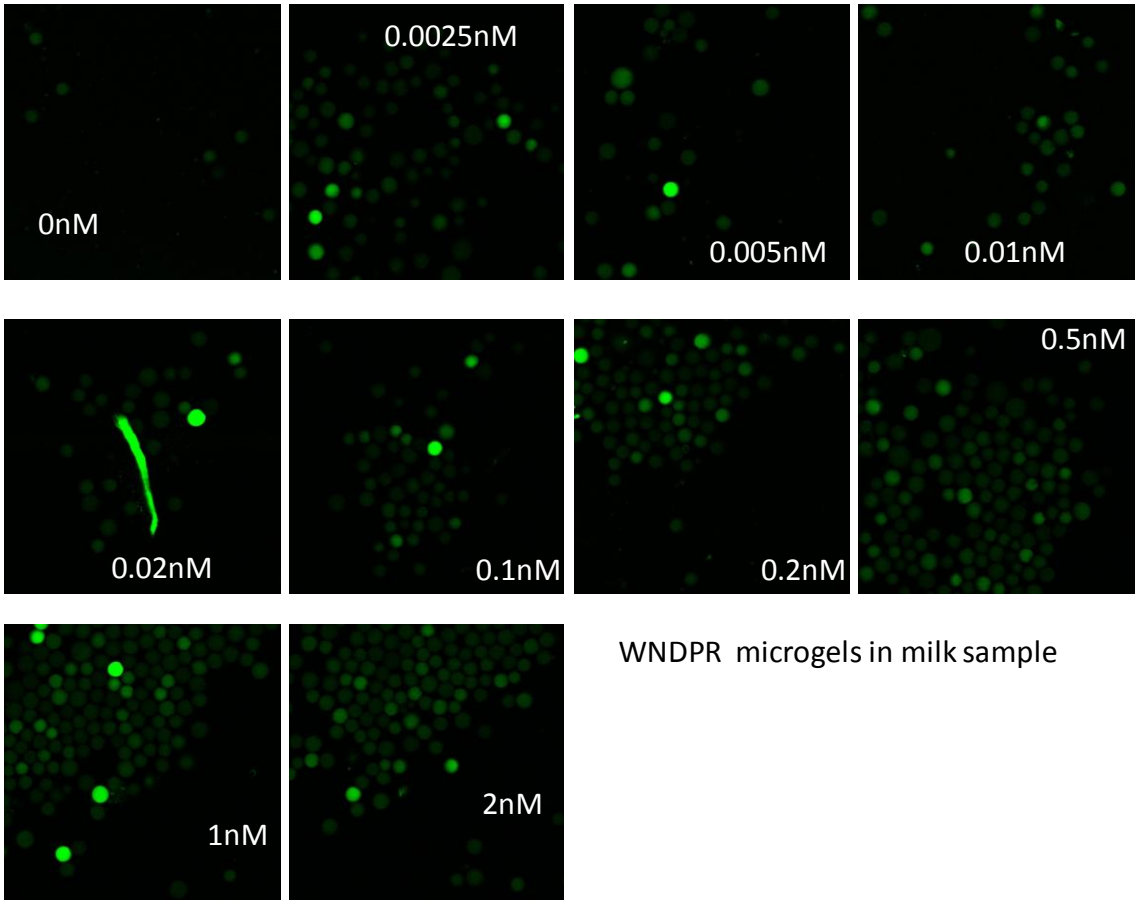

B

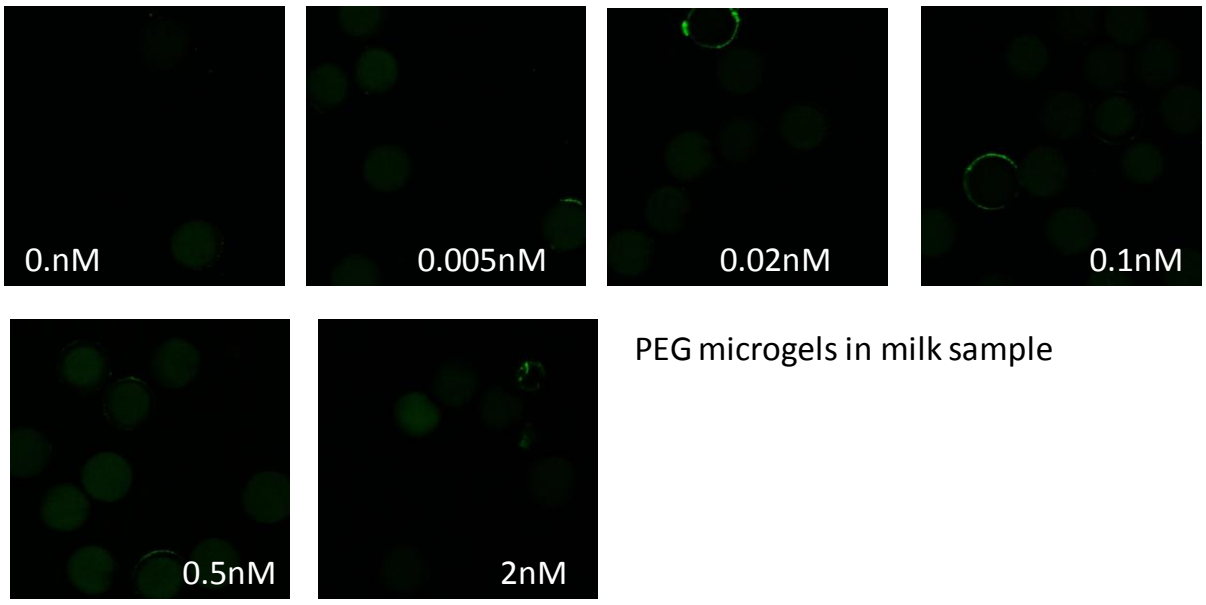

Figure 3.22: Multiphoton confocal images of binding between Aflatoxin M1-BSA conjugated and (A) WNDPR peptide and (B) control negative microgels in milk sample. Excitation laser 700nm, emission 400-500nm.

A

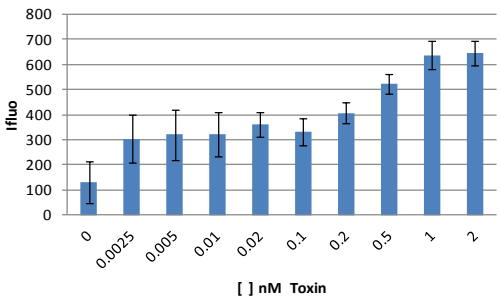

B

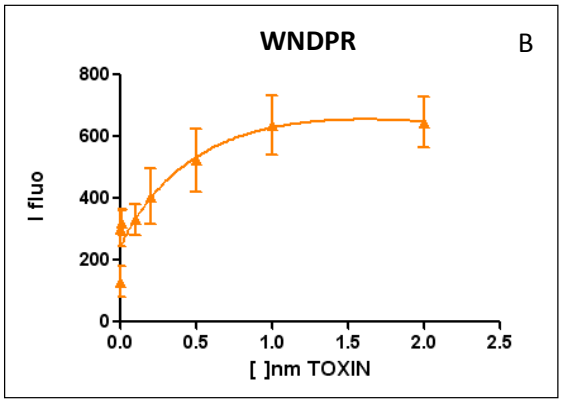

C

One site -- Total	
Best-fit values	
Bmax	923.3
Kd	0.8075
NS	-127.5
Background	245.5
Std. Error	
Bmax	1569
Kd	1.575
NS	398.2
Background	42.49
95% Confidence Intervals	
Bmax	-3432 to 5279
Kd	-3.566 to 5.181
NS	-1233 to 977.9
Background	127.5 to 363.4
Goodness of Fit	
Degrees of Freedom	4
R^2	0.9067
Absolute Sum of Squares	20908
Sy.x	72.30
Number of points	
Analyzed	8

K_D= 0.81±1.57nM

Figure 3.23: Quantification of fluorescent intensity of WNDPR microgels in milk sample. A) Quantification of fluorescent signal of single microgels using ImageJ tools. B) Fitting of binding event between WNDPR peptide and Aflatoxin M1-BSA conjugated using a One-site total binding as model with a non linear regression approach (C).

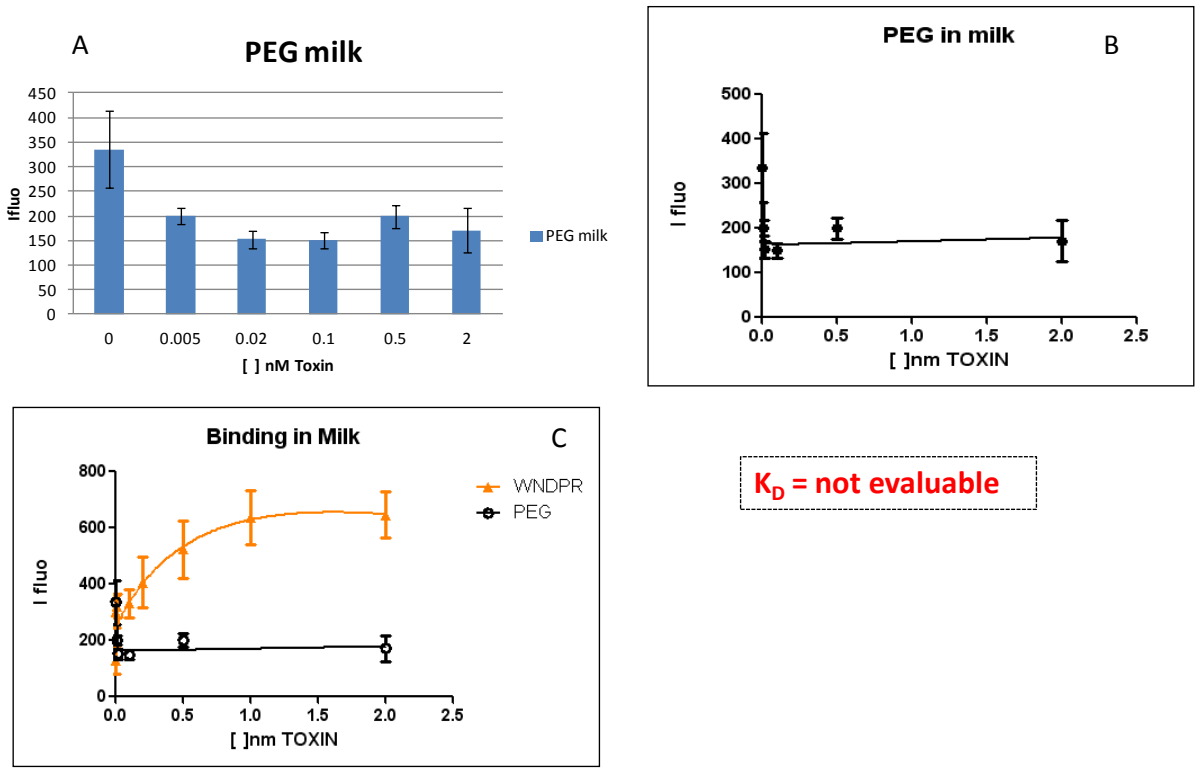

Figure 3.24: Quantification of fluorescent intensity of control negative microgels in milk sample. A) Quantification of fluorescent signal of single microgels using ImageJ tools. B) Fitting of binding event between control negative microgels and Aflatoxin M1-BSA conjugated using a One-site total binding as model with a non linear regression approach, K_D not evaluable. C) Comparison of fitting of WNDPR microgels and control negative microgels using a One-site total binding as model with a non linear regression approach.

In order to improve sensibility of our biosensor, we decided to change microgels numbers in binding experiments. A dilution of 1:10 about microgel solution was used to perform new binding experiments, in this case the number of microgels in contact with aflatoxin was about 80. Using a lower number of microgels, we were able to improve biosensor sensibility in aflatoxin recognition at very low concentrations (Figure 3.25). On the basis of these new results, we can confirm that our system could be a promising discovery in aflatoxin detection in milk samples.

3.3.8.1 Aflatoxin M1 binding and characterization in milk samples

With the aim to confirm the real specificity and sensibility of our biosensor, a binding assay between WNDPR microgels and the only Aflatoxin M1 without BSA conjugation was performed. For this experiment four different concentrations of aflatoxin were used: 0, 0.01, 0.1, 2 nM. All images were performed by multiphoton confocal scanning microscopy using 700 nm as excitation laser and 400-500 nm as emission laser. The quantification of Aflatoxin M1 auto-fluorescence into microgels was performed by ImageJ tools, analyzing the fluorescence of the single microgel. As it is possible to see in figure 3.26 A and B,C,D, the biosensor developed in this work was able to recognize aflatoxin contamination in milk sample in a very specific manner, opening an important way in aflatoxin food contamination in the agricultural and industrial fields.

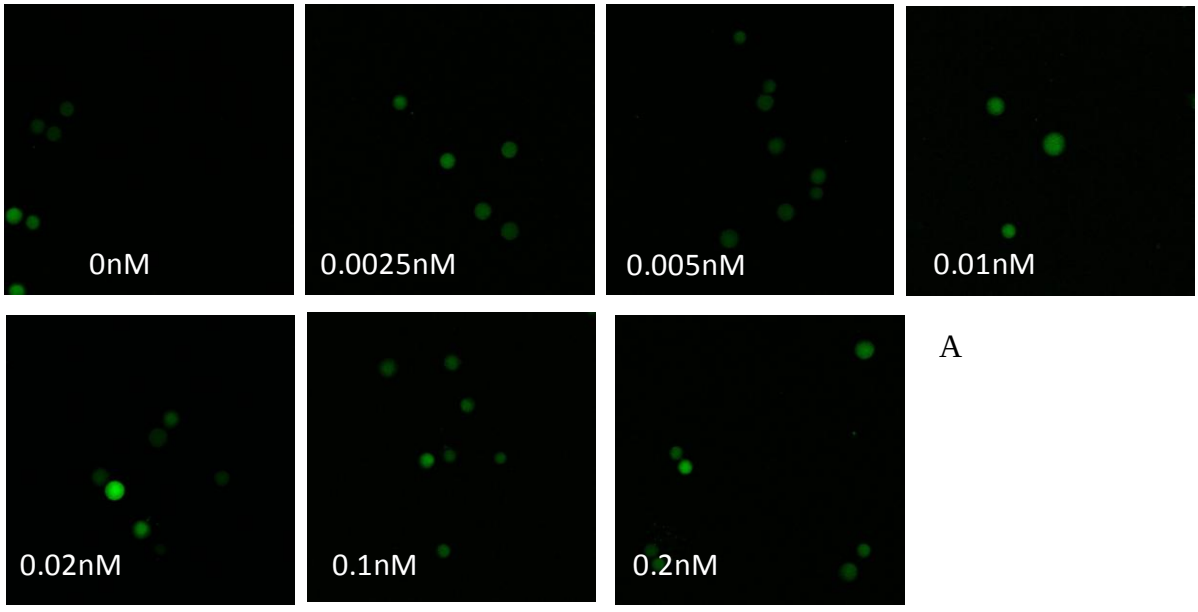

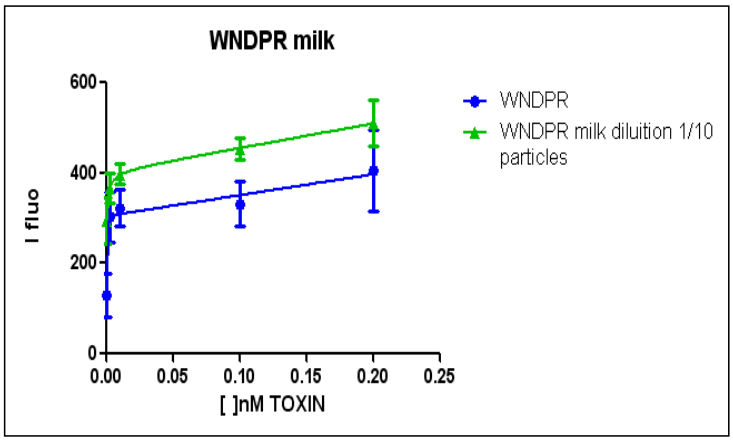

Figure 3.25: Binding between Aflatoxin M1-BSA conjugated and WNDPR microgels using a number of microgels diluted 1:10. A) Multiphoton confocal images of binding between Aflatoxin M1-BSA conjugated and WNDPR peptide microgels in milk sample. Excitation laser 700nm, emission 400-

500nm. B) Comparison of fluorescence signal between WNDPR microgels and WNDPR one diluted 1:10 after toxin binding. Using a lower number of microgels, there was an improvement on biosensor sensibility.

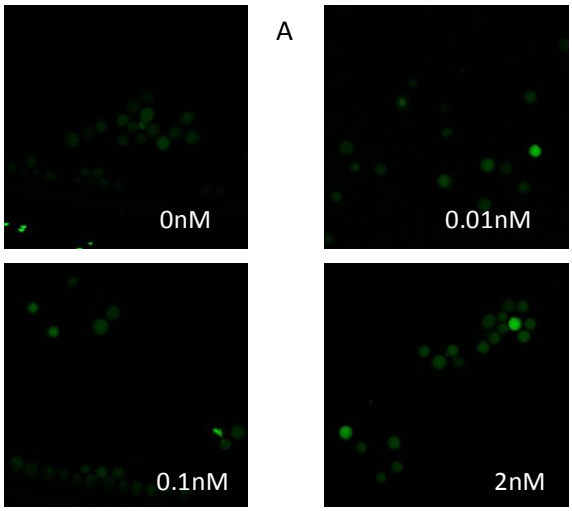

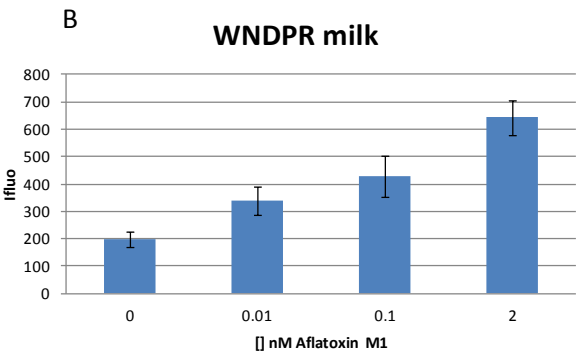

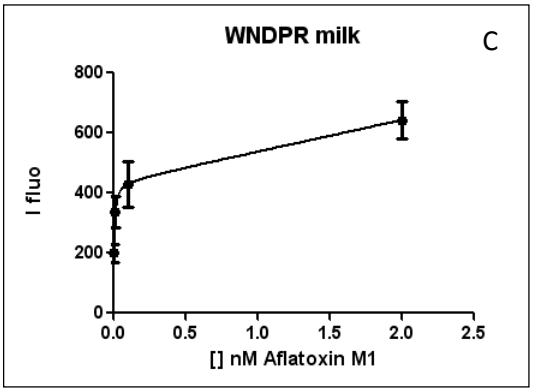

D

One site -- Total and nonspecific binding	Perfect fit
Best-fit values	
Bmax	235.8
Kd	0.007045
NS	104.3
Background	198.9
Std. Error	
Bmax	
Kd	
NS	
Background	
95% Confidence Intervals	
Bmax	
Kd	
NS	
Background	
Goodness of Fit	
Degrees of Freedom	
R^2	1.000
Analyzed	4

Figure 3.26: Binding assay between WNDPR microgels and Aflatoxin M1 no BSA conjugated in milk sample. A) Multiphoton confocal images of binding between Aflatoxin M1 and WNDPR peptide microgels in milk sample. Excitation laser 700nm, emission 400-500nm. B) Quantification of fluorescent signal of single microgels using ImageJ tools. C) Fitting of binding event between WNDPR peptide and Aflatoxin M1 using a One-site total and no specific binding as model with a non linear regression approach (D). The K_D evaluated was about low picomolar range.

3.4 CONCLUSIONS

Aflatoxins are a group of highly toxic secondary metabolites produced by *Aspergillus flavus* and *Aspergillus parasiticus*. They are strong hepatotoxins and are internationally recognized as carcinogens [18]. Because of their strong chemical and thermal stability it is very difficult

to eliminate them from contaminated food. For this reason, over the last few decades, several methods for the identification and quantification of the aflatoxins have been developed [13]; however all of them present high costs and skilled quality control operators. So our work was based on the development of a peptide-based biosensor for autofluorescence aflatoxin M1 detection in milk samples, in a sensitive, specific and unsophisticated manner. With our synthetic and computational combinatorial approach we discovered a new synthetic peptide WNDPR that was able to recognize Aflatoxin M1. The affinity power of this peptide sequence was after improved, integrating it in PEGDA microgels and developing a real sensitive and specific biosensor for Aflatoxin detection in milk samples. The use of our biosensor could be open the rout towards a direct detection of aflatoxins in small volume both in liquid and solid environments. Our approach could be also applicable to other small molecules or contaminants whose sensitive detection is indispensable for food, biochemical or medical applications.

References

[1] Bennett W., and M. Klich, Mycotoxins. Clin. Microbiol. Rev. J. 2003.

[2] Rai M.K., Bonde S.R., Ingle A.P., Gade A.K., Mycotoxin: rapid detection, differentiation and safety. J Pharm Educ Res 2012 Vol. 3, Issue No. 1.

[3] Zain M.E., Impact of mycotoxins on humans and animals. Journal of Saudi Chemical Society 2011 15, 129–144.

[4] Bennett, J.W., 1987. Mycotoxins, mycotoxicoses, mycotoxicology and mycopathology. Mycopathlogia 100, 3–5.

[5] CAST, 2003. Mycotoxins: Risks in Plant, Animal and Human Systems. Report No. 139. Council for Agricultural Science and Technology, Ames, Iowa, USA.

[6] Haouet M.N. and Altissimi M.S. (2003a). Micotossine negli alimenti e micotossicosi animale umana. Webzine Sanità Pubblica Veterinaria, n.18.: http://www.spvet.it/arretrati/numero_18/micot.html.

[7] Haouet M.N., and Altissimi M.S. (2003b) Micotossine negli alimenti e micotossicosi animale umana - Elaborazione dei dati ottenuti dal 1992 al 1998 (2a parte). Webzine Sanità

Pubblica Veterinaria, n. 19. Disponibile all'indirizzo: http://www.spvet.it/arretrati/numero_19/micot.html.

[8] Parker C, PhD thesis, 2008.

[9] Parker C.O., Lanyon Y. H., Manning M., Arrigan D. W., Tothill I. E., Electrochemical immunochip sensor for aflatoxin M1 detection. Analyt Chem 2009; 81:5291–5298.

[10] Ammida N.H.S., Micheli L., Piermarini S., Moscone D., Palleschi G., Detection of aflatoxin B1 in barley: comparative study of immunosensor and HPLC. Analyt. Lett 2006; 39:1559– 1572.

[11] Tan Y., Chu X., Shen G.L., Yu R.Q. , A signal-amplified electrochemical immunosensor for aflatoxin B1 determination in rice. Analyt Biochem 2009; 387:82–86.

[12] Alarcon S. H., Palleschi G., Compagnone D., Pascale M., Visconti A., Barna-Vetro´ I., Monoclonal antibody based electrochemical immunosensor for the determination of ochratoxin A in wheat. Talanta 2006; 69:1031–1037.

[13] Cigić I.K., Prosen H., An overview of conventional and emerging analytical methods for the determination of mycotoxins. Int J Mol Sci 2009; 10:62–115.

[14] Goryacheva I.Y., De Saeger S., Eremin S.A., Van Peteghem C., Immunochemical methods for rapid mycotoxin detection: Evolution from single to multiple analyte screening: A review. Food Addit. Contam. 2007, 6, 1169–1183.

[15] Lamberti I., Tanzarella C., Solinas I., Padula C., Mosiello L., An antibody-based microarray assay for the simultaneous detection of aflatoxin B1 and fumonisin B1. Mycotoxin Research 2009 Vol. 25 No 4, pp. 193-200, 0178-7888.

[16] Reis C.P., Ribeiro A.J., Neufeld R.J., Veiga F., Alginate micro- particles as novel carrier for oral insulin delivery. Biotechnol. Bioeng. 2007;96(5):977–989. 49.

[17] Tkachenko A.G., Xie H., Ryan J., Glomm W., Franzen S., Feldheim D.L., Assembly and Characterization of Biomolecule-Gold Nanoparticle Conjugates and their Use in Intracellular Imaging in Bionanotechnology Protocols, Edited by Sandra Rosenthal and David Wright, Humana Press Inc. New Jersey, 2005.

[18] Tozzi C., Anfossi L., Baggiani C., Giovannoli C., Giraudi G., A combinatorial approach to obtain affinity media with binding properties towards the aflatoxins. Anal Bioanal Chem. 2003 Apr;375(8):994-9. Epub 2003 Feb 22.

[19] In Silico Systems Biology (Methods in Molecular Biology) 2013th Edition. by Maria Victoria Schneider (Editor). Book.

[20] Sugumar R., Adithavarman A.P., Dakshinamoorthi A., David D.C, Ragunath P.K., Virtual Screening of Phytochemicals to Novel Target (HAT) Rtt109 in Pneumocystis Jirovecii using Bioinformatics Tools. Journal of Clinical and Diagnostic Research [serial online] 2016 March [cited: 2016 Mar 30]; 10:FC05-FC08. Available from http://www.jcdr.net/back_issues.asp?issn=0973709x&year=2016&month=March&volume=10&issue=3&page=FC05-FC08&id=7374.

[21] Wu G., Robertson D. H., Brooks C. L., III; Vieth M., Detailed Analysis of Grid-Based Molecular Docking: A Case Study of CDOCKER - A CHARMm-Based MD Docking Algorithm. J. Comp. Chem. 2003, 24, 1549.

[22] Tirado-Rives J., and Jorgensen W. L., "Contribution of Conformer Focusing on the Uncertainty in Predicting Free Energies for Protein-Ligand Binding." J. Med. Chem. 2006, 49, 5880-5884.

[23] Vachali P., Li B., Nelson K., Bernstein P.S., Surface plasmon resonance (SPR) studies on the interactions of carotenoids and their binding proteins. Archives of Biochemistry and Biophysics (2012), doi 10.1016/j.abb.2012.01.006.

[24] Teh S.-Y., Lin R., Hung L.-H., Lee A. P., Droplet microfluidics. Lab on a Chip 2008, 8 (2), 198-220.

[25] Chung B. G., Lee K.-H., Khademhosseini A., Lee S.-H., Microfluidic fabrication of microengineered hydrogels and their application in tissue engineering. Lab on a Chip 2012, 12 (1), 45-59.

[26] Udenfriend S., Stein S., Böhlen P., Dairman W., Leimgruber W. & Weigele M., Fluorescamine: A Reagent for Assay of Amino Acids, Peptides, Proteins, and Primary Amines in the Picomole Range. Science 178 871-872 (1972).

[27] Lorenzen A., and Kennedy S.W., A Fluorescence-Based Protein Assay for Use with a Microplate Reader. Anal. Biochem. 214 346-348 (1993).

[28] De Bernardo S., Weigele M., Toome V., Manhart K., Leimgruber W., Böhlen P., Stein, S. & Udenfriend, S. Studies on the Reaction of Fluorescamine with Primary Amines. Arch. Biochem. Biophys. 163 390-399 (1974).

[29] Hamid Mohammadi (2011). A Review of Aflatoxin M1, Milk, and Milk Products, Aflatoxins - Biochemistry and Molecular Biology, Dr. Ramon G. Guevara-Gonzalez (Ed.), ISBN:978-953-307-395-8,InTech,Availablefrom: http://www.intechopen.com/books/aflatoxins-biochemistry-and-molecular-biology/a-review-of-aflatoxin-m1-milk-and-milk-products.

Chapter 4

Miniaturized microfluidic peptide-based device for biomedical and diagnostic applications; a specific case: Endometriosis disease

ABSTRACT. There is always a great interest in the fabrication of protein-detecting arrays using immobilized capture agents in biomedical and diagnostic field [1]. While most efforts in this area have focused on the use of biomolecules such as antibodies and nucleic acid aptamers as capture agents, synthetic peptides might present many potential advantages. However, synthetic molecules isolated from combinatorial libraries generally are able to bind target proteins with the high affinity necessary for array applications. In this work three different peptides (CRP-1, VEGF-114 and ΦG6) were used as capture agents to detect serum levels of vascular endothelial growth factor (VEGF), tumor necrosis factor-alpha (TNF-a), and C-reactive protein (CRP): three serum markers of endometriosis in menstrual blood [2]. The selected peptides have been covalently immobilized on a microfluidic PDMS device, previously derivatized with 10% of PAA (Poly(acrylic acid)) solution. The so built device has been used to capture and recognize endometriosis markers both in buffer and biologic fluids matrices such as human serum with a good specificity and sensitivity. Our idea is to make up a miniaturized microdevice that is able to diagnose endometriosis from the earliest stages using peptides as capture agents in order to have a sensitive but not invasive and not expansive biosensor tool.

4.1 INTRODUCTION

There is great interest in the development of micro-arrays that are able to monitor the levels and activities of a large numbers of proteins simultaneously [1]. One approach is to construct protein-detecting arrays using DNA, antibody and/ or aptamers as capture agents that recognize target protein with high affinity and specificity [3, 4]. The use of these macromolecules are very expensive and for this reason the biosensor applications in medical fields are still very low. A significant challenge in the development of such technology could be the isolation of large numbers of suitable protein binding compounds [1]. Synthetic molecules can be produced in large quantities with efficient quality control and can be tailored to allow attachment to surfaces in a defined manner [1]. Also, macromolecules can easily lose their folded structure and so their activity at surface-solution interfaces, whereas this is not an evident issue with synthetic molecules. However, synthetic molecules isolated from combinatorial libraries generally can be able to bind target proteins with the high affinity necessary for array applications. Finally, some types of protein binding synthetic molecules like peptides can be economically produced and purified in large quantities than antibodies or aptamers. In this work three different peptides, were selected as ligand of three different biomarkers in menstrual blood related to endometriosis insurgence: tumor necrosis factor-α (TNF-α), vascular endothelial growth factor (VEGF), and C-reactive protein (CRP) respectively. These sequences screened by SPR, phage display and FACS methodology respectively, showed high affinity for studied biomarkers [5-11]. Their affinity was confirmed by SPR-One step injection in this work. The selected peptides was covalently immobilized on a microfluidic PDMS device, previously derivatized with 10% of PAA (Poly (acrylic acid)) solution. The so built device was used to capture and recognize endometriosis markers both in buffer and biologic fluids matrices such as human serum with a good specificity and sensitivity. Endometriosis is an often painful disorder in which tissue that normally lines inside of uterus, the endometrium, grows outside uterus (endometrial implant) [12, 13]. The generation of new capillary blood vessels is probably required for the implant to grow larger than 2–3 mm, favoring an angiogenesis-dependent mechanism in endometriosis disease [12, 13]. Tumor necrosis factor-alpha (α) and vascular endothelial growth factor (VEGF) are important angiogenic factors. TNF-α is secreted by macrophages and it is a potent inducer of new blood vessel growth that produces proliferation of endometriotic stromal cells [14]. VEGF is a heparin binding growth factor with potent mitogen, morphogen and chemoattractant properties for endothelial cells. It increased in endometrium of

endometriosis patients, reflecting a critical pathogenic role. Serum C-reactive protein (CRP) is widely used as a marker of ongoing inflammation in several clinical diseases. CRP seems to be increased in women with endometriosis, especially in those with more advanced disease [15]. Although the use of serum biomarkers was still controversial, because of their low specificity in endometriosis disease and the low sensitivity of detection techniques performed, a non-surgical diagnostic approach could be of great benefit to both physicians and women alike [16]. In recent years, many efforts were made up to try to identify an easy way to diagnose endometriosis. The direct visualization of lesions at surgery preferably coupled with histologic confirmation of endometrial glands and stroma is the gold standard detection for endometriosis diagnosis. A surgical diagnosis has multiple drawbacks such as the risks inherent to the procedure (organ damage, hemorrhage, infection, and adhesion formation), as well as general anesthetic complications. Also patients need to travel to a hospital or outpatient surgicenter, with associated financial costs to the patient and the healthcare system [17]. For all these reasons, to develop a non-surgical diagnostic approach is very important in order to detect this disease from early stages. So the aim of this project was to make up a miniaturized microdevice that was able to diagnose endometriosis from the earliest stages using specific peptides as capture agents for these three VEGF, TNF-α and CRP biomarkers in order to have a sensitive but not invasive and not expansive biosensor tool for their determination and quantification.

4.2 MATERIALS AND METHODS

4.2.1 Materials

Reagents for peptide synthesis (Fmoc-protected amino acids, resins, activation, and deprotection reagents) were purchased from Iris Biotech GmbH (Waldershofer Str. 49-51 95615 Marktredwitz, Deutschland) and InBios (Naples, Italy). 1-ethyl-3-(3-dimethylaminopropyl)car-bodiimide hydrochloride(EDC), N-hydroxysuccinimide (NHS),PDMS and CRP (C-Reactive Protein)protein were fromSigma-Aldrich. VEGF (Recombinant Human $VEGF_{165}$) was purchased from Peprotech. Anti-CRP (Anti-C Reactive Protein antibody (FITC) (ab19174)) and Anti-VEGF (Anti-Recombinant Human VEGF antibody (FITC)) were from Abcam. TNF-α and Anti-TNF-α (Anti-Tumor Necrosis Factor-α antibody (FITC)) were from Prospec. Solvents for peptide synthesis and HPLC analyses were purchased from Sigma-Aldrich; reversed phase columns for peptide analysis and the LC–MS system were supplied respectively from Agilent Technologies and Waters (Milan, Italy). All

SPR reagents and chips were purchased from AlfaTest (Rome, Italy). PMMA substrates used in this study were purchased from the same batch of the polymer supplier (GoodFellow Cambridge Limited, England), Fluorolink S10 was from Solvay. Pooled human serum from healthy donors was supplied by Lonza (Life Technology Ltd, Paisley, UK). All chemicals were used as received.

4.2.2 Peptide Synthesis

Solid phase peptide synthesis of CRP-1, VEGF-114, G6 peptides and a model peptide was performed on a fully automated multichannel peptide synthesizer Biotage® Syro Wave™. The peptides were synthesized in the amidate version, employing the solid phase method on a 50 μmol scale following standard Fmoc strategies. Rink-amide resin (substitution 0.7 mmol/g) was used as solid support. Activation of amino acids was achieved using HBTU/HOBt/DIPEA (1:1:2). All couplings and deprotections were performed for 15 and 10 min, respectively. Peptides were then removed from the resin, by treatment with a TFA/TIS/H_2O (95:2.5:2.5, v/v/v) mixture for 90 min at room temperature; then, crude peptides were precipitated in cold ether, dissolved in a water/acetonitrile (1:1, v/v) mixture, and lyophilized. Products were purified by preparative RP-HPLC on a Waters 2535 Quaternary Gradient Module, equipped with a 2489 UV/Visible detector and with an X-Bridge^{TM} BEH300 preparative 10 × 100 mm C8, 5μm column, applying a linear gradient of 0.1% TFA CH_3CN in 0.1% TFA water from 5% to 70% over 30 min at a flow rate of 5 mL/min. Peptides purity (97%) and identity was confirmed by LC–MS analyses carried out on an Agilent 6530 Accurate-Mass Q-TOF LC/MS spectrometer with Zorbax RRHD Eclipse Plus C18 2.1 x 50 mm, 1.8 μm columns. CRP-1 and VEGF-114 peptides were cyclized to obtain their active version. The cyclization process was performed using a concentration of 0.1 mg/mL of peptides dissolved in 10mM phosphate buffer pH 7.4 for two days. The occurred reaction was confirmed by LC–MS analyses (See Appendix Chapter 4). Products were purified by preparative RP-HPLC applying a linear gradient of 0.1% TFA CH_3CN in 0.1% TFA water from 5% to 95% over 5 min at a flow rate of 5 mL/min. Purified peptide were lyophilized and stored at −20 °C until use.

4.2.3 PDMS-PAA (Poly (acrylic acid)) derivatization

All PDMS samples were submerged for 1’ in a 10% Benzophenone solution in ethanol and after they were treated with 15uL of different concentrations of PAA solution and covered with a rim glass [18-21]. They were irradiated with UV lamp at 360nm from 3 minutes to 1h.

The correct PAA- derivatization at different time of irradiation was monitoring by IR (Infra-Red) spectroscopy, analyzing the presence of the acid band at 1717 cm^{-1}.

4.2.4 Peptide grafting on PDMS-PAA surface optimization by IR (Infra-red spectroscopy) and HPLC (High performance liquid chromatography)

The peptide grafting was optimized with a model peptide: Ac-βA-G-R-A-A-Y-A-K-NH_2. Different concentrations of peptide from 0 to 2mg/mL were used to grafted it on PDMS-PAA surface. In order to have a better and more stable complex we decided to link the peptide on our substrate with a covalent bond. The PAA surface was at first treated with 0.1M EDC/ 0.2M NHS mixture in water for 10 minutes [22] and after peptide was grafted dissolving it in carbonate buffer 10 mM pH 8.5 at different concentrations. The formation of amide-bond was monitoring by IR analyzing the presence of peaks corresponding to amide I and amide II at 1660 and 1550 nm, respectively. In order to confirm the good amidation of PAA surface and to calculate the amount of adsorbed moles, peptide solutions were analyzed before and after PDMS-PAA grafting process by RP-HPLC, following tyrosine signal at 275nm.

4.2.5 SPR (Surface Plasmonic Resonance)

In order to evaluate and confirm the binding constant between peptide and biomarkers, SPR experiments were performed by One step injection. VEGF and CRP protein were immobilized at a concentration of 100 µg/mL in a 10 mM acetate buffer pH 4.5 and 3.5 respectively, (flow 10 µL/min, injection time 20 min) on a COOH1 SensiQ sensor chip, using EDC/NHS chemistry (0.4 M EDC - 0.1 M NHS, flow 25µl/min, injection time 4 min), achieving a 800 RU signal. Groups reactive residues were deactivated by treatment with ethanolamine hydrochloride 1 M, pH 8.5. The reference channel was prepared by activation with EDC/NHS and deactivation with ethanolamine Analyte concentration of 30 µM for VEFG -114 peptide and 245 µM for CRP-1 peptide was used with a flow rate of 100 µL min^{-1} and a 300 sec of dissociation time. In this kind of experiment, the volume of sample was configured as a percentage of the dispersion loop volume so in order to have a longer plateau at full concentration, the largest percentage (100%) was used. As to bulk standard cycles, a 3% of sucrose was used. For all experiments Kinetic parameters for both peptides were estimated assuming a 1:1 binding model and using QDAT software (SensiQ Technologies). For G6 peptide, the affinity against TNFα was previously estimated by our research group in a recent study [9].

4.2.6 Microfluidic device

The depth and width of the three microchannel is equal, 300 µm width and 300 µm depth, and the chamber with an area of 67 mm^2 is located at the end of the parallel microchannels. The pillars are 300 µm in diameter and 300 µm depth. The fabrication process consists of 4 steps: (1) preparing the chip draft using Draftsight (Cad Software), (2) micromachining of PMMA layers; (3) the double PDMS replica (4) and finally the bonding process via oxygen-plasma treatment. A micromilling machine (Minitech Machinery Corporation) was used to fabricate the PMMA master with the features of the final device. The certified positioning accuracy of the three-axis are 12”/300mm in x-axis, 9”/228mm in y-axis, and 9”/228 mm in z-axis. To standardize the fabrication process, the PMMA substrates used in this study were purchased from the same batch of the polymer supplier (GoodFellow Cambridge Limited, England). The microtools used in the microfabrication process were two flute endmills 300 and 889 µm in diameter (Performace microtool, USA). During micromilling, spindle speed, feed speed and plunge rate per pass were set to 12.000 rpm, 15 mm s-1, and 20, respectively. After preparation of a PMMA master with negative features, open microchannels in PDMS were obtained by double replica molding onto the starting master. PDMS replica were fabricated from a mixture of PDMS precursor mixed in ratio 10:1 with curing agent and by using a thermal curing protocol at 80 °C for 2 h. Particularly, in order to prevent adhesion of the negative PDMS replicas on the positive PDMS mold, the latter was treated with oxygen plasma to activate the surface using a plasma chamber (Plasma prep II, SPI) for 1 min at a pressure of 0.3 mbar and power of 37 W and then immersed for about 2 min into a silane solution (i.e., a mixture of 94% v/v isopropanol,1% acetic acid, 1% Fluorolink S10 and 4% deionized water) and then placed in an oven at 75 °C for 1 h, thus allowing a complete reaction of the master surface with the fluorinated polymer [23]. To obtain the closed PDMS chip, we treated the final PDMS replica and a glass slide preciously coated with a thin PDMS layer through oxygen plasma activation , using a plasma chamber (Plasma prep II, SPI) for 1 min at a pressure of 0.3 mbar and power of 37 W. The glass coating process involved depositing a small undiluted PDMS droplet (around 1 ml) onto the center of the glass and then spinning at high speed (2000 rpm for 20 s). Finally the bonding was then finalized in a controlled environment (temperature 80 °C for 2 h).

4.2.7 Selection of protein-binding peptides for specific marker detection and quantification

Three peptides, V114; CRP-1; φG6, whose sequences are reported in Table 3 were derived from biopanning procedures[9-11], and synthesized by solide phase peptide synthesis. **Table 3 peptide sequences binnding endometriosis biomarkers VEGF, CRP, TNF-α.**

Peptide	Biomarker target	Sequence
φG6	TNF-α	SSYYPQWPTDRF
V114	VEGF	VEPNCDIHVMWEWECFERL
CRP-1	CRP	EWACNDRGFNCQLQR

The sequences were selected as ligand of three different biomarkers in menstrual blood related to endometriosis insurgence: tumor necrosis factor-α (TNF-α), vascular endothelial growth factor (VEGF), and C-reactive protein (CRP) respectively.

Each peptide was immobilized on the PDMS-PAA surface in a microfluidic channels following the procedure above described (4.2.4) and filling the channel with a peptide solution at a concentration of 2 mg/mL. Different concentrations of pure human recombinant TNF-α (Abcam) VEGF (Abcam), and CRP (Sigma Aldrich) proteins were solubilized in Phosphate-buffered saline (PBS) and incubated by flushing 25 µl of biomarker solutions into the corresponding channel for 2 hours. After incubation, the channels were washed 3 times with 3 ml of PBS.

Biomarkers detection was performed by immunofluorescent detection through primary anti-TNF-α, anti-VEGF, and anti-CRP antibody (Abcam), labeled with Alexa Fluor® 488, Alexa Fluor® 568, and Pacific Blue™ dye, respectively, by Molecular Probes® Antibody Labeling Kits (ThermoFisher Scientific). Fluorescence analysis was performed by Leica SP5 confocal microscope. Bright field and fluorescence images using a HCX IRAPO L 25×/0.95 water objective were acquired; Images were acquired with a resolution of 1024 × 1024 pixels, zoom 1, 2.33A.U. All experiments were performed at room temperature. LOD range related to each was determined by image analysis through ImageJ tool [31] (https://**imagej**.nih.gov/ij/).

4.2.8 Setting of microfluidic device for endometriosis biomarkers

Microfluidic device channels were functionalized for multiplex detection of endometriosis biomarkers. V114, CRP-1, and φG6 peptides were immobilized filling any channel with a PBS solution containing 2 mg/mL of one peptide as wall as previously described in 4.2.6. the device was tested flushing 1 ml of a testing solution containing 5pmol of VEGF, CRP and TNF-α proteins in PBS. Functionalization through a scramble peptide (Ac-βA-G-R-A-A-Y-A-K-$NH_{2)}$ was used for negative controls. The resident time of the testing solution was 2 hours. After proteins incubation, the device was washed by 30ml of PBS and incubated with a mixed solution of primary fluorescent anti-VEGF, anti-CRP and anti-TNF-α antibody (dilution 1:10 in PBS) overnight. Fluorescence analysis was performed by Leica SP5 confocal microscope. Bright field and fluorescence images using a HCX IRAPO L 25×/0.95 water objective were acquired; Images were acquired with a resolution of 1024 × 1024 pixels, zoom 1, 2.33A.U. Analogous experiments were performed detecting endometriosis biomarkers in human serum (1x), dissolved at 5 nM final concentration. Autoflorescence and background signal was determined by analysis of each channel surface incubated with PBS or human serum solution not containing biomarkers. All experiments were performed in triplicate at room temperature. For each sample 10 images of different zone of the surface was acquired under the microscope.

4.3 RESULTS AND DISCUSSIONS

In this work three different peptides (CRP-1, VEGF-114 and φG6), selected by literature, have been used as capture agents for human biomarkers: VEGF, TNF-α and CRP. The area of interest for these biomarkers spread in several diagnostic research fields. In particular, it has been postulated a future diagnostic tool for endometriosis will consist of a panel containing these proteins as biomarkers. As a fact, recent studies suggested that peritoneal fluid of endometriosis patients contains an increased number of activated macrophages that secrete local products with important angiogenic properties, including VEGF and TNF-α [24-26]. Moreover, serum C-reactive protein (CRP) is widely used as a marker of ongoing inflammation in clinical practice [2]. A health history and a physical examination can lead the health care practitioner to suspect endometriosis. Although doctors can often feel the endometrial growths during a pelvic exam, and these symptoms may be signs of endometriosis, diagnosis cannot be confirmed by exam only. Use of pelvic ultrasound may identify large endometriotic cysts (called endometriomas) [27]. However, smaller

endometriosis implants cannot be visualized with ultrasound technique. Our idea is to set up a miniaturized microdevice that is able to diagnose endometriosis from the earliest stages using peptides as capture agents in order to have a sensitive but not invasive and not expansive biosensor tool. Thus, the selected peptides were covalently immobilized on a microfluidic PDMS device, previously derivatized with 10% of PAA (Poly(acrylic acid)) solution, and tested for detection of VEGF, TNF-α and CRP in solution.

4.3.1 PDMS-PAA (Poly (acrylic acid)) derivatization

PAA brushes were grown on PDMS surface previously actived with a 10% Benzophenone solution in ethanol. The correct PAA-derivatization at different UV-irradiation time was monitoring by IR (Infra-Red) spectroscopy, analyzing the presence of the acid band at 1717 cm^{-1}. In figure 4.1, IR spectra of PDMS-PAA functionalization (10% of PAA-solution) at different UV-irradiation time periods, from 3 to 10 minutes were reported. The improvement of acid band at 1710 nm with the increasing time was very clear. From 7 to 10 minutes the saturation was reached.

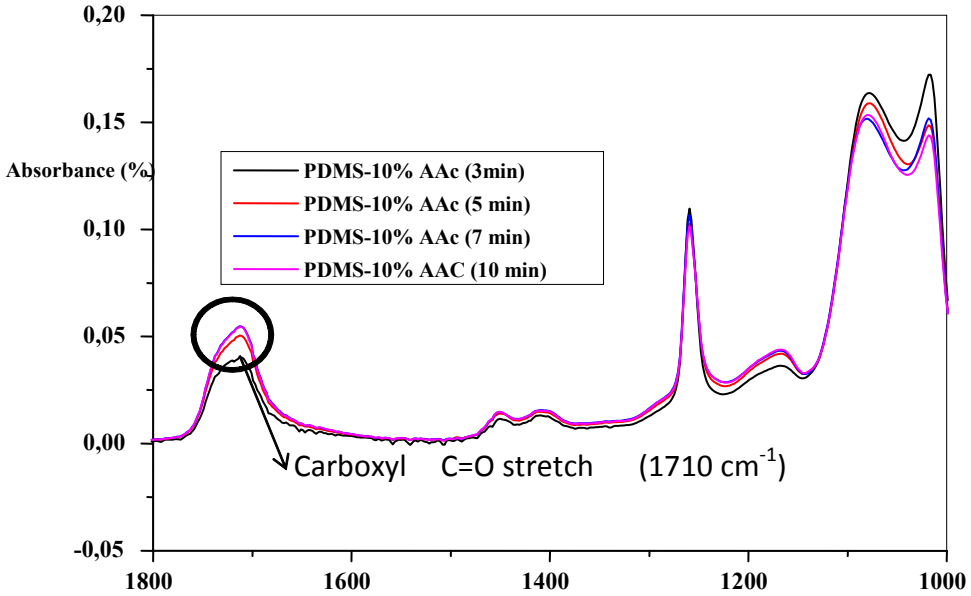

Figure 4.1: IR spectra of PDMS-PAA functionalization at different time periods from 3 to 10 minutes. It was clear the improvement of acid band at 1710 cm^{-1} with the increasing time. From 7 to 10 minutes the saturation was reached.

The figure 4.2 displayed the deconvolution of carbonyl stretching regions showed in figure 4.1. The PAA-grafted surface increased during the time, reaching the saturation point of around 1.3-1.4 mg/cm^2 between 10 and 15 minutes.

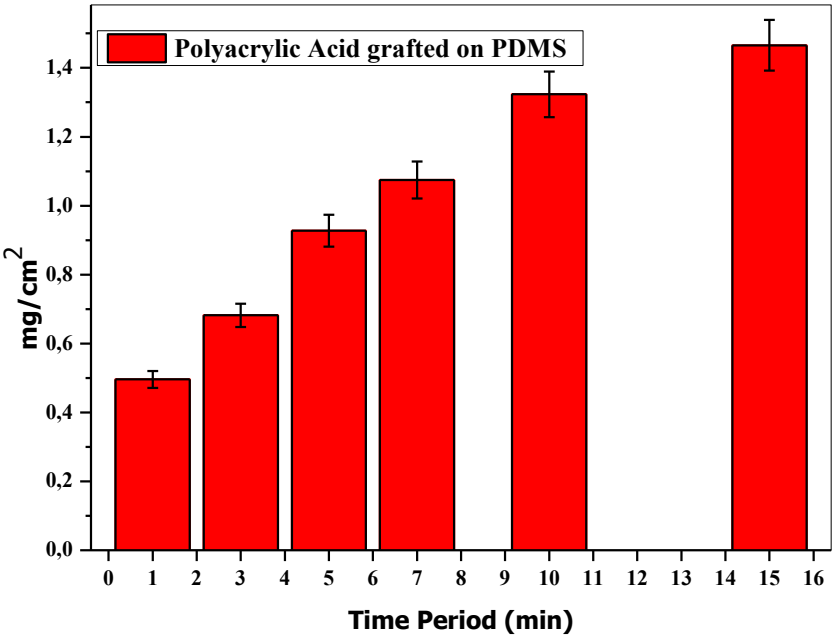

Figure 4.2: Deconvolution of carbonyl stretching region at different time periods. The PAA grafted surface increased during the time, reaching the saturation point of around 1.3-1.4mg/cm^2 between 10 and 15 minutes.

4.3.2 Peptide grafting on PDMS-PAA surface optimization by IR (Infra-red spectroscopy) and HPLC (High performance liquid chromatography)

The peptide grafting was optimized with a model peptide: Ac-βA-G-R-A-A-Y-A-K-NH_2. Different concentrations of peptide from 0 to 2mg/mL were used to grafted it on PDMS-PAA surface. The PAA surface was at first treated with 0.1M EDC/ 0.2M NHS mixture in water for 10 minutes [22] and after with different concentrations of model peptide dissolved in carbonate buffer 10 mM pH 8.5. Figure 4.3 A showed the overlay of infrared spectra of PDMS-PAA surface before and after activation of PAA brushes with EDC/NHS mixture. The characteristic infrared bands classified as NHS-ester showed triplex bands at 1740, 1780, and 1815 cm^{-1}; while the degradation product of reaction, N-acylurea was associated to doublet bands of amide at 1550 and 1650 cm^{-1} (Figure 4.3 B).

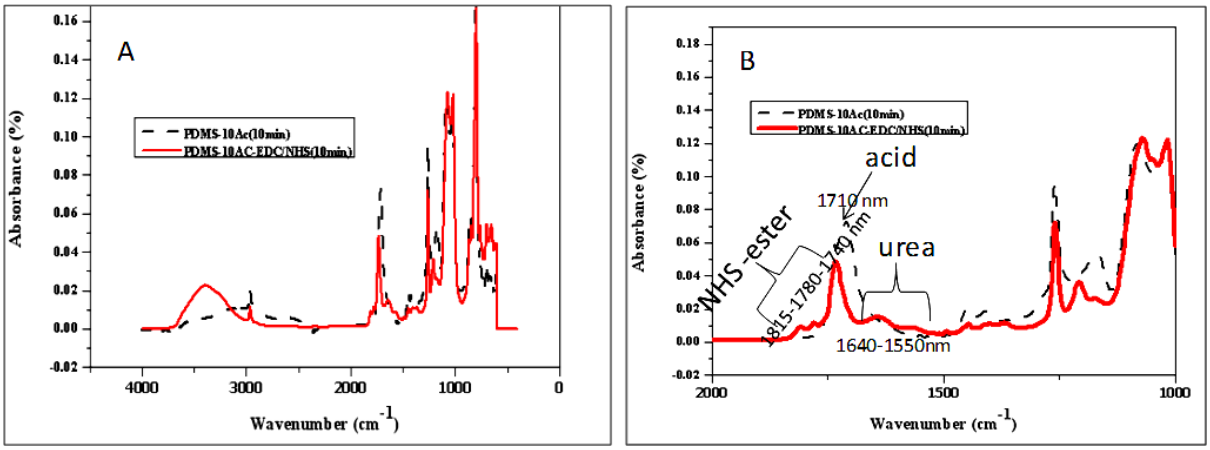

Figure 4.3: A) IR spectra of PDMS-PAA surface before and after activation treatment with EDC/NHS (0.1M-0.2M). B) Zoom of the observed region before and after EDC/NHS treatment: NHS-ester three bands (1740-1780-1815cm^{-1}), N-acylurea, degradation product of reaction, two bands (1550-1640cm^{-1}). The dotted line showed the acid band (1710cm^{-1}) before treatment that disappeared after activation.

The main goal of EDC/NHS activation of carboxylic acids is to couple free amine-containing biomolecules [22]. Figure 4.4 showed the occurred amidation on PDMS-PAA surface after incubation with different solutions of model peptide (from 0.125 mg/mL to 2mg/mL), (figure 4.4 A). The presence of two bands at 1550 and 1670 cm^{-1}, corresponding to amide I (peptide C=O stretch) and amide II (mostly peptide N=H bend), stressed the proper peptide grafting on the surface (figure 4.4 C). Unlike, the presence of two amide bands on PDMS-PAA surface without pre-activation by EDC/NHS solution was very weak, (figure 4.4 B, D). In figure 4.5 (A,B) the quantification of the area of the amide and acid bands according to peptide concentrations, both for EDC/NHS treated surface and not was showed. The data were analyzed by software GraphPad Prism version 5.04.

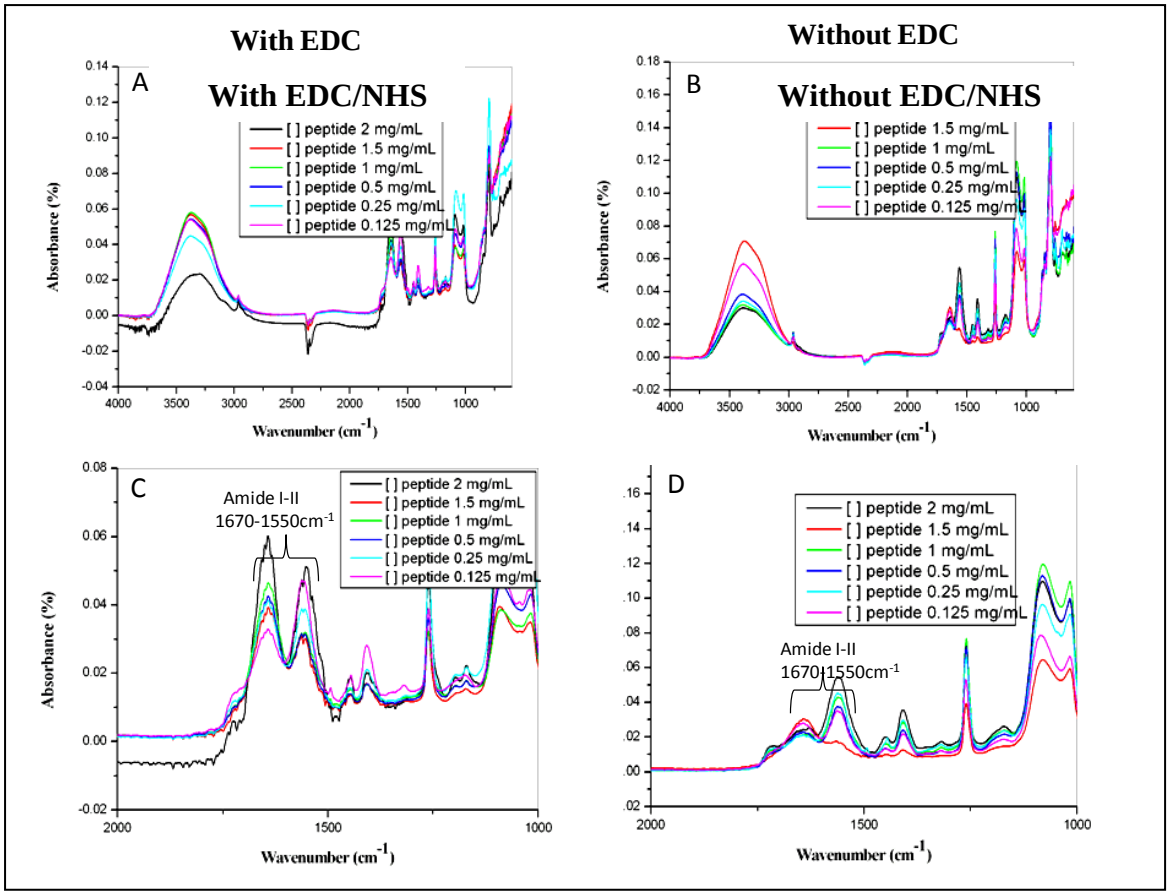

Figure 4.4: IR spectra of PDMS-PAA after peptide amidation. A) Whole IR spectra of amidation reaction after EDC/NHS reaction at different concentrations of peptide from 0.125mg/mL to 2mg/mL. B) IR spectra of amidation reaction without EDC/NHS treatment. C) and D) Zoom of observed area with activation treatment and without it respectively. In the first case the presence of the two amide bands (1550 and 1670 cm^{-1}, amide I and II) was clear and they increase with improving peptide concentration. In the second one the presence of two amide bands was very weak.

A

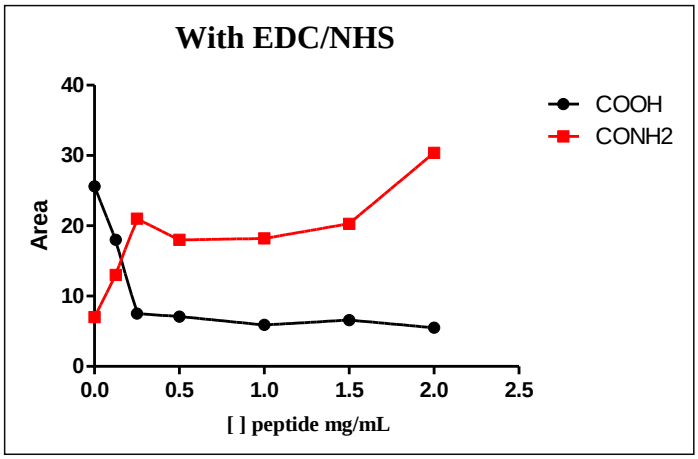

B

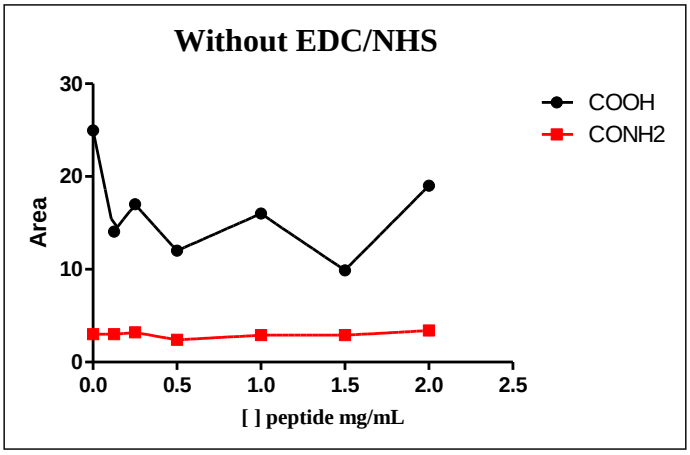

Figure 4.5: Quantification of the area of the amide and acid bands according to peptide concentrations. A) Sample treated with activation reaction. In this case the amide band was increased with peptide concentration, while acid band at 1710 cm^{-1} decreased. B) Sample without activation reaction. In this case only the acid band at 1717 cm^{1} was observed.

In order to confirm the good amidation of PAA surface and to calculate the amount of adsorbed moles, peptide solutions were analyzed before and after PDMS-PAA grafting process by RP-HPLC, following tyrosine signal at 275nm. In the table 4 and 5 the amount of adsorbed moles were reported both for EDC/NHS treated surface and not treated PDMA-PAA. The adsorbed moles were evaluated measuring peptide concentrations of unbound fraction after grafting process. A saturation point on treated surface was reached at 1 mg/mL of peptide concentration. A no linear response was obtained for not treated surface. The titration curve used for quantification was reported in the Appendix of chapter 4. In figure 4.6 A the absorbance of bound fractions corresponding to different concentrations of peptide was reported for both surface. Also the amount of adsorbed moles/cm^2 was reported, (Figure 4.6

B). For 2 mg/mL of peptide concentration, about 500 nanomoles/cm^2 were linked on our device.

Table 4: Quantification of adsorbed moles by RP-HPLC on PDMS-PAA surface previously activated by EDC/NHS

[ ] peptide mg/mL (surface with EDC/NHS treatment)	C bound mg/mL	Moles adsorbed
0.25	0.18	53nmol
0.5	0.19	56nmol
1	0.43	126nmol
1.5	0.43	126nmol
2	0.43	126nmol

Table 5: Quantification of adsorbed moles by RP-HPLC on PDMS-PAA surface not activated by EDC/NHS

[ ] peptide mg/mL (surface without EDC/NHS treatment)	C bound mg/mL	Moles adsorbed
0.25	0.036	10nmol
0.5	0.022	6.5nmol
1	0.09	26nmol
1.5	0.09	26nmol
2	0	0nmol

A

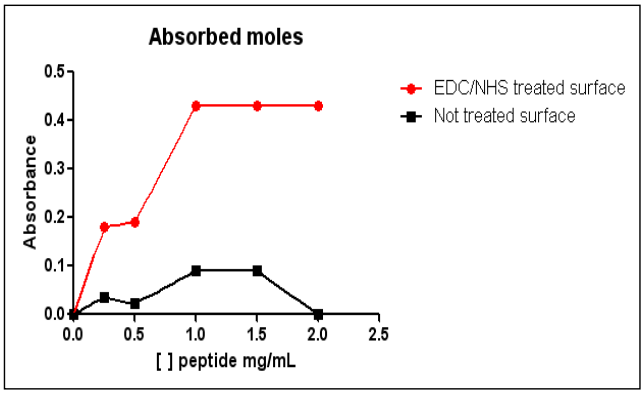

B

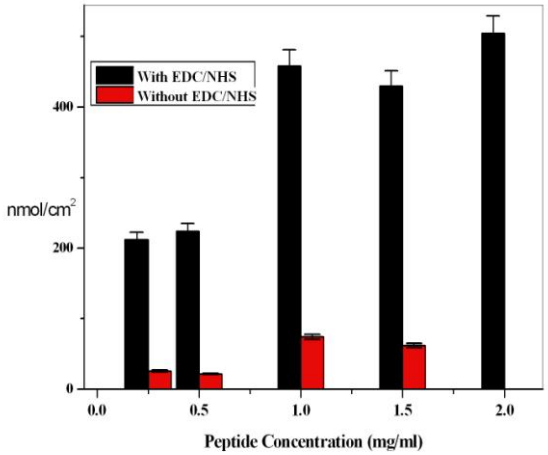

Figure 4.6: A) the absorbance of bound fractions corresponding to different concentrations of peptide was reported for both surface. B) the amount of adsorbed moles/cm^2 was reported, For 2 mg/mL of peptide concentration, about 500 nanomoles/cm^2 were linked on our device.

4.3.3 SPR (Surface Plasmonic Resonance)

In order to evaluate and confirm the binding constant between peptide and biomarkers SPR experiments were performed by One step injection. Analyte concentration of 30 µM for VEFG -114 peptide and 245 µM for CRP-1 peptide was used. One step experiment was based on Taylor dispersion theory, so a unique concentration of peptide was dispersed into running buffer directly in the flow cell in order to have a final sigmoidal profile [28-30] (Figure 4.7 A,B). Employing a 1:1 interaction model, a low micromolar dissociation value for peptides/biomarkers was shown; it was in according to conventional SPR experiment reported in literature [10, 11]. For G6 peptide, the affinity against TNFα protein was previously estimated by our research group in a recent study (data not shown), [9].

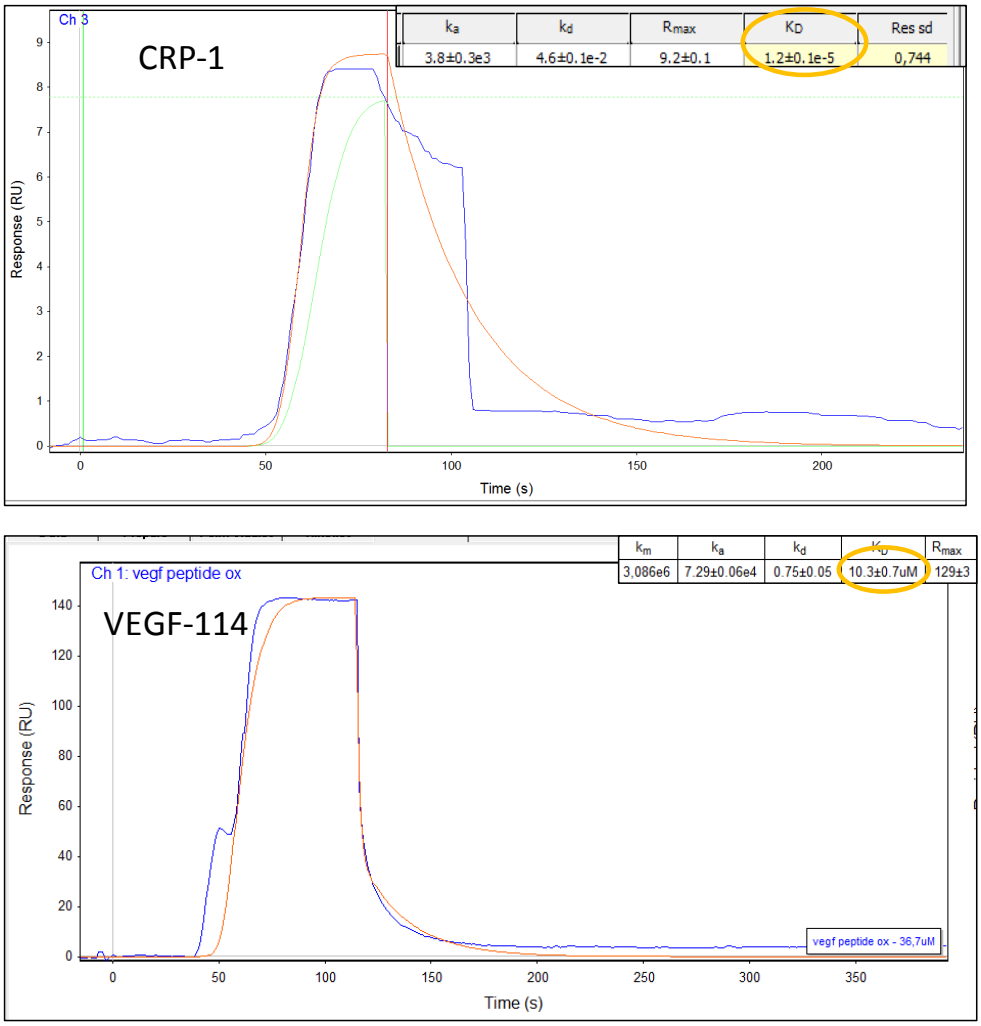

Figure 4.7: One Step injection experiments. A) Binding of CRP-1 (245µM) and CRP protein. The evaluated KD was 12±0.1 µM. B) Binding of VEGF-114 (30µM) and VEGF protein. The evaluated KD was 10 ±0.7 µM.

4.3.4 Microfluidic device

Microfluidic chip was obtained by coupling micromilling and soft lithography technology based on polydimethylsiloxane (PDMS). PDMS has been the most widely used material in the research and development of microfluidics for several reasons including its optical transparency. In addition, the fabrication of systems of microchannels in PDMS is particularly straightforward. They can be replicated on masters of different materials including poly methyl methacrylate (PMMA). Such material can be easily machined by a low cost and fast prototyping technique such as micromilling. Microfluidic chips can then be easily sealed by oxygen plasma treatment of the PDMS substrate. As shown in figure 4.8 by the CAD (Figure 4.8 A) and SEM image (Figure 4.8B) the microfluidic device is composed

of three parallel channel converging in a chamber with micropillars which function is to support the large channel once bonded.

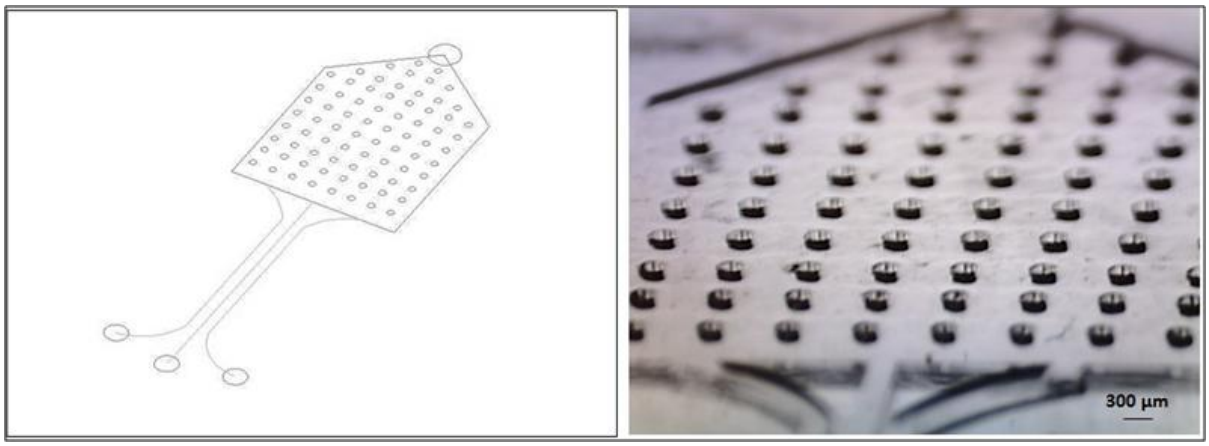

Figure 4.8 CAD layout (A) and SEM image (B) of the microfluidic chip.

4.3.5 Endometriosis biomarkers detection through peptide functionalized microfluidic device

The affinity peptides V114; CRP-1; φG6, identified from phage display peptide libraries and FACS methodology [9-11], were employed here as biorecognition element for human VEGF, CRP and TNF-α biomarkers.

The conjugation of each peptide to the channel surface was carried out allowing specific binding and detection of only one biomarker per channel. Thus, each channel was tested with different concentrations of the corresponding protein target in PBS and biomarker sequestration was revealed by immunofluorescent detection through primary fluorescent labeled antibodies. For each biomarker the LOD was determined by image analysis of the fluorescence detectable on the surface as reported in figure 4.9.

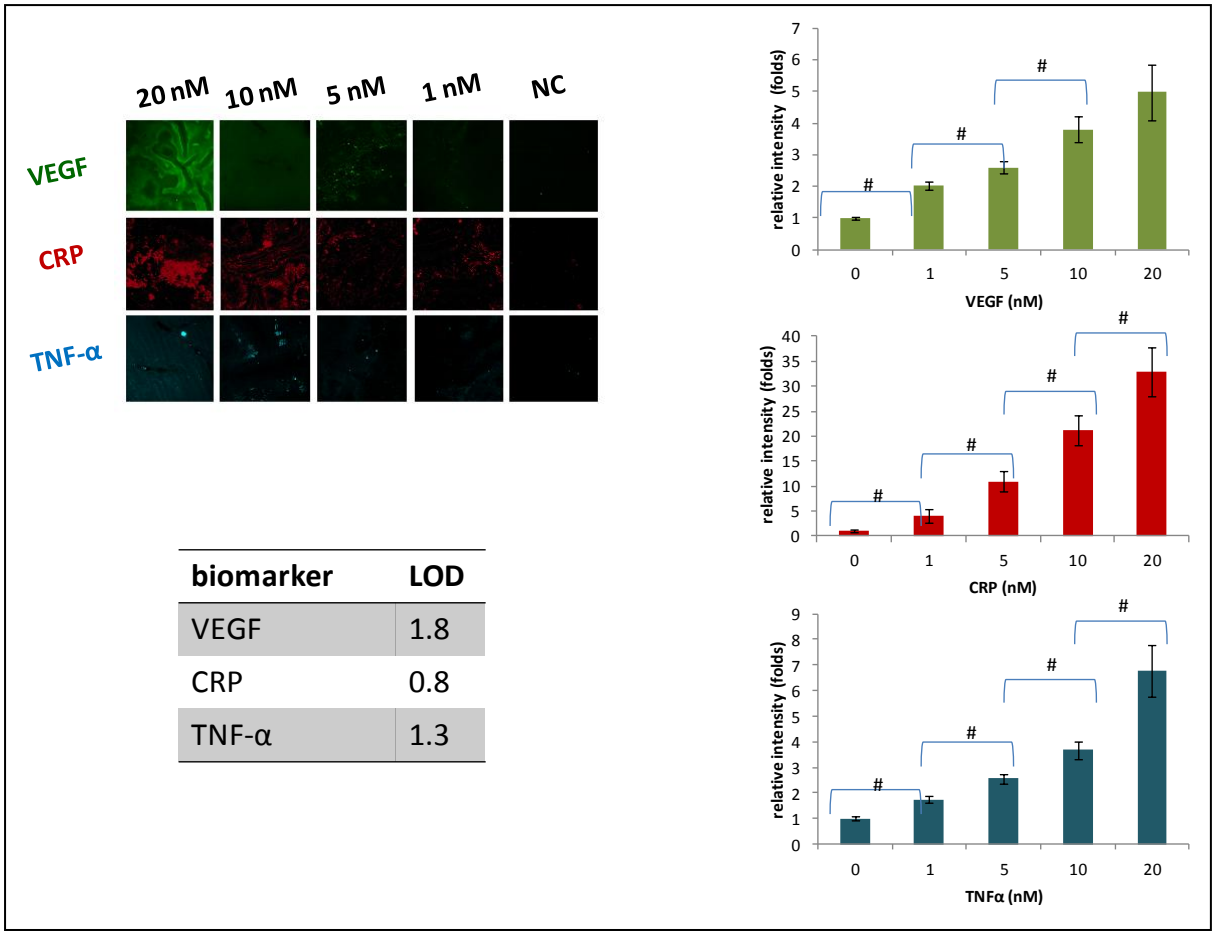

biomarker	LOD
VEGF	1.8
CRP	0.8
TNF-α	1.3

Figure 4.9: LOD determination and fluorescence analysis of studied biomarkers.

The device is able to reveal the presence of biomarkers in solution at a nM order concentration, compatible with the physiological range of VEGF, CRP and TNF-α in menstrual blood of patient affected by endometriosis. In order to test suitability and specificity of the functionalized channels for multiplex analysis of endometriosis biomarkers, the microfluidic device was tested by flashing 1ml of PBS solution containing recombinant human VEGF, CRP and TNF-α proteins at 5nM final concentration. In this case the immunodetection was performed by incubating each microchannel of our device with a unique solution containing fluorescent anti-VEGF, anti-CRP and anti-TNF-α antibodies. The device was able to specifically detect the presence od each biomarker displaying the fluorescent signal only in the dedicated microchannel (figure 4.10)

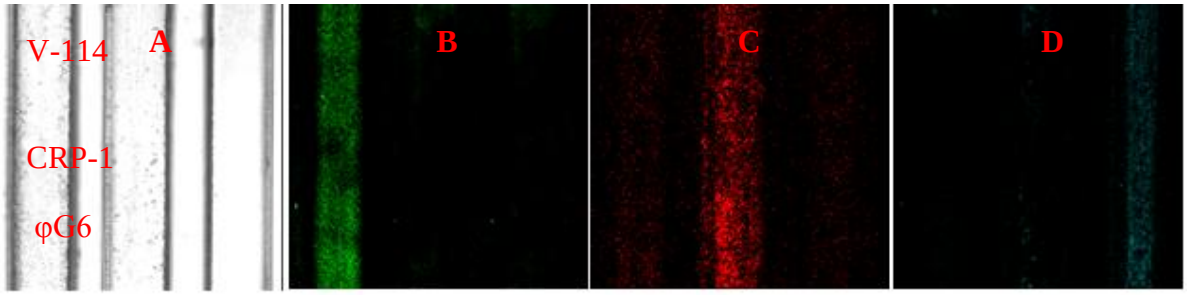

Figure 4.10: Detection of endometriosis biomarkers dissolved in PBS solution flushed in functionalized microfluidic channel device. From left to the right the channels were functionalized with three different binding peptides as follow: V114; CRP-1; φG6 (figure 4.10 A). immunofluorescence was performed with three different fluorescent antibodies: anti-VEGF (figure 4.10 B), anti-CRP (figure 4.10 C), anti-TNF-α (figure 4.10 D).

Finally, we conducted the same experiments in a complex biological modelby processing an human serum sample that contained the human EGF, CRP and TNF-α biomarkers at 5nM final concentration (figure 4.11). The fluorescence analysis display that the presence of human serum proteins does not affect the interaction of biomarkers with the corresponding binding peptides. Thus, the reported data confirmed the effective applicability of our system in the multiplex analysis for diagnostic purposes.

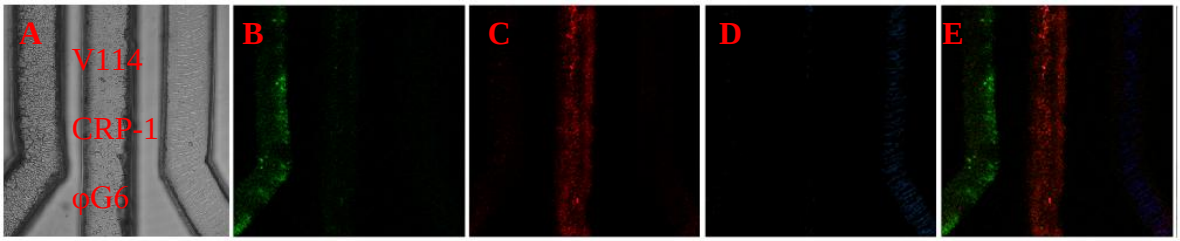

Figure 4.11: Detection of endometriosis biomarkers dissolved in human serum solution flushed in functionalized microfluidic channel device. From left to the right the channels were functionalized with three different binding peptides as follow: V114; CRP-1; φG6 (figure 4.11 A). Immunofluorescence was performed with three different fluorescent antibodies: anti-VEGF (figure 4.11 B), anti-CRP (figure 4.11 C), anti-TNF-α (figure 4.11 D). A merge of the fluorescent signals is reported in figure 4.11 E.

4.4 CONCLUSIONS

There is great interest in the construction of protein-detecting microarrays agents in biomedical and diagnostic fields [1]. One approach is to construct protein-detecting arrays using macromolecules as capture agents [3,4]. The use of these macromolecules are very expansive and for this reason the biosensor applications in medical fields are still very low. A significant challenge in the development of such technology could be the isolation of large numbers of suitable protein binding compounds [1]. Synthetic molecules can be economically produced in large quantities with efficient quality control and can be tailored to allow attachment to surfaces in a defined manner. In this work three different peptides, selected by literature, was used as capture agents for three endometriosis protein markers: VEGF, TNF-α and CRP [5-8]. The selected peptides was covalently immobilized on a microfluidic PDMS device, previously derivatized with 10% of PAA (Poly (acrylic acid)) solution. The so built device was used to capture and recognize endometriosis markers both in buffer and biologic fluids matrices such as human serum with a good specificity and sensitivity. With our approach, we proposed a simply but efficient strategy to bind a peptide on a polymer surface in order to use it as capture protein agent. Our idea was to set up a miniaturized microdevice that was able to diagnose endometriosis from the earliest stages in order to have a sensitive but not invasive and not expansive biosensor tool. The obtained results could represent a new challenge in endometriosis diagnosis avoid all drawbacks (organ damage, hemorrhage, infection, and adhesion formation) connected to surgical diagnosis that today seems to be the gold standard method used in the diagnosis of endometriosis disease.

References

[1] Naffin J.L., Han Y., Olivos H.J., Reddy M.M., Sun T., Kodadek T., Immobilized peptides as high-affinity capture agents for self-associating proteins Chem. Biol., 10(3), 251-9.

[2] Xavier P., Belo L., Beires J., Rebelo I., Martinez-de-Oliveira J., Lunet N., Barros H., Serum levels of VEGF and TNF-a and their association with C-reactive protein in patients with endometriosis. Arch Gynecol Obstet 273: 227-231.

[3] Kodadek, T., Protein microarrays: prospects and problems. Chem. Biol. 8, 2001 105–115.

[4] Kodadek, T. Protein-detecting microarrays. Trends Biochem 2002 Sci. 27, 295–300.

[5] Karayiannakis A.J., Syrigos K.N., Polychronidis A., Zbar A., Kouraklis G., Simopoulos C., Karatzas G., Circulating VEGF levels in the serum of gastric cancer patients: Correlation with pathological variables, patient survival, and tumor surgery. Ann. Surg. 2002, 236, 37–42.

[6] Poon R.T., Lau C., Pang R., Ng K.K., Yuen J., Fan, S.T. High serum vascular endothelial growth factor levels predict poor prognosis after radiofrequency ablation of hepatocellular carcinoma: importance of tumor biomarker in ablative therapies. Ann. Surg. Oncol. 2007, 14, 1835–1845.

[7] Balkwill F., TNF-α in promotion and progression of cancer. Cancer Metastasis Rev. 2006 25, 409–416.

[8] Mocellin S., Rossi C.R., Pilati P., Nitti D., Tumor necrosis factor, cancer and anticancer therapy. Cytokine Growth Factor Rev. 2005 16, 35–53.

[9] Cusano A. M., Causa F., Della Moglie R., Falco N., Scognamiglio, P. L.; Aliberti A., Vecchione R., Battista E., Marasco D., Savarese M., Integration of binding peptide selection and multifunctional particles as tool-box for capture of soluble proteins in serum. Journal of The Royal Society Interface 2014, 11 (99), 20140718.

[10] Kenrick S.A., and Daugherty P.S., Bacterial display enables efficient and quantitative peptide affinity maturation. Protein Engineering, Design and Selection. 2010;23(1):9-17. doi:10.1093/protein/gzp065.

[11] Bessette P.H., Rice J.J., Daugherty P.S., Rapid isolation of high-affinity protein binding peptides using bacterial display Protein Engineering, Design and Selection (2004) 17 (10): 731-739 first published online November 5, 2004 doi:10.1093/protein/gzh084.

[12] Donnez J., Smoes P., Gillerot S., Casanas-Roux F., Nisolle M., Vascular endothelial growth factor (VEGF) in endometriosis. Hum Reprod 1998 13:1686–1690.

[13] Healy D.L., Rogers P.A., Hii L., Wingfield M., Angiogenesis: a new theory for endometriosis. Hum Reprod 1998 Update 4:736–740.

[14] Iwabe T., Harada T., Tsudo T., Nagano Y., Tanikawa M., Terakawa N.,Tumor necrosis factor-a promotes proliferation of the endometriotic stromal cells by inducing interleukin-8 gene and protein expression. J Clin Endocrinol Metab 2000 85:824–829.

[15] May K.E., Conduit-Hulbert S.A., Villar J., Kirtley S., Kennedy S.H., Becker C.M., Peripheral biomarkers of endometriosis: a systematic review .Hum Reprod Update. 2010 Nov-Dec; 16(6): 651–674. Published online 2010 May 12. doi: 10.1093/humupd/dmq009.

[16] Foda A.A. and Abdel Aal I.A., Role of some biomarkers in chronic pelvic pain for early detection of endometriosis in infertile women. Middle East Fertil Soc J 2012 17:187–194.

[17] Fassbender A., Burney R.O., Dorien F. O, D'Hooghe T., Giudice L., Update on Biomarkers for the Detection of Endometriosis. BioMed Research International, vol. 2015, Article ID 130854, 14 pages, 2015. doi:10.1155/2015/130854.

[18] Hu S., Ren X., Bachman M., Sims C.E., Li G. P., Allbritton N.L., Surface-directed, graft polymerization within microfluidic channels. Anal Chem. 2004 April 1; 76(7): 1865–1870. doi: 10.1021/ac049937z.

[19] Wong I., and Ho,C.-M., Surface molecular property modifications for poly(dimethylsiloxane) (PDMS) based microfluidic devices. Microfluidics and Nanofluidics, 2009 7(3), 291–306. http://doi.org/10.1007/s10404-009-0443-4.

[20] De Prijck K., De Smet N., Rymarczyk-Machal M., Van Driesschec G., Devreesec B., Coenyea T., Schachtb E., Nelisa H.J., Candida albicans biofilm formation on peptide functionalized polydimethylsiloxane, Biofouling, vol. 26, no. 3, pp. 269–275,2010.

[21] Seo H.S., Ko Y.M., Shim J.W., Lim Y.K., Kook J., Cho D., Kim B. H., Characterization of bioactive RGD peptide immobilized onto poly(acrylic acid) thin films by plasma polymerization. Appl. Surf. Sci. 2010 257 (2), 596–602.

[22] Wang C., Yan Q., Liu H.B., Zhou X.H., Xiao S.J. Different EDC/NHS Activation Mechanisms between PAA and PMAA Brushes and the Following Amidation Reactions. Langmuir 2011 27 (19), 12058-12068 DOI: 10.1021/la202267p.

[23] Occhipinti L.G., and Porro F., Surface treatment of an organic or inorganic substrate for enhancing stability of a lithographically defined deposited metal layer, 2010, US Pat. App. 12/835,011.

[24] Herington J. L., Bruner-Tran K. L., Lucas J. A., Osteen K. G., Immune interactions in endometriosis. Expert Review of Clinical Immunology, 2011 7(5), 611–626. http://doi.org/10.1586/eci.11.53.

[25] Haider S., and Knöfler M., Human Tumour Necrosis Factor: Physiological and Pathological Roles in Placenta and Endometrium. Placenta, 2009 30(2), 111–123. http://doi.org/10.1016/j.placenta.2008.10.012

[26] Hoeben A., Landuyt B., Highley M.S., Wildiers H., Van Oosterom A.T., De Bruijn E.A. Vascular endothelial growth factor and angiogenesis. Pharmacol Rev 2004;56:549-580.

[27] A. Bokor, Semi-invasive Diagnosis of Endometriosis. PhD thesis, Semmelweis University, 2010.

[28] Vachali P.P, Li B., Besch B.M, Bernstein P.S., Protein-Flavonoid Interaction Studies by a Taylor Dispersion Surface Plasmon Resonance (SPR) Technique: A Novel Method to Assess Biomolecular Interactions. Biosensors 2016, 6(1), 6; doi 10.3390/bios6010006

[29] Quinn J.G.,Evaluation of Taylor dispersion injections: Determining kinetic/affinity interaction constants and diffusion coefficients in label-free biosensing. Analytical Biochemistry (2011)doi:10.1016/j.ab.2011.11.023 (Free Download)

[30] Quinn J.G., Modeling Taylor dispersion injections: Determination of kinetic/affinity interaction constants and diffusion coefficients in label-free biosensing. Analytical Biochemistry (2011) doi:10.1016/j.ab.2011.11.02.

[31] Armbruster D.A.,and Pry T.,Limit of Blank, Limit of Detection and Limit of Quantitation. Clin Biochem Rev. 2008 Aug; 29(Suppl 1): S49–S52.

CHAPTER 3

Di-peptide sequences of Cdocker results.

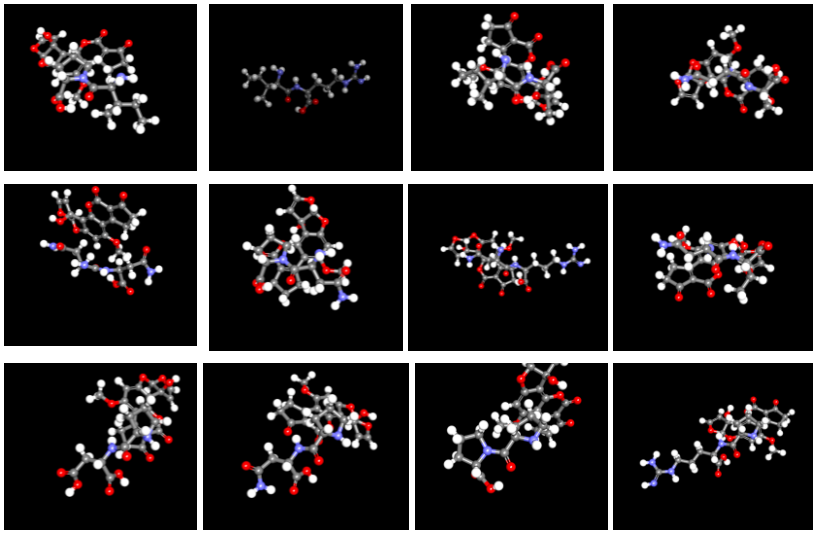

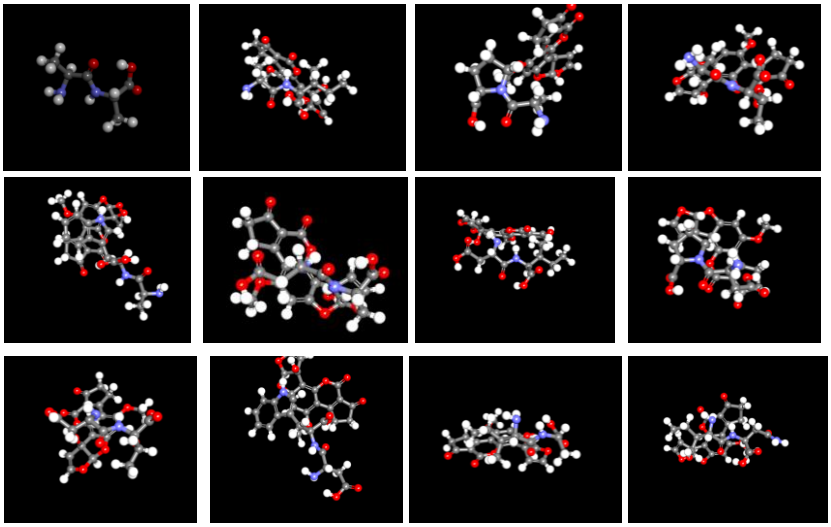

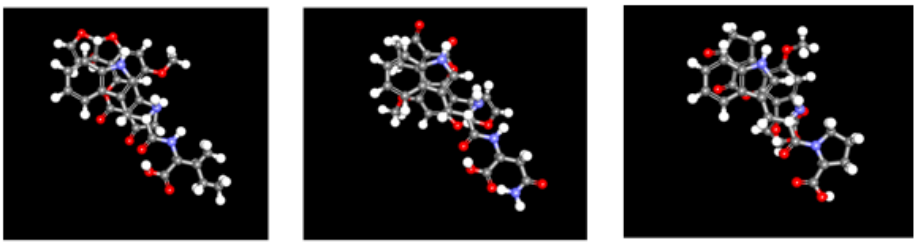

Tetra-peptide sequences of Cdocker results.

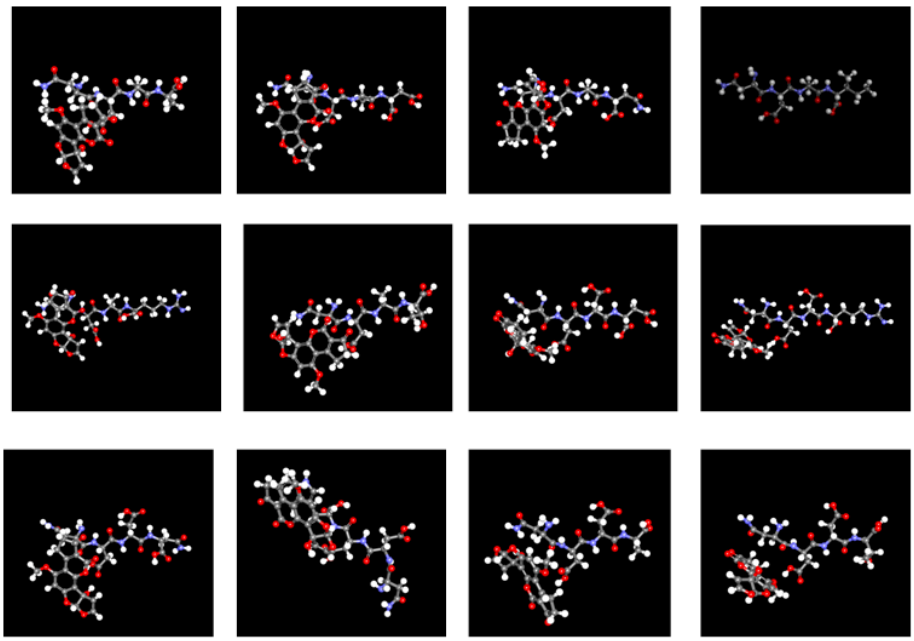

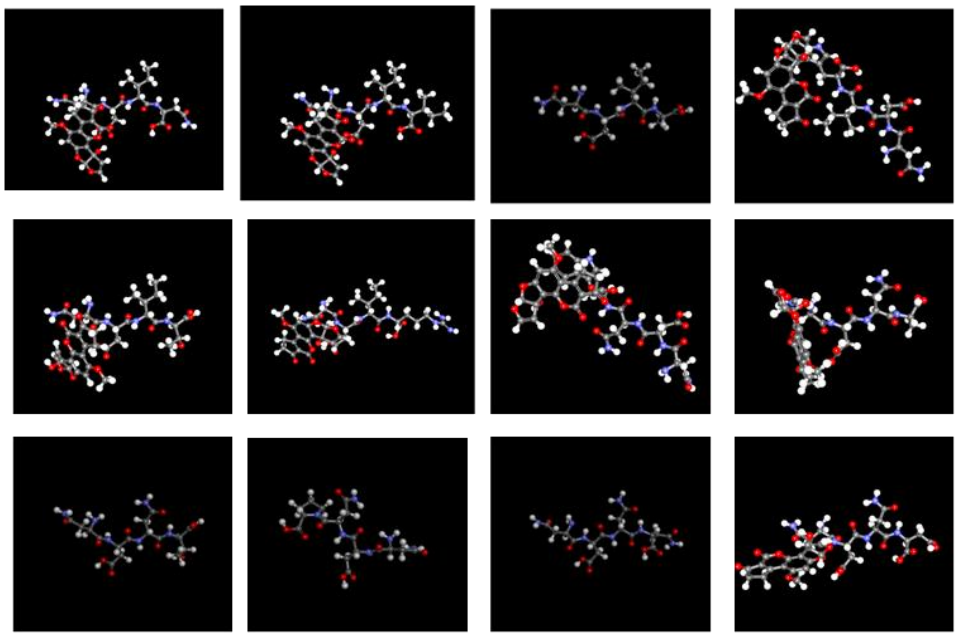

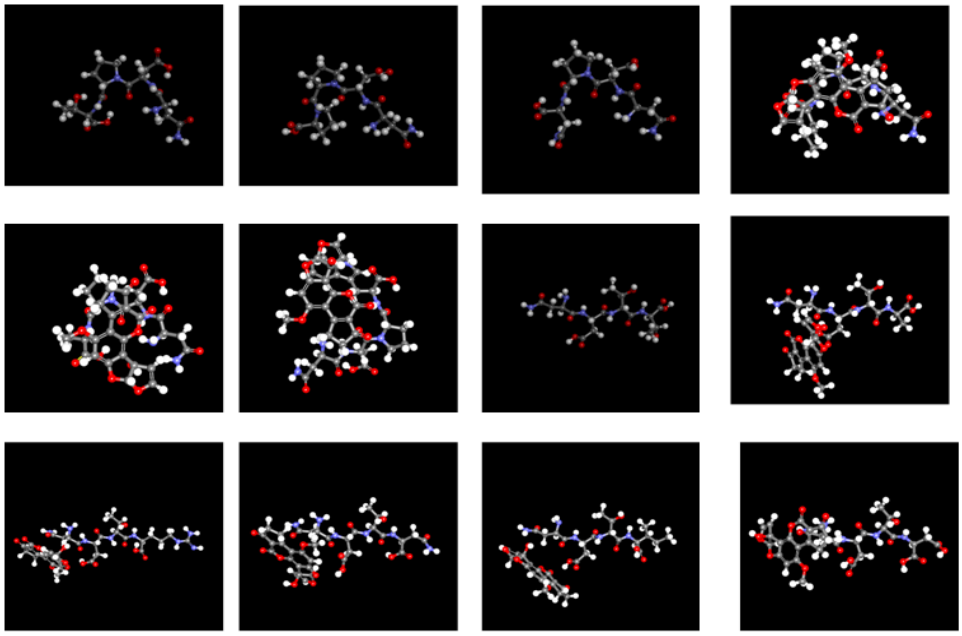

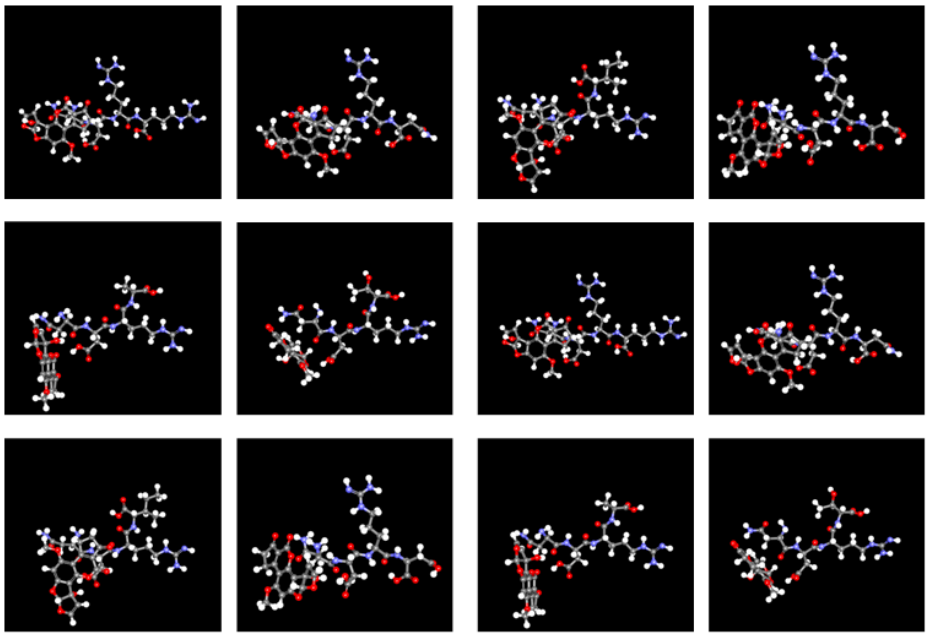

Di-peptide screening by SPR ([ ] 3mM of each sequence)

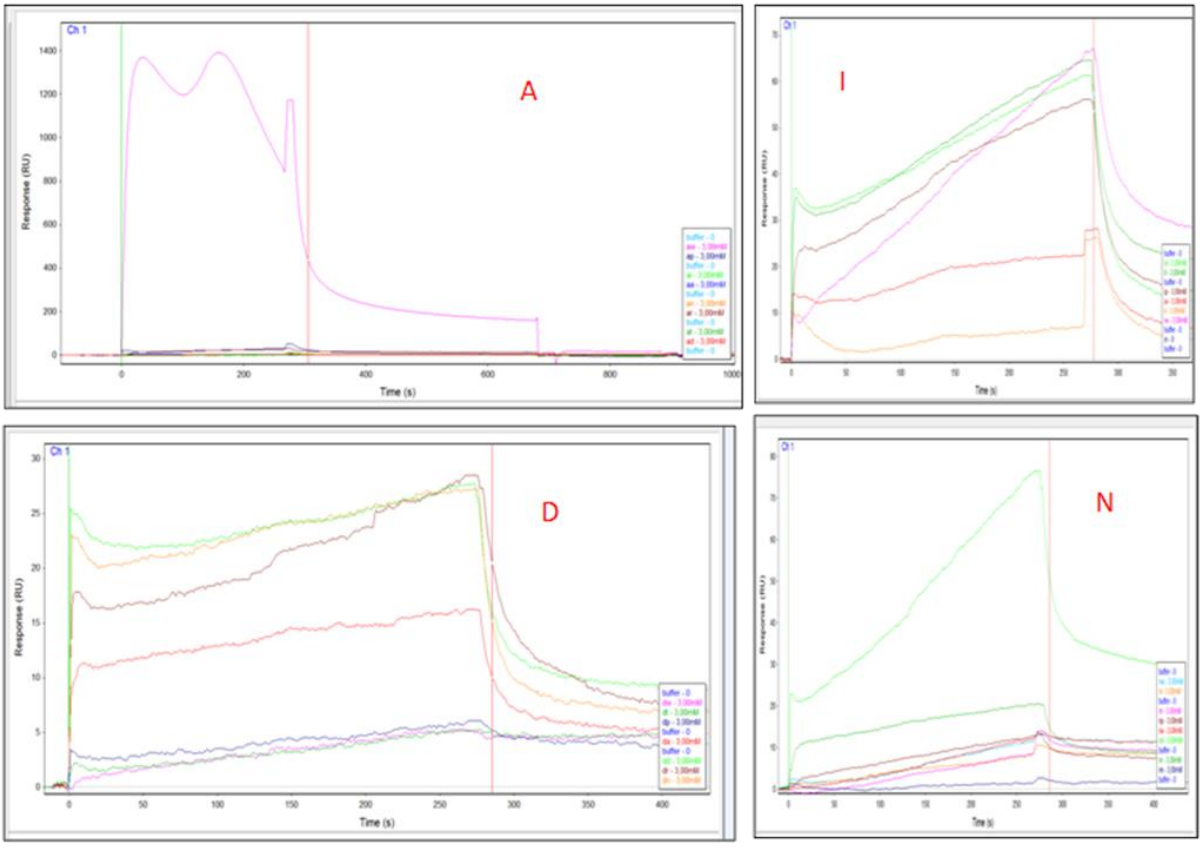

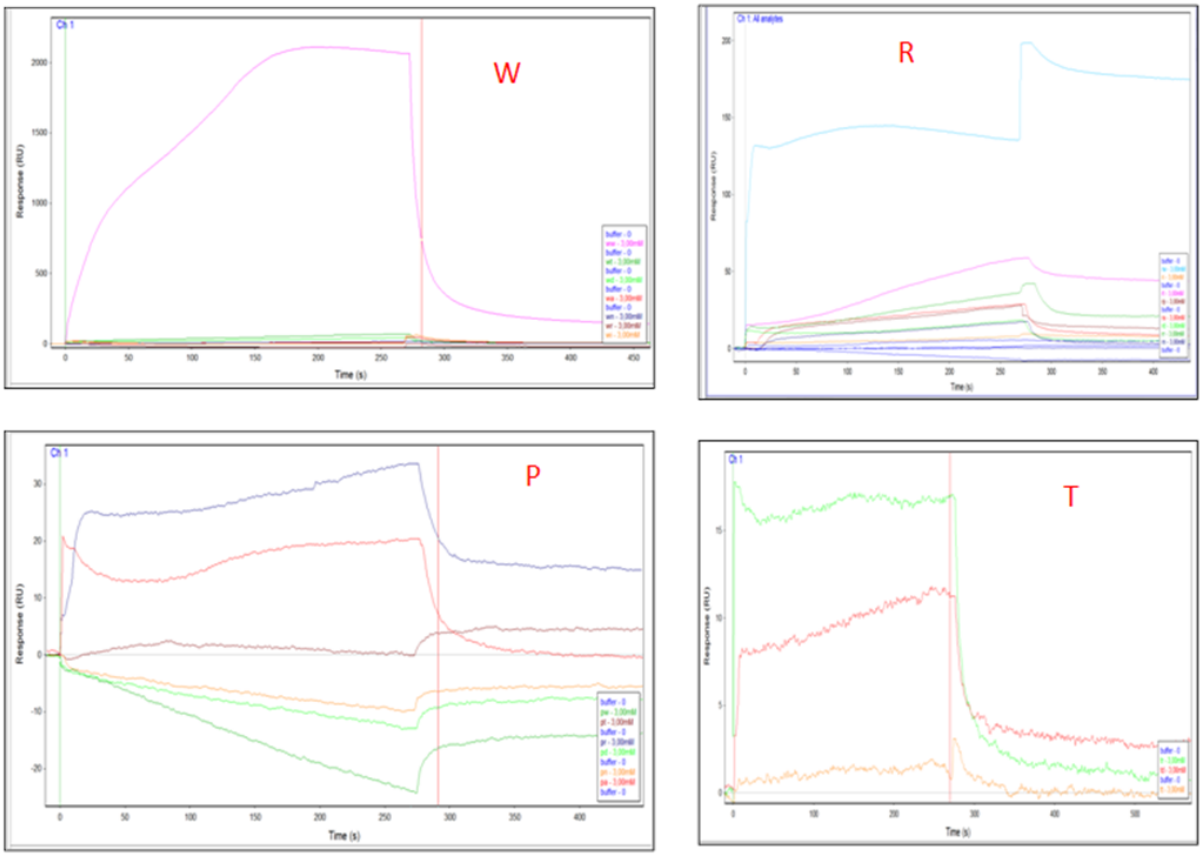

Tetra-peptide screening by SPR ([ ] 1mM of each sequence), K_D= high micromolar range. No good fitting for all sequences.

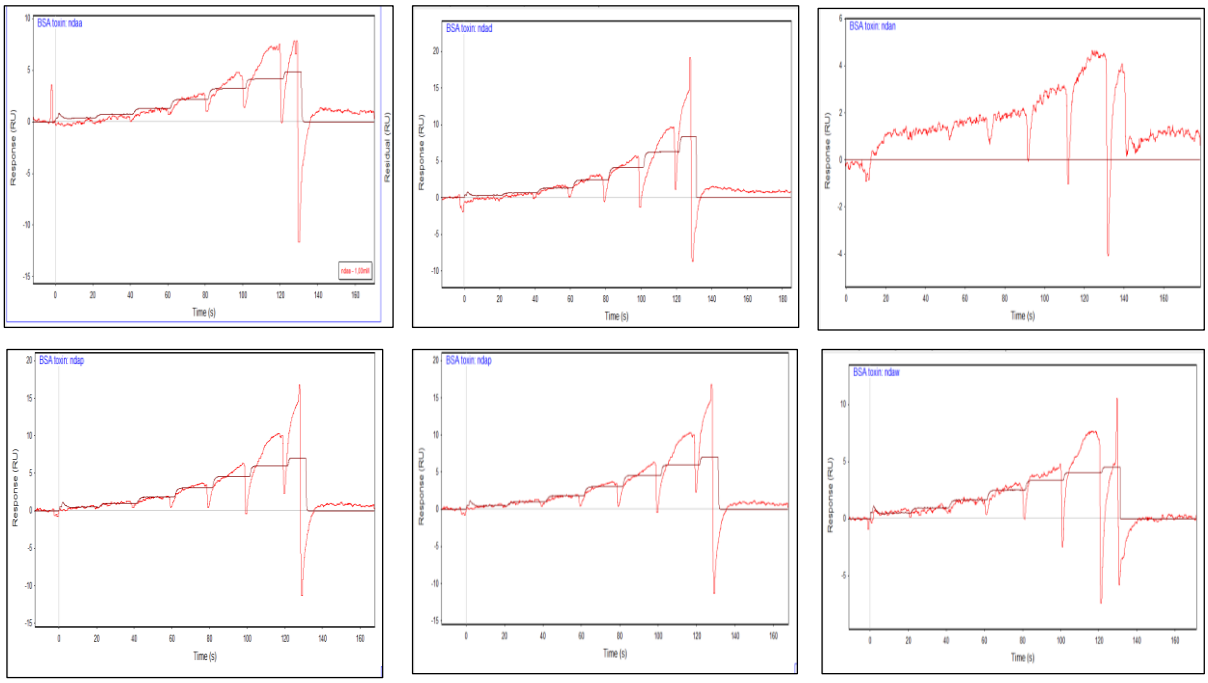

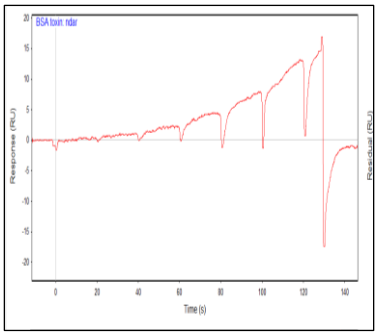
BSA toxin: ndar
Response (RU)
Time (s)

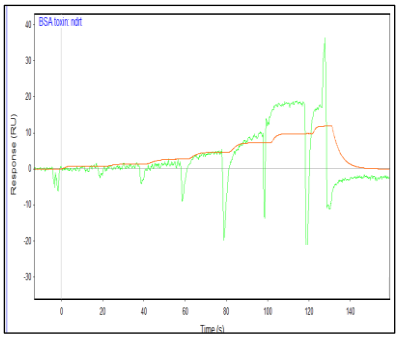
BSA toxin: ndrt
Response (RU)
Time (s)

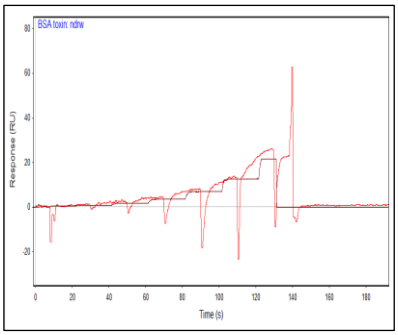
BSA toxin: ndrw
Response (RU)
Time (s)

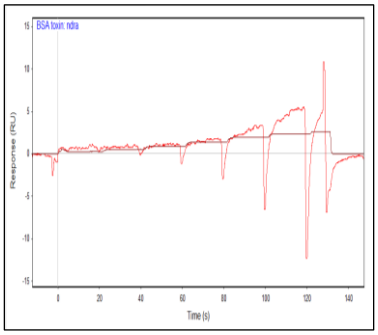
BSA toxin: ndra
Response (RU)
Time (s)

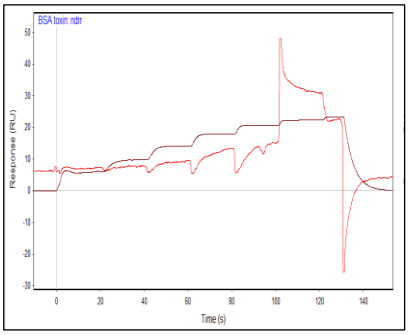
BSA toxin: ndrr
Response (RU)
Time (s)

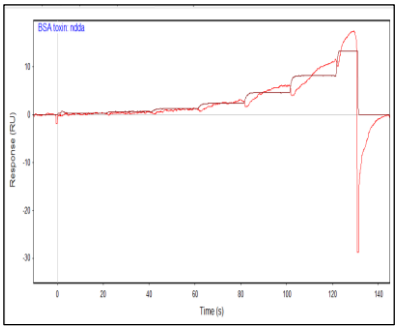
BSA toxin: nddа
Response (RU)
Time (s)

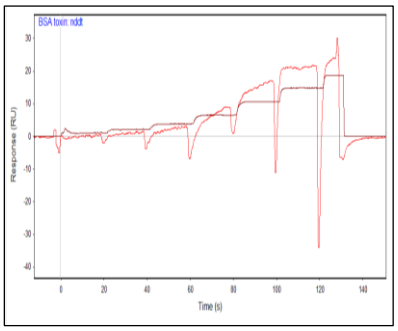
BSA toxin: nddt
Response (RU)
Time (s)

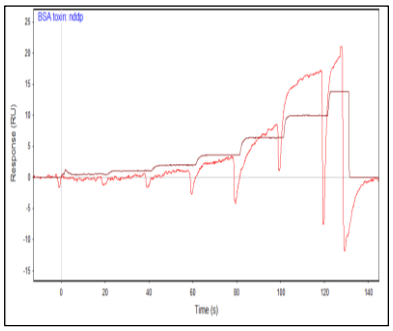
BSA toxin: nddp
Response (RU)
Time (s)

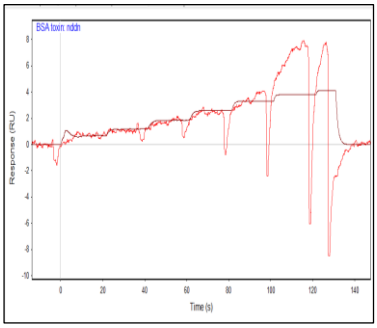
BSA toxin: nddn
Response (RU)
Time (s)

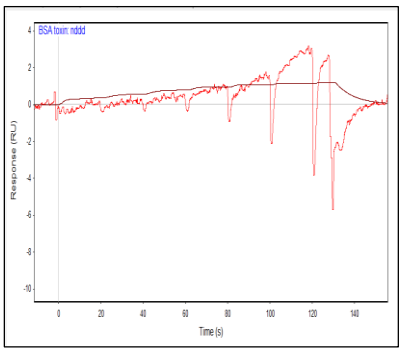
BSA toxin: nddd
Response (RU)
Time (s)

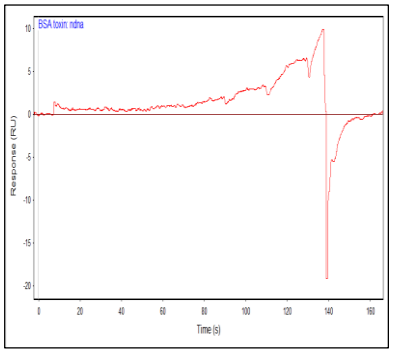
BSA toxin: ndna
Response (RU)
Time (s)

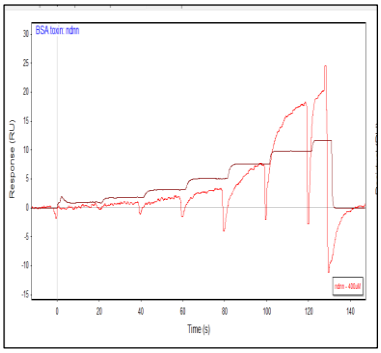
BSA toxin: ndm
Response (RU)
Time (s)

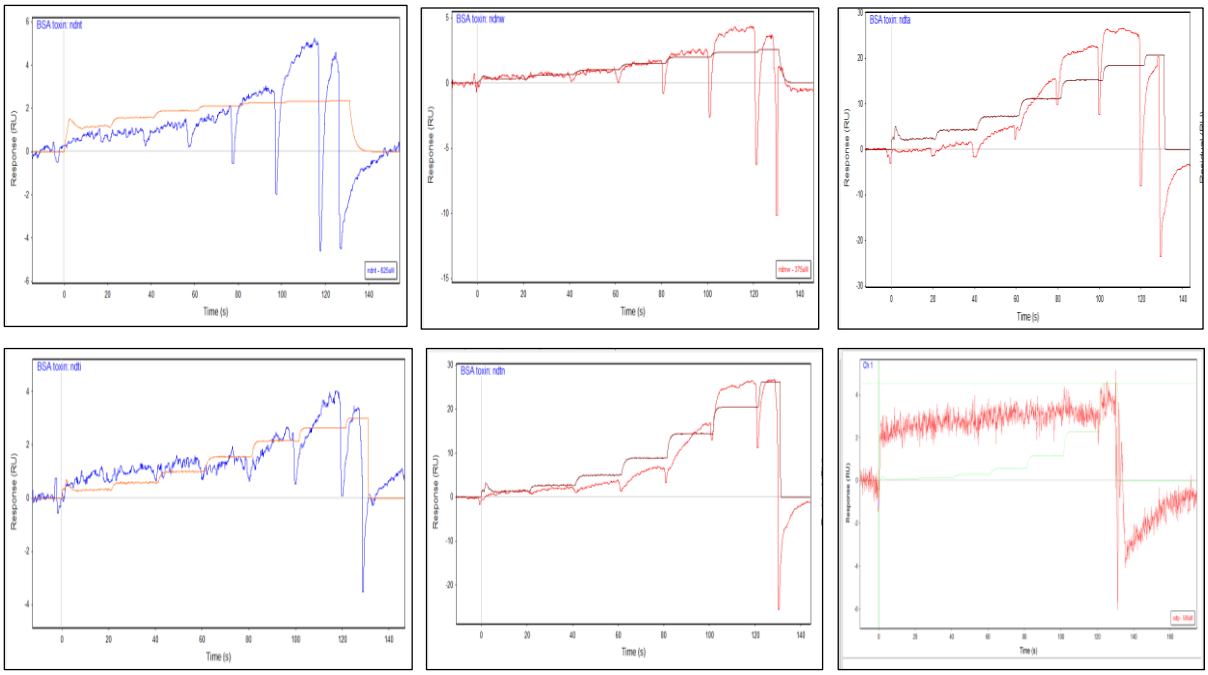
BSA toxin: ndnt
BSA toxin: ndnw
BSA toxin: ndta
BSA toxin: ndtl
BSA toxin: ndtn
Response (RU)
Time (s)

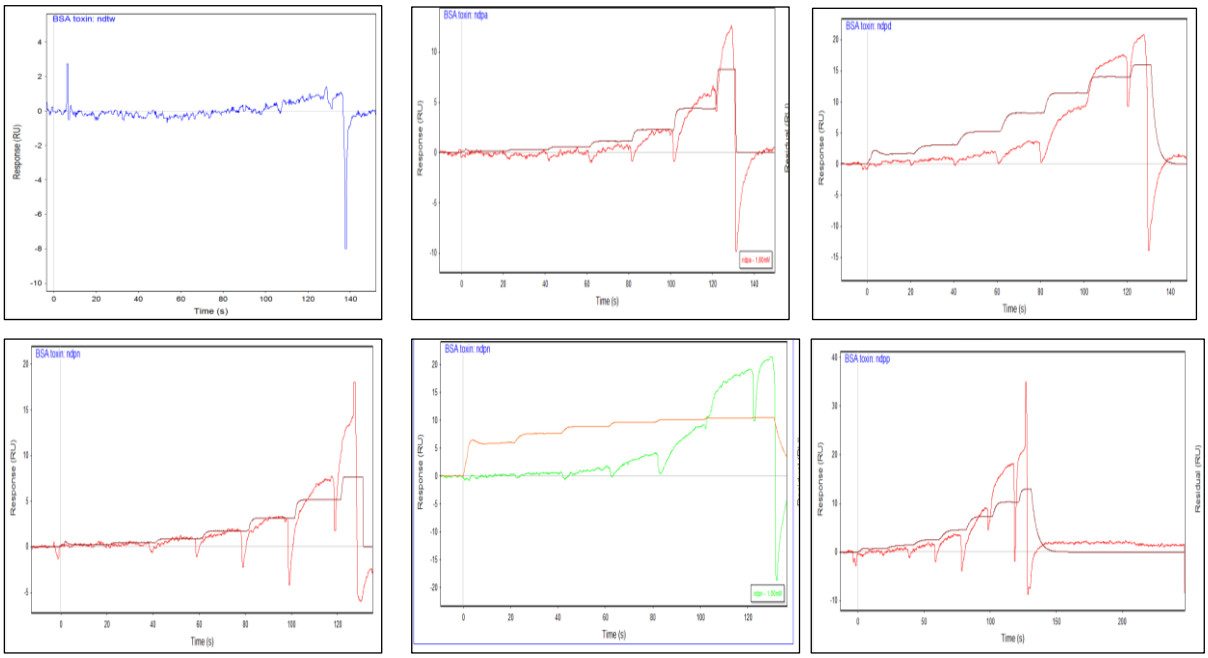
BBA toxin: ndtw
BSA toxin: ndpa
BSA toxin: ndpd
BSA toxin: ndpn
BSA toxin: ndpp
Response (RU)
Time (s)

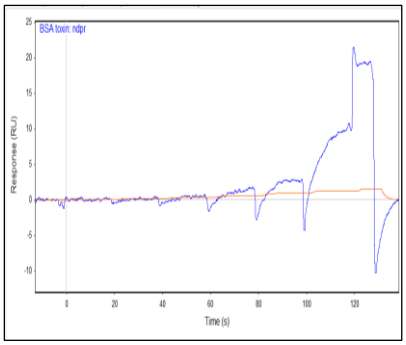
BSA toxin: ndpr
Response (RU)
Time (s)

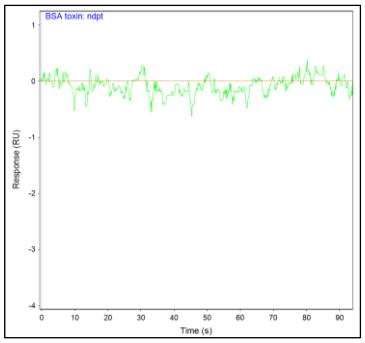
BSA toxin: ndpt
Response (RU)
Time (s)

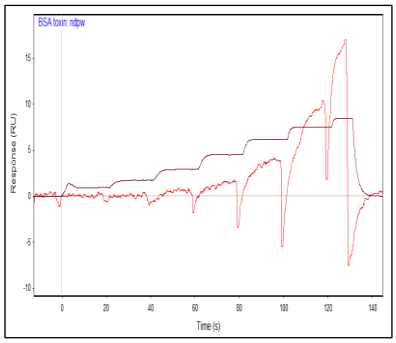
BSA toxin: ndpw
Response (RU)
Time (s)

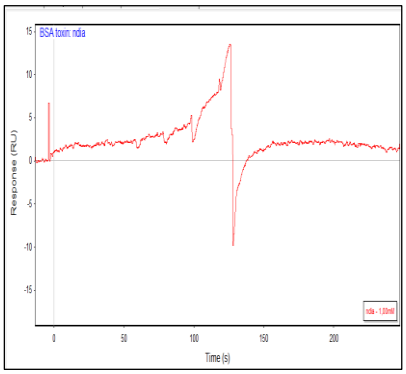
BSA toxin: ndia
Response (RU)
Time (s)

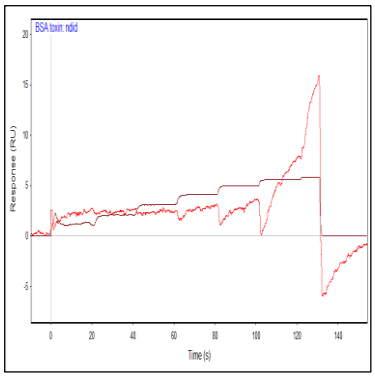
BSA toxin: ndid
Response (RU)
Time (s)

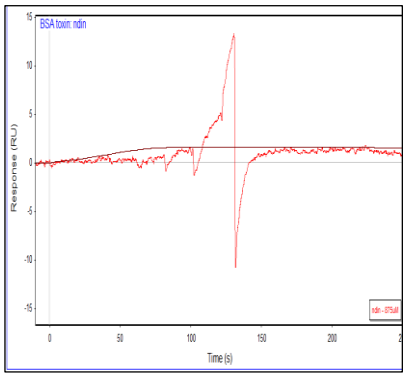
BSA toxin: ndin
Response (RU)
Time (s)

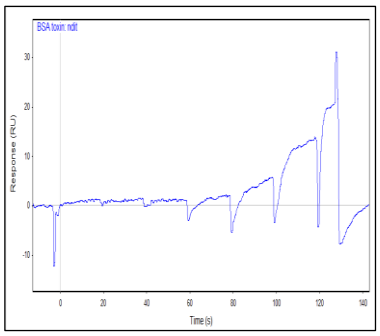
BSA toxin: ndit
Response (RU)
Time (s)

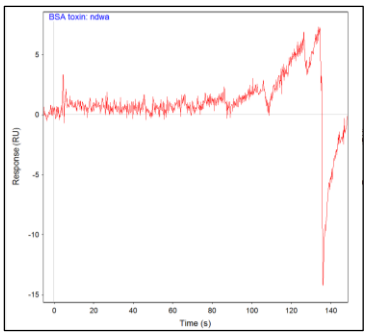
BSA toxin: ndwa
Response (RU)
Time (s)

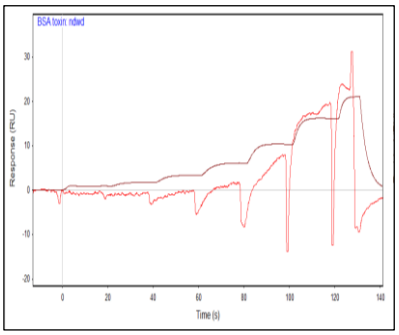
BSA toxin: ndwd
Response (RU)
Time (s)

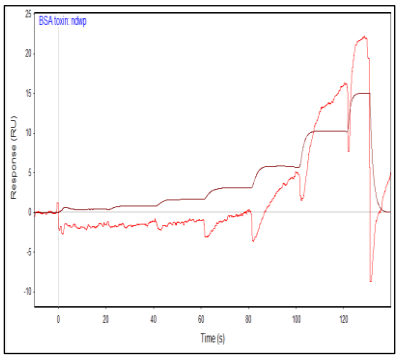
BSA toxin: ndwp
Response (RU)
Time (s)

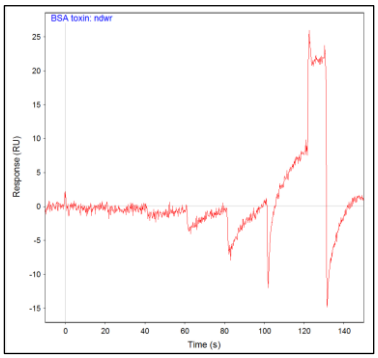
BSA toxin: ndwr
Response (RU)
Time (s)

CHAPTER 4

LC-MS of VEGF-114, ΦG6 and CRP-1 peptides.

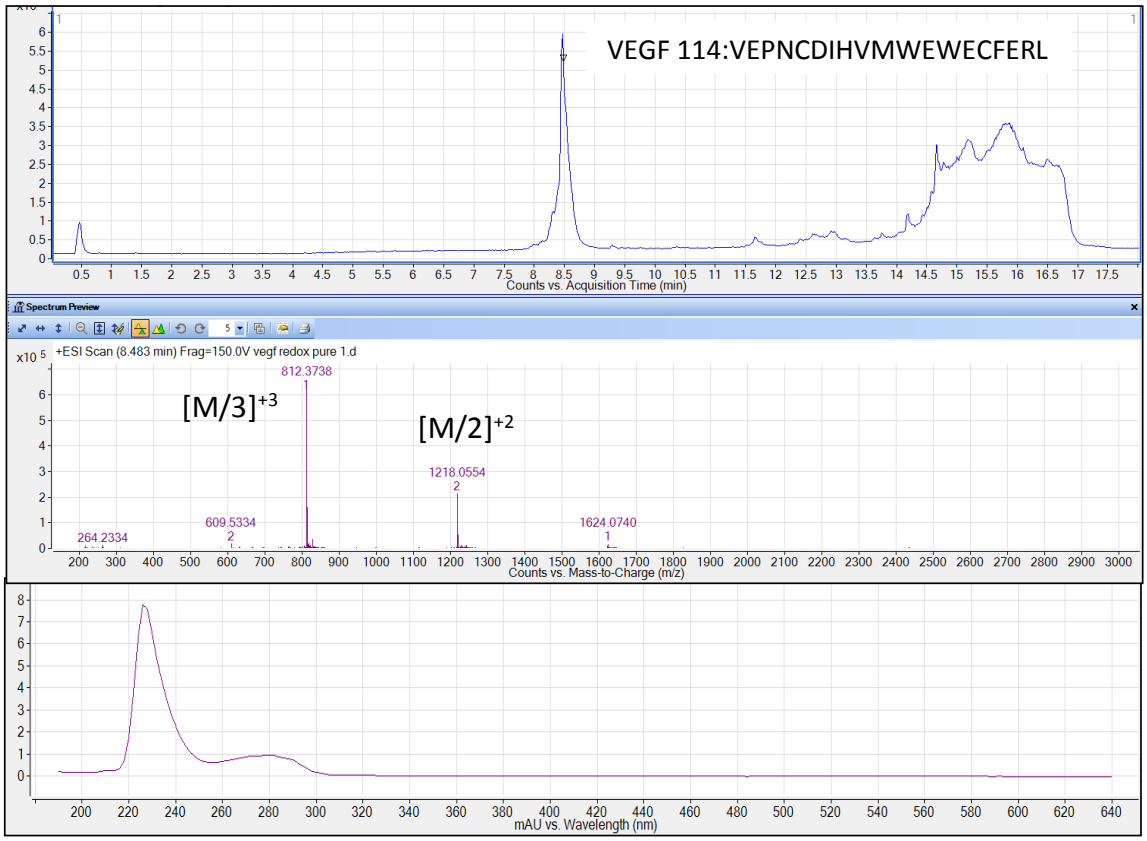

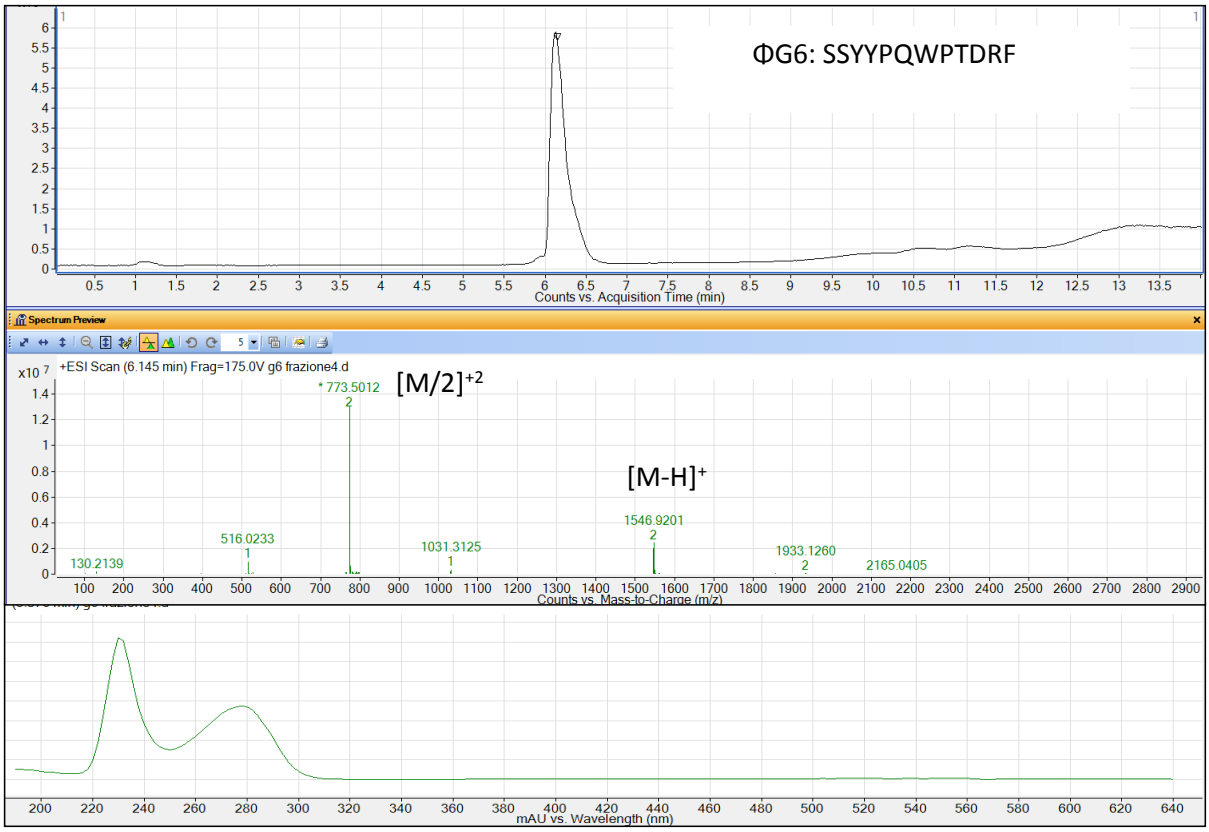
ΦG6: SSYYPQWPTDRF
Counts vs. Acquisition Time (min)
Spectrum Preview
+ESI Scan (6.145 min) Frag=175.0V g6 frazione4.d
[M/2]+2
773.5012
[M-H]+
1546.9201
516.0233
1031.3125
1933.1260
130.2139
2165.0405
Counts vs. Mass-to-Charge (m/z)
mAU vs. Wavelength (nm)

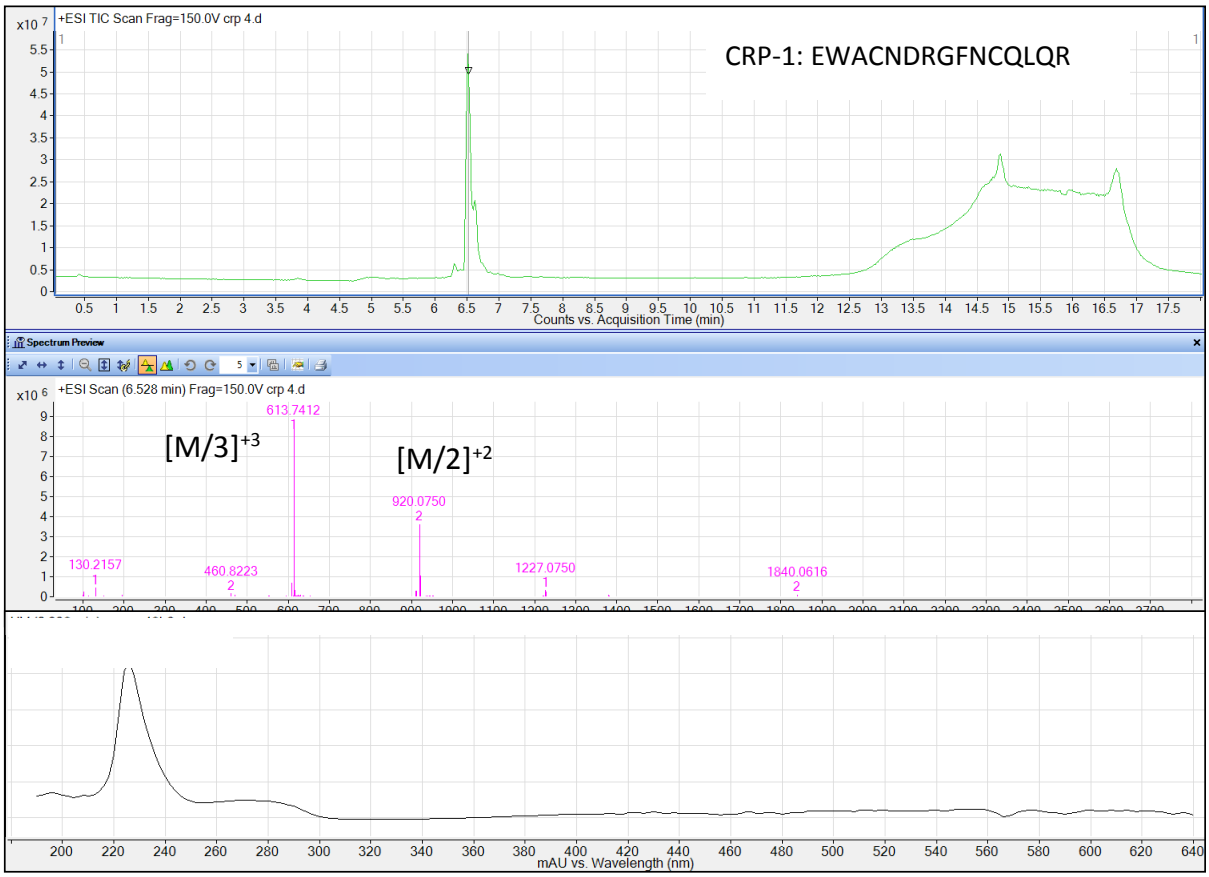
+ESI TIC Scan Frag=150.0V crp 4.d
CRP-1: EWACNDRGFNCQLQR
Counts vs. Acquisition Time (min)
Spectrum Preview
+ESI Scan (6.528 min) Frag=150.0V crp 4.d
[M/3]+3
[M/2]+2
613.7412
920.0750
130.2157
460.8223
1227.0750
1840.0616
mAU vs. Wavelength (nm)

LC-MS of VEGF-114 and CRP-1 oxidized peptides.

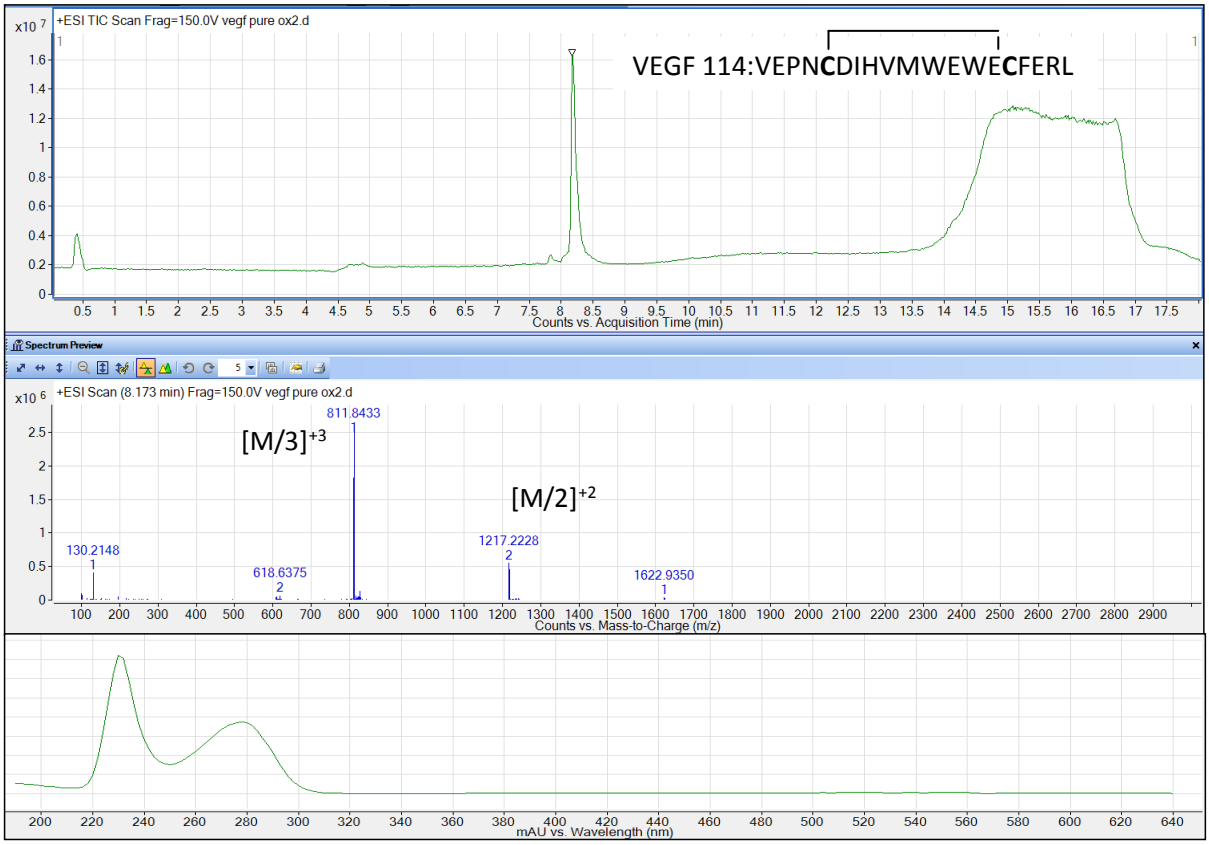

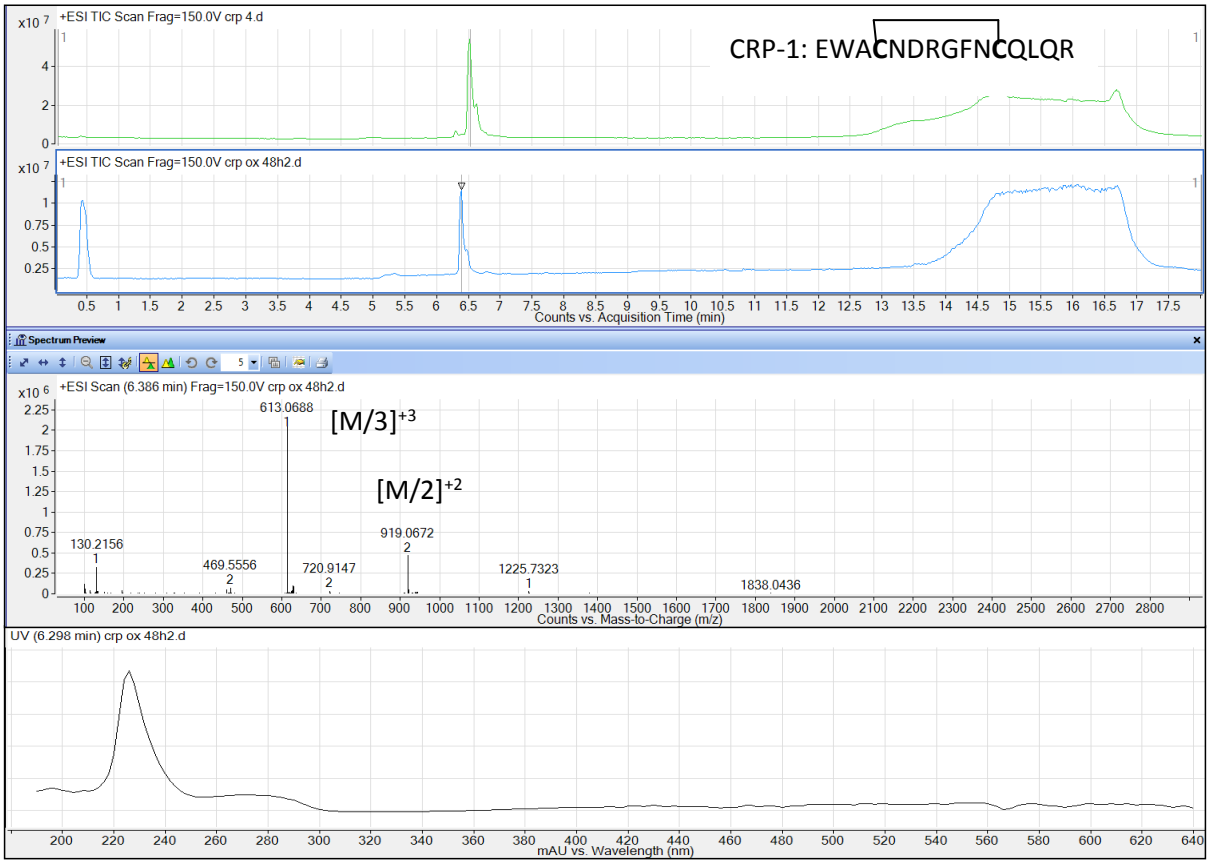

POSTER COMMUNICATIONS

1. **C. Di Natale**, D. Marasco , M. Leone , P.L. Scognamiglio, L. De Rosa and L. Vitagliano: Structural studies of Nucleophosmin1 helical peptides. EPS European Peptide Symposium-September 2012-Athens.

2. **C. Di Natale**, F.A. Mercurio, P.L. Scognamiglio, L. Pirone, E. Pedone. D. Marasco, M. Leone and M. Pelleccchia. SAM domains heterotypic interactions:functional and structural characterization of minimum interacting protein regions.13th Naples Workshop on Bioactive Peptides, Naples June 7-10, 2012

3. **C.Di Natale**, P.L.Scognamiglio, V.Punzo, M.Leone, G.Tell and D.Marasco. Conformational studies of nucleophosmin C-terminal leukemia associated regions: new insights from protein dissection approach. 14th Naples Workshop on Bioactive Peptides, Naples June 12-14, 2014

4. F.A. Mercurio,**C.Di Natale**, P.L. Scognamiglio, L. Pirone, E. Pedone. D. Marasco, M. Leone and M. Pelleccchia. Conformational and binding studies of peptides spanning the EphA2 interacting region of the first Sam domain of Odin.14th Naples Workshop on Bioactive Peptides, Naples June 12-14, 2014

5. **C. Di Natale**, C.Cosenza, N.R. Naganna Gari, E.Battista and F.Causa.

Development of peptide-based biosensor for aflatoxin detection in food ISSON14 and 11th NN14 Thessaloniki,Greece, 2014

6. D. Marasco, **C.Di Natale**, V. Punzo, D. Riccardi, P.L. Scognamiglio, R. Cascella, C. Cecchi, F. Chiti, M. Leone and L. Vitagliano. Amyloid-like aggregation of Nucleophosmin regions associated with acute myeloid leukemia mutations. The 29th Annual Symposium of the Protein Society, Barcelona July 22-25, 2015

7. F.A. Mercurio,**C.Di Natale**, L. Pirone, P.L. Scognamiglio, D. Marasco, E. Pedone, M. Saviano and M. Leone. Odin-Sam1 peptides NMR conformational and binding studies with Epha2-Sam. XLIV National Congress on Magnetic Resonance, Rome September 28-30, 2015

ORAL COMMUNICATIONS

1. **C. Di Natale**, C. Cosenza, P.L. Scognamiglio, E.Battista, F. Causa and P.A.Netti . Selection of peptide motifs for the detection of small molecules in biotechnological applications. NANOTECH FRANCE 2015, CONFERENCE & EXHIBITION NANOTECH FRANCE 2015 15 JUNE 15-17, 2015 PARIS , FRANCE.

2. **C. Di Natale** Selection of peptides for small molecules capture. WORKSHOP SPR - USER MEETING SENSQ, July 1,2015, Milan.

PUBLICATIONS

1. Scognamiglio PL, **Di Natale C**, Perretta G, Marasco D. From peptides to small molecules: an intriguing but puzzled way to new drugs. Curr Med Chem. 2013;20(31):3803-17. Review.

2. Scognamiglio PL, **Di Natale C**, Leone M, Poletto M, Vitagliano L, Tell G, Marasco D. G-quadruplex DNA recognition by nucleophosmin: new insights from protein dissection. Biochim Biophys Acta. 2014 Jun;1840(6):2050-9.

3. Mercurio FA, Scognamiglio PL, **Di Natale C**, Marasco D, Pellecchia M, Leone M. CD and NMR conformational studies of a peptide encompassing the Mid Loop interface of Ship2-Sam. Biopolymers. 2014 Nov;101(11):1088-98.

4. **Di Natale C**, Scognamiglio PL, Cascella R, Cecchi C, Russo A, Leone M, Penco A, Relini A, Federici L, Di Matteo A, Chiti F, Vitagliano L, Marasco D. Nucleophosmin contains amyloidogenic regions that are able to form toxic aggregates under physiological conditions. FASEB J. 2015 May 14. pii: fj.14-269522.

5. Mercurio FA, **Di Natale C**, Pirone L,Scognamiglio PL, Marasco D, Pedone EM, Saviano M, Leone M. Peptide fragments of Odin-Sam1: Conformational Analysis and Interaction Studies with EphA2-Sam. ChemBioChem.2015 May.

6. Celetti G., **Di Natale C**., Causa F., Battista E and P.A. Netti Peptide-functionalized polymeric network: microgels synthesis for in

serum protein detection with high affinity by droplet microfluidic device, Colloid and Interface B: Biointerface, submitted.

7. F. A. Mercurio, S. Guarriniello, **C. Di Natale**, L. Pirone, D. Marasco, S. Costantini, E.M. Pedone, and M. Leone Structural Investigation of a C-terminal EphA2 mutant associated to cataracts: does mutation affect the End-Helix Interface in the Sam domain?, Molbiosyst,2016,submitted.

8. Pasqualina Liana Scognamiglioa, **Concetta Di Natale**, Marilisa Leone, Roberta Cascella, Cristina Cecchi, Lisa Lirussi,Giulia Antoniali, Domenico Riccardi, Giancarlo Morelli, Gianluca Tell, Fabrizio Chiti and Daniela Marasco Destabilisation, Aggregation, Toxicity and Cytosolic Mislocalisation of Nucleophosmin Regions Associated with Acute Myeloid Leukemia,Oncotarget 2016,submitted